SVERIGES METEOROLOGISKA OCH HYDROLOGISKA INSTITUT

MEDDELANDEN. SERIE B. Nr 28
(COMMUNICATIONS. SERIES B. No. 28)

SCIENTIFIC PAPERS DEDICATED TO DR ANDERS ÅNGSTRÖM

STOCKHOLM 1968

Meddelanden. Serien uppsatser.

Communications. Series of papers.

Nr 1. A. Ångström: Teleconnections of climatic changes in present time
Utgången (out of print)

2. *G. Slettenmark: Axel Wallén* . . . . . Utgången (out of print)

3. Hydrologisk bibliografi år 1934 . . . . . Kr. 1: —

4. Hilding Olsson: Sunshine and radiation, Mount Nordenskiöld, Spitzbergen
Utgången (out of print)

5. A. Ångström: Jordtemperaturen i bestånd av olika täthet. (Soil temperature in stands of different densities, with an English summary.) . . . . Kr. 2: —

6. Walter Persson: Vindhastighetens dagliga gång vid några svenska stationer. (The daily variation of wind velocity at some Swedish stations, with an English summary.) . . . . . » 1: —

7. Olof Tryselius: On the turbidity of polar air . . . . . » 1: —

8. A. Ångström: Effective radiation during the second international polar year . . . . . » 1: 50

9. A. Ångström: A simple actinometer . . . . . Utgången (out of print)

10. Folke Bergsten: A contribution to the knowledge of the influence of the Gulf Stream on the winter temperature of Northern Europe . . . . . Kr. 1: —

11. A. Ångström: A coefficient of humidity of general applicability . . . » 1: —

12. Hilding Olsson: Radiation measurements on Isachsen's Plateau . . . . » 1: 50

13. Tor Bergeron: Physik der troposphärischen Fronten und ihrer Störungen
Utgången (out of print)

14. Ragnar Melin: Forecasting spring run-off of the forest rivers in North Sweden . . . . . Kr. 0: 50

15. G. Slettenmark: Väderlekstjänstens organisation och arbete.
Utgången (out of print)

16. T. E. Aurén: Luminous efficiency of solar radiation . . . . . Kr. 1: 50

17. A. Ångström: On the formation of ice in the river Götaälv as a function of meteorological factors . . . . . » 0: 50

18. G. Slettenmark: Issignaltjänsten, dess organisation samt några erfarenheter beträffande isförhållandena i Gävlebukten . . . . . » 1: 50

19. A. Ångström: On the standardization of photo-electric cells by means of sun radiation . . . . . » 0: 50

20. G. Köhler: Några aktinometrars egenskaper med hänsyn till mätning av artificiell strålning i samband med växtodling . . . . . » 3: —

21. Bibliographie Hydrologique des Années 1935 et 1936. Suède.
Utgången (out of print)

22. Tor Bergeron: Hydrometeorbeschreibungen mit den vom Internationalen Meteorologischen Komitee in Salzberg 1937 angenommenen Änderungen. (Deutscher, englischer und französischer Text.) . Utgången (out of print)

23. A. Ångström: Actinometric measurements near Stockholm 1930—1936 Kr. 2: —

24. B. Rolf and J. Olsen: Contributions to the study of overhead current systems in the arctic during magnetic storms, based on observations during the first and second international polar year . . . . . » 1: 50

25. Bibliographie Hydrologique de l'Année 1937, Suède . . . . . » 1: —

26. A. Ångström: Temperaturklimatets ändringar i nuvarande tid och dess orsak . . . . . Utgången (out of print)

27. A. Nyberg: Temperature measurements in an air layer very close to a snow surface . . . . . Kr. 2: 50

28. A. Ångström: Bemerkungen betreffs Verdunstung von dem Wasser eines eingetauchten Kessels mit artificieller Umrührung und von freien Wasseroberflächen . . . . . » 0: 50

29. H. Modén: Beräkning av medeltemperaturen vid svenska stationer. (Computation of the mean monthly temperature at Swedish stations.)
Utgången (out of print)

SVERIGES METEOROLOGISKA OCH HYDROLOGISKA INSTITUT

MEDDELANDEN. SERIE B. Nr 28
(COMMUNICATIONS. SERIES B. No. 28)

SCIENTIFIC PAPERS DEDICATED TO DR ANDERS ÅNGSTRÖM

STOCKHOLM 1968

Kungl. Boktryckeriet P. A. Norstedt & Söner Stockholm 1968

Contents

Dr. Anders Ångström, 80 years on February 28, 1968

Dr. Anders K. Ångström was born on 28 February 1888. Both his father and grandfather were world famous professors of physics at the university of Uppsala and devoted much of their scientific activity to solar radiation. Anders Ångström thus had a good background for work in the field of radiation and started early his studies in various parts of the world. He is by now so well known in the meteorological community that it seems unnecessary to discuss here the numerous scientific papers that he has published. It may suffice to mention that many of his papers especially on radiation and climatology including energy transformations in the atmosphere have been of pioneering character.

Dr. Ångström has been much appreciated for his contributions to international meteorological work in the International Union of Geodesy and Geophysics as well as in the World Meteorological Organization and its predecessor the International Meteorological Organization (IMO). In 1962 he got the seventh IMO prize "in recognition of his distinguished contributions to the advancement of meteorological knowledge in the field of actinometry, heat balance, agrometeorology and climatology and his pioneering works on instruments and observations of solar radiation and his services to the cause of international collaboration in meteorology".

Dr. Ångström has spent a large part of his life at the Swedish Meteorological and Hydrological Institute in various positions and finally as director. His activity has been of great importance for the successful functioning and development of the institute. His positive attitude towards his cooperators and their efforts and his gentle and friendly manners created an excellent atmosphere highly appreciated by the staff.

Dr. Ångström is still active as a scientist giving valuable contributions to the field of radiation. It is a great pleasure for his students, cooperators and friends to honour him by dedicating this volume of articles to him at the occasion of his 80th anniversary at the same time as we bring him our best wishes for a successful continuation of his work.

Alf Nyberg

On the causes of climate variations

By M. I. BUDYKO *Main Geophysical Observatory, Leningrad*

ABSTRACT

The problem of causes of climate variations at the present time and in the geological past has been considered. Physical explanation of the regularities of climate variations has been suggested which is based on the general ideas of factors determining the genesis of the Earth's climate.

One of the basic trends in modern physical climatology is connected with studying the income of solar radiation and its transformations in the atmosphere and hydrosphere.

The works by A. ÅNGSTRÖM (1920, 1925, 1935 and others) have made an important contribution to the development of investigations of this kind. In these works the first data on the heat balance of the earth's surface were obtained, factors determining the climate genesis studied and the influence of the radiation regime changes on the climate variations investigated.

During recent years in connection with the rapid progress of physical climatology the possibilities of applying the methods of this science to the study of climate variations have considerably widened (WEXLER, 1953; FLOHN, 1961, 1964; MITCHELL, 1961, 1965 and others).

In this work we shall proceed with discussion of the problem on the causes of climate variations, using the data available on the transformations of solar energy in the atmosphere and at the Earth's surface.

When dealing with this problem we shall start with the survey of the empirical data on the climatic conditions of the past. As is well known, there are three main sources of such an information.

The most accurate data available on the climatic regime are those for the period of instrumental meteorological observations. Since mass meteorological observations with the help of instruments started in the second half of last century, this period does not exceed a hundred of years.

Some information on the climatic regime for the period of several thousands of years can be obtained from the data of non-instrumental observations presented in different historical sources.

And at last the data on the climate of remote ages of up to hundreds of millions of years can be found in the palaeographic investigations in which to determine the climatic conditions of the past the dependences of biological, hydrological processes and the processes of lithogenesis etc. on meteorological factors are used.

Interpretation of the data on the natural conditions of remote ages, for reconstruction of the climatic regime of that time, is connected with great difficulties some of which are of principle character. Among them, in particular, is the necessity to use the principle of actualism in such investigations. In this case it means to accept an assumption that the relations between climate and other natural phenomena in the past were the same as at the present time. Though such an assumption is not always unquestionable the variety of natural processes depending on climate makes it possible to verify independently the results of restoration of climatic conditions of the past by different palaeographic data. In this connection one can be sure of the reliability of the most general features of climatic conditions in the geological past that have been established in palaeographical investigations, though some particular results of these investigations are disputable and require additional study.

The main results of empiric investigation of the climatic conditions of the past can be presented as the following conclusions.

1. During the last several hundreds of millions of years the climatic conditions great-

ly different from the present ones have prevailed. During that time, except for the last relatively short quarternary period, the difference in temperature between the low and high latitudes was comparatively small. The temperature in the tropical latitudes was close to that of present time, and the temperature in temperate and high latitudes was much higher than that observed at present.

2. The development of considerable contrast in temperature between the equator and the poles began 70 million years ago, at the beginning of the tertiary period. This process developed quite slowly and till the beginning of the quarternary period (about a million years ago) the difference in temperature between the high and low latitudes was still far smaller than the present one.

3. In the quarternary period the temperature in high latitudes decreased sharply, which fact was connected with the formation of polar glaciation. The glaciation appeared in the northern hemisphere underwent considerable fluctuations in the course of which it increased several times, extending to the temperature latitudes, and then it receded again to the high latitudes. The last onset of glaciers in Euroasia finished about 10 thousands years ago and after that permanent ice cover in the northern hemisphere (except for mountain regions) remained only in the Arctic Ocean and on the islands of high latitudes.

4. In the post-glacial period the climatic conditions in the high and temperate latitudes changed several times in the direction of warming and cooling, which fact was connected with the corresponding variations of the polar ice area.

5. In the last century according to the instrumental observations the fluctuations of climate continued, warming taking place in the first half of our century that was particularly marked in the twenties and thirties. In the forties the warming stopped and cooling began but it does not achieve the size of preceding warming. The present climatic changes were most noticeable in the temperate and particularly in high latitudes of the northern hemisphere.

To explain the above features of climatic fluctuations, many hypotheses were suggested that connected the climate changes with various terrestrial and space factors.

Without aiming at the discussion of many suggestions on factors causing the climate changes, we shall dwell upon this problem basing on the data available and on the methods of physical climatology. In the course of this consideration causes can be singled out the effect of which on the climate changes is more or less evident. If these causes are sufficient to explain the above-mentioned regularities of climate changes, the use of additional hypotheses will not be necessary for interpretation of the phenomena under study.

It is generally known that the climate of the Earth is determined by the solar radiation coming to the outside boundary of the atmosphere as well as by the structure of the underlying surface. The previous widespread opinion that the atmospheric circulation is also a factor forming climate cannot be accepted, since the motions of the atmospherric air are one of the elements of climate and not an external factor with respect to climate.

Admitting that the given chemical composition of the atmosphere, the solar radiation and the structure of the underlying surface are the basic factors determining the climate, the meaning of term "the structure of the underlying surface" as a factor of genesis of climate should be explained.

It is evident that the climate genesis in the broad sense of the word involves not only the processes occurring in the atmosphere but also physical processes in the hydrosphere and the whole complex of hydrometeorological processes at the surface of land, including the development of glaciation if it takes place.

Thus, the underlying surface as a factor of genesis of climate should be understood as the relief structure determining the values of the surface and depth of seas and oceans, as well as the values of the continents surface and height. Though the change in the underlying surface due to, for example, glaciation can be considered as a factor of genesis of the given epoch climate in some particular investigations, when dealing with the problem in general it should be regarded as one of the climate elements which is caused by the same

external factors forming climate—the radiation income and the relief structure.

Now we shall dwell upon the question to what extent it is possible to explain the principal features of the climate change, taking into account the information on the change of factors of climate genesis.

Let us begin with the nearest period of instrumental meteorological observations for which there is a detailed information available on the climatic regime.

It is evident that during the period under consideration there were no changes in the condition of the underlying surface that could influence the climate of the Earth as a whole.

At the same time, as the analysis of the data on radiation regime shows, the solar radiation income to the lower atmosphere for the last century was not constant.

To clear up this problem, one can use the data on the secular radiation variation which were prepared by the results of actinometric observations from 1883 to 1920 by KIMBALL (1924), from 1910 to 1938 by WILLETT (see MITCHELL, 1961) and for the later period were supplemented with the data available at the Main Geophysical Observatory. These data characterize the average for a number of stations values of the intensity of direct solar radiation incident on a normal surface.

It is seen from the above-mentioned data that the direct radiation grew from the beginning of our century to the forties, increasing by about 5 %. Then its value began decreasing.

Apart from these comparatively slow changes, several shortterm but sharp decreases in radiation are clearly seen on the curve of the secular radiation variation. Four such decreases accounting for 12 to 22 % of the normal values of direct radiation took place at the end of the 19th and at the beginning of the 20th centuries. HUMPHREYS (1929) and other scientists have established that these decreases in radiation were observed after great volcanic eruptions of an explosive character, and as a result of them considerable amount of dust came to the lower stratosphere that remained there and was spread by stratospheric wind either over the whole planet or within the hemisphere where the eruption occurred. After the last of these eruptions that took place in 1912. (the Katmai volcano eruption on Alaska) there were no great eruptions for several decades and a new large eruption of explosive character occurred only in 1963 (the Agung volcano in Indonesia), the effect of this eruption on the radiation being less than that of the eruptions at the end of the 19th and at the beginning of the 20th centuries.

One can think that an increase in radiation in the twenties-thirties was explained by gradual purification of the atmosphere from the fine volcanic dust (WEXLER, 1953). The causes of the radiation decrease started in the forties are less clear. Probably, it was due to penetration of dust into the atmosphere from industrial air pollution that increased in those years.

It should be noted that a sharp increase in the atmosphere pollution during the last decades has been established in the experimental investigations by F. F. DAVITAYA (1965) and other authors.

Let us analyse the influence of the change in the solar radiation intensity on the thermal regime of the Earth. For this purpose we shall use the data on the variations of the annual mean temperature of the northern hemisphere for the period of 1881 to 1960, that have been prepared at the Main Geophysical Observatory. It must be pointed out that unlike the analogous calculations made by WILLET and MITCHELL who had averaged the results of observations at individual meteorological stations to study the secular variation of the Earth temperature, the above data have been obtained by using the maps of temperature anomalies which were made for each month of the period under consideration.

The analysis of this material shows that beginning from the end of last century to the end of the thirties of our century the temperature of the Earth gradually increases, this increase achieving about 0.6°. From the beginning of the forties the temperature began decreasing and by the end of the fifties it decreased approximately by 0.2° as compared to the period of maximum warming.

Alongside with these comparatively slow changes in temperature, on the curve of its secular variation there can be seen shortterm fluctuations reaching several tenths of a degree and relating to the periods of time of several months to several years.

HUMPHREYS (1929), ÅNGSTRÖM (1935) and other authors have established that such short-term decreases in temperature were observed, in particular, after volcanic eruptions of explosive character when a decrease in solar radiation income occurred.

Thus, the main regularities of the secular temperature variation are in good agreement with the regularities of the secular solar radiation variation. At the same time it can be found that the effect of short-term sharp decreases after volcanic eruptions on temperature fall is relatively lower than that of weaker but longer-term change of radiation in secular course.

The observed regularities of temperature changes can be explained quantitatively as a result of calculation determining the dependence of temperature of the Earth on the change of direct radiation.

In such calculation it should be established how the total solar radiation changes with a certain decrease of the direct radiation intensity. As numerous observations have shown the stratospheric dust, through the decrease of direct radiation. considerably increases the diffuse radiation. In this case due to prevailing diffusion of radiation on dust particles in the direction of falling ray (Mie effect) the increase of diffuse radiation compensates a considerable portion of the direct radiation decrease. If such a compensation were complete the change of atmospheric transparency would not influence the climatic conditions. On the basis of the results of calculations using formulae of atmospheric optics it is possible to say that in the given case the total radiation decreases, its decrease being about 10—20 % of the decrease in the intensity of direct radiation.

It should be borne in mind that, as it has been established by HUMPHREYS (1929), the stratospheric dust changing the shortwave radiation income almost does not influence the long-wave radiation due to small size of particles as compared to the corresponding wave-length.

In the works on climate theory (RAKIPOVA, 1966 and others) the solar constant decrease by 10 % has been proved to lower the mean temperature of the Earth approximately by 8°. Taking into account this result, we shall find that the increase of the direct radiation intensity by 5 % by the end of the thirties that corresponds to the total radiation increase by 0.5—1.0 % should result in the increase of the Earth temperature by 0.4—0.8°. This conclusion agrees well with the observational results mentioned above.

Let us estimate how the temperature of the Earth must change with comparatively short-term sharp decreases in radiation after volcanic eruptions. It is evident that in this case the changes of temperature will be less due to considerable effect of the heat inertia of the Earth when it is cooled for a short period of time.

Among factors determining the heat inertia of the Earth the change of heat content of the oceans is of greatest importance. The influence of oceans on the fluctuations of thermal regime of the Earth can be estimated empirically by the data on temperature changes over the oceans as a result of the annual variation of solar radiation.

The data available on the radiation and thermal regime show that in the regions of ocean situated far from continents the temperature of the upper water layers and the lower air layer decreases by approximately 1° with the decrease in radiation for 6 months by 10 %. Comparing this value with the above estimation of the effect of solar constant changes on the Earth temperature, it is easy to determine that the thermal inertia of ocean diminishes cooling for 6 months 8 times as compared to the value reached at stationary regime.

Taking into account that the dust of volcanic eruptions is maintained in the atmosphere in considerable amounts on an average for 1—2 years, the role of thermal inertia of oceans should be estimated for lowering radiation during that period of time.

Considering that under the influence of heat inertia of the ocean water the change of temperature in time with the radiation decrease is characterized by the curve of exponent type, the temperature decrease within a definite interval of its values can be considered to be approximately proportional to time. In this connection it should be concluded that if the radiation decrease by 10 % remained for 1—2 years the corresponding decrease in temperature of oceanic surface would be 2—4°.

As one can see, this value is 2—4 times as large as the corresponding value at stationary regime which fact can be considered as approximate estimation of the effect of oceanic heat inertia on the thermal regime after eruption. Taking into account this conclusion, we shall compute how individual eruptions of explosive type influence the mean temperature of the Earth.

If we assume that after an eruption of explosive type the radiation intensity decreases by 10—20 %, it should be considered that the total radiation decreases in this case by 2 %. If such a decrease were of significant duration it would lead to the decrease in temperature of the Earth by 1.6°. Since an appreciable decrease in total radiation after eruption takes place for 1—2 years the corresponding decrease in temperature should be 2—4 times less, i.e. it should have on an average the order of several tenths of a degree which is in good agreement with observational data.

In this connection a conclusion can be drawn that the climate changes during the last hundred years seem to be explained to a considerable extent by changes in the atmospheric transparency.

Basing on this conclusion some peculiarities of thermal regime fluctuations can be explained which have been established as a result of observations.

Thus, in particular, it is known that the thermal regime variations in the temperate and high latitudes were noticeably greater than analogous variations in the tropics. It is evident that analogous effect must have place with changes in atmospheric transparency since the optical thickness of the atmosphere increases with the growth of latitude as a result of which the dependence of radiation regime on the transparency conditions increases.

Now we shall proceed to the problem of causes of climatic changes in the geological past.

As paleogeographic investigations have shown, the relief of the Earth in the period of its geological history changed substantially the form and position of continents and oceans changing accordingly.

It follows from the investigations available that during the last several hundreds of millions of years the continents were lower and took smaller area than they do at present.

In the mesozoic period the sea that took the polar zone was connected with tropical oceans through wide straits providing free circulation of oceanic water. In the tertiary period these straits became more narrow as the land rose, though up to the middle of the tertiary period, alongside with connection of polar sea with the Atlantic there was a wide strait crossing along meridian the whole continent in the region of West Siberia.

With further rise of continents this strait disappeared and the Polar sea was mainly connected with the Atlantic Ocean and this connection gradually weakened as mountain ridges became higher at the bottom of the Northern Atlantic.

The change of conditions for the oceanic water circulation between the tropical and polar zones could be of decisive importance for the change of climate in high and temperate latitudes.

In the works on the theory of climate it has been established long ago that due to heat advection to the high latitudes the air temperature in the polar zone is much higher than that which could take place with the absence of advective heat income, i.e. under the conditions of "solar climate". In the investigations of the heat balance of the Earth it was established (BUDYKO, et al, 1962) that under the present climate conditions the meridional heat transfer in the hydrosphere is comparable by value with the analogous transfer in the atmosphere though it is smaller than the latter.

Thus, the changes in meridional heat transfer in the hydrosphere should affect considerably the climate of high latitudes.

In the works concerning the genesis of the arctic ice cover there was suggested a method for estimation of the influence of changes in meridional heat flux in the hydrosphere on the climatic conditions of polar zone (BUDYKO et al, 1962).

As a result of applying this method the above conclusion was confirmed that the temperature regime in temperate and, particularly, in high latitudes substantionally depends on the heat amount transferred by sea currents in meridional direction.

As is well known, under the existing conditions the annual mean difference in temperature between the equator and the North Pole is approximately 50°. As the calculations have shown, if the amount of heat given by the Gulf Stream and in the Northern Atlantic is transferred by sea currents to the polar area this difference will be only 15—20°. In this case the transfer of the corresponding heat amount to the high latitudes almost will not change the heat balance and thermal regime of tropical zone which fact is explained by the relatively small area of the polar zone as compared to that of tropics.

It should be indicated that a sharp growth of temperature in the high latitudes with increasing the meridional heat influx in the hydrosphere is explained to a considerable extent by inevitable melting of polar ice.

In this connection one can imagine the following picture of successive changes of climate that have taken place since the beginning of the tertiary period.

After a long period without strong meridional thermal contrast, that corresponded to the conditions of free water circulation between high and low latitudes. the temperature in high latitudes started decreasing in the tertiary period due to fall in meridional heat exchange in the hydrosphere.

As the computation have shown, with small income from sea currents the water temperature in the polar sea should approach the freezing point and then small additional cooling could cause the formation of ice cover.

Since the ice cover is characterized by great reflectivity for short-wave radiation it considerably decreases the amount of absorbed solar heat which fact results in further sharp fall in temperature over the ice surface.

For this reason in the quarternary period after the polar ice formation the mean difference in temperature between the pole and equator became several times as great as that in the previous periods, which corresponded to formation of the marked meridional thermal contrast that exists now.

The polar ice of quarternary period was very unstable and changed its surface both on the sea and on the land relatively quickly. The repeated onsets of glaciers on the land of the northern hemisphere gave place to their retreats which fact was connected with the corresponding temperature fluctuations.

The substantial cause of instability of ice cover was the presence of factors promoting its self-development. Among these factors, beside the decrease in temperature over ice, is the proportionality of solid precipitation income on the surface of a large ground glacier to its area with the proportionality of loss for ablation to its perimeter.

Without going into details of the theory of quarternary glaciation dynamics we shall note that this dynamics seemed to depend substantially on the solar radiation changes caused by the atmospheric transparency fluctuations.

Some conclusions can be drawn on the influence of eruptions on the climate of the past, basing on the above data on the effect of volcanic eruptions on the radiation income and thermal regime under present conditions.

To this end we shall mention the following important regularity of the influence of volcanic activity on thermal regime of the Earth. If the influence of individual eruptions on the Earth temperature is comparatively small due to limited amount of dust that comes to the atmosphere after each eruption then it is evident that the temperature of the Earth will change far more greatly at coincidence of many eruptions of explosive type for short intervals of time. The possibility and inevitability of such coincidences during long periods of time is a consequence of general statistical regularities.

If we consider individual eruptions to be independent of each other it can be shown that the ratio of maximum number of eruptions for some interval is equal to square root of the ratio of duration of the period under study to the duration of the given time interval.

For the last century there have been four great eruptions of explosive type, which corresponds to the mean frequency of eruptions of 0.2 for five years. If we assume that such frequency corresponds to the mean for long periods of time we shall find that maximum number of eruptions for one century for the period of 10,000 years will reach 40, and for 100,000 years about 130.

Under the same conditions the maximum number of eruptions for five years will be

approximately 100 for the period of 1 million years, and several hundreds for periods of tens of millions of years.

A question of possibility to apply such an approach to estimation of maximum number of simultaneous eruptions for longer periods of time requires additional discussion as in this case the number of eruptions becomes comparable with the number of existing active volcanoes. Though it is well known that in the epochs with higher volcanic activity the number of active volcanoes was considerably larger than it is now, for the purposes of this work it is enough to use only the estimates given in this paper.

Let us consider the question how the temperature of the Earth should change at coincidence of many volcanic eruptions.

If during hundred years 50—100 eruptions of explosive type take place the order of their influence on the thermal regime can be approximately estimated basing on the fact that in this case the direct radiation will decrease by 10—20 % during the whole century.

In accordance with the above calculation for stationary conditions the mean air temperature showed decrease in this case by about 1—3°. Considerable changes of radiation will take place at the coincidence of tens or hundreds of eruptions during five years.

Using the above-mentioned formulae for the estimation of the atmospheric transparency effect on radiation it can be established that the coincidence of several tens of eruptions during 5 years will decrease the direct radiation, as compared to the norm, 3 to 5 times and the total radiation by 10 to 20 % in the low latitudes and by somewhat larger value in the high ones.

When several hundreds of eruptions coincide for 5 years a dust sheet appears which, according to calculation, will be practically impenetrable to direct radiation. In this case the total radiation in the low latitudes decreases by approximately 50 %, and in the high latitudes by 80 % and more. Under such conditions the temperature of the Earth could decrease by a value of 10° and even by larger values.

Taking into account the estimates mentioned above one can conclude that the volcanic activity many times led to a decrease in the mean temperature of the Earth for a century by several degrees for the period of time of hundreds of thousands of years. The value of decrease in temperature was larger in the higher latitudes and smaller in the low latitudes.

It should be noted that such a conclusion can be of great importance for explanation of the origin of quarternary glaciations. As it has been established in the above calculations, the shape of relief and the position of the coastline of continents formed by the beginning of the quarternary period created possibility of formation of ice cover in the high latitudes with a comparatively small general decrease in the air temperature.

The formation of this ice resulted in a sharp additional decrease of temperature in the high and temperate latitudes, which was a precondition for the development of quarternary glaciations.

With the above mentioned high instability of polar ice the relatively small temperature decreases as a result of volcanic activity had to increase considerably the area of sea ice and promote the formation of ground glaciations. Long periods of low volcanic activity led to warming during which the ice cover on the land and seas retreated. New volcanic activity could result in resumption of glaciation.

If in the quarternary period, when the heat transfer by sea currents to the high latitudes was small, the decreases in temperatures as a result of eruptions led to glaciations, in the earlier period such decreases could not create lasting changes in climate.

However, it can be supposed that if a decrease in temperature in the prequarternary time did not influence for a long period of time the climatic conditions they still could be of great importance as a factor affecting the change of successive faunas during the history of the Earth.

As modern palaeontologic investigations have shown, the different biological groups of animals belonging to different oceological types often died out simultaneously. Thus, in particular, most of extinct orders and suborders of reptiles and amphibians vanished during three critical moments of geological

history corresponding to the ends of Permian, triassic and cretaceous periods.

It should be pointed out that all these three periods of geological history took place in the epochs of high volcanic activity when the probability of simultaneous eruptions of a large number of volcanoes was the greatest.

A considerable peculiarity of reptiles and amphibians is, as is well known, the absence of thermal regulation, which fact makes these animals particularly sensitive to temperature regime. As we have noted above, the climate of the end of palaezoic and mesozoic times was characterized by homogenous thermal conditions, higher temperature in the low latitudes as compared to the present epoch, and by much higher temperature in the extra-tropical regions, which fact created favourable conditions for the existence of animals throughout the Earth that have no thermal regulation.

Without dwelling upon the problem of extinction of dinosaurs and some other groups of animals in the indicated epoch, we shall note that in spite of the large number of investigations on this question palaeontologists consider that this problem has not yet been solved.

One can suppose that the short-term sharp decreases in temperature at coincidence in time of many volcanic eruptions that are inevitable for periods of tens of millions of years, could be a sufficient cause for dying out of animals not adapted to such cooling.

Thus, we have analysed in the present paper two factors one of which is associated with the atmospheric transparency fluctuations, and the second factor with the changes in the relief in the geological past.

The effect of both of these factors on climatic conditions can be established as a result of quantitative calculations, the obtained results being in agreement with the data observations of current climate fluctuations and with palaeographic materials on climates of the past.

In the light of the results presented here it is possible to explain the basic regularities of climate changes mentioned at the beginning of the paper by the effect of only the two indicated factors. Such a conclusion does not exclude the possibility of influence of many other causes on the change and fluctuations of climate. It must be, however, supposed that the effect of these causes, if it takes place, occurs on the background of climatic changes caused by the factors considered.

REFERENCES

BUDYKO, M. I., 1949, The heat balance of the northern hemisphere. *Trudy G.G.O., vyp. 18.* (in russian).

BUDYKO, M. I., 1962, Polar ice and climate. *Izvestia AN SSSR, ser. geograf. No. 6.* (in russian).

DAVITAYA, F. F., 1965, On possible influence of the dusty atmosphere on reduction of glaciers and climate warming. *Izvestia AN SSSR, ser. geograf. No. 2,* pp. 3—28. (in russian).

FLOHN, H., 1961, Man's activity as a factor affecting the climate change. Solar variations, climatic change and related geophysical problems. Ed. R. W. Fairbridge. *Annals of the N. Y. Academy of Sciences, V. 95,* Art. I.

FLOHN, H., 1964, Grundfragen der Paläoklimatologie im Lichte einer theoretischen Klimatologie. *Geologische Rundschau. B. 54,* pp. 504—515.

HUMPHREYS, N. J., 1929, *Physics of the air.* Second edition. McGraw-Hill Book Company. N.Y.

KIMBALL, 1924, Variation in solar radiation intensities measured at the surface of the Earth. *Monthly Weath. Rev. V. 52,* pp. 527—529.

MITCHELL, J. M., 1961, Recent secular changes of global temperature. Solar variations, climatic change and related geophysical problems. Ed. R. W. Fairbridge. *Ann. of N. Y. Academy of Sciences, V. 95,* Art. I, pp. 235—250.

MITCHELL, J. M., 1965, *Theoretical palaeoclimatology.* The Quarternary of the United States. Princeton University Press, pp. 881—901.

RAKIPOVA, L. R., 1966, The change of zonal temperature distribution in the atmosphere as a result of active climate modification. Modern problems of climatology. Ed. M.I. Budyko. Gidrometeoizdat, Leningrad, pp. 358—383. (in russian).

WEXLER, H., 1953, Radiation balance of the Earth as a factor of climatic changes. Climatic change: evidence, causes and effects. Ed. H. Shapley. Harvard University Press. Cambridge, pp. 73—105.

ÅNGSTRÖM, A., 1920, Applications of heat radiation measurements to the problems of the evaporation from lakes and the heat convection at their surfaces. *Geog. Ann., B II,* pp. 237—252.

ÅNGSTRÖM, A., 1925, On radiation and climate. *Geog. Ann., B VII,* pp. 122—142.

ÅNGSTRÖM, A., 1935, Teleconnections of climate changes in present time. Geog. Ann., B XVII, pp. 242—258.

Direct solar radiation and aerosol structure of the atmosphere from balloon measurements in the period of IQSY

By K. Y. KONDRATYEV and G. A. NIKOLSKY, *University of Leningrad*

ABSTRACT

The results of the actinometric balloon sounding V. 1962-XI. 66 are used to analyse the irregularity of extinction of the direct solar radiation in the troposphere and stratosphere. The beginning of this period is characterized by the great extinction (up to 8 %) above the sounding level; later the influence of the "upper" extinction becomes somewhat less but there appears another source of extinction, that is, volcanic dust.

The aerosol structure of the atmosphere up to the heights of 30 km and its relationship to the temperature profile are discussed. The solar constant for the period studies is evaluated.

1. Introduction

In recent years the collaborators of the Department of Atmospheric Physics, the University of Leningrad, have carried out an extensive programme of balloon actinometric soundings of the troposphere and lower stratosphere. One of the main purposes of the investigations was a study of the vertical profiles of solar radiation (S) and aerosol.

Data on S values at various heights are accorded due attention since from the vertical profile of the direct solar radiation one can determine not only extinction values of S and the radiative flux divergence due to the absorption of solar radiation but also obtain the notion on the aerosol structure of the atmospheric portion sounded. Besides, the S measurements in the stratosphere allow one to understand the reasons of anomalous changes in transparency for both the atmospheric portion sounded and the layers above. Upon obtaining sufficient amount of data one can evaluate the solar constant and its variations.

Since the balloon measurements of S are usually followed by filter measurements in the ultraviolet and by humidity measurements we have the opportunity to obtain the aerosol extinction component vertical distribution in the atmospheric layer investigated (KONDRATYEV, NIKOLSKY, and ESIPOVA, 1966).

The present paper treats the data obtained in 1962—66 to find out the peculiarities in the extinction of the direct solar radiation occurring in the period of the International Quiet Sun Year (I Q S Y).

2. Instrumentation

Since 1965 the measurements of the direct solar radiation have been conducted using a sealed-in actinometer with a quartz window. Simultaneously an exposed actinometer was raised. These simultaneous measurements permitted us to specify the pressure correction of the actinometer which was introduced in the data of 1962—64 measurements. The S values with the old pressure correction were overestimated (KONDRATYEV, NIKOLSKY, and ESIPOVA, 1966).

Block-scheme of automatic device for a continuous measurement of the direct solar radiative flux is represented in Fig. 1. The biaxial pointing control (5) permits simultaneous measurement of the direct solar radiation with two actinometers. This possibility was used to obtain pressure correction. The radiation detector-actinometer (1) receives solar radiation through the quartz window (2) which was carefully examined to determine the dependence of transmission on the incident light wavelength. In the 0.25—3.0 μ spectral range the window

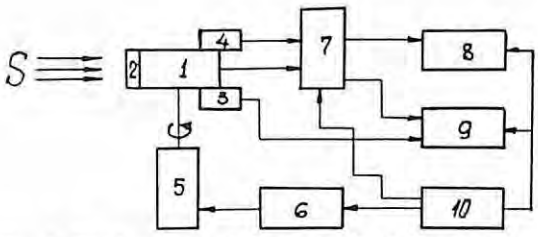

FIG. 1. Block scheme of the device for the automatic measurement of the direct solar radiation flux from a balloon. 1.—sealed-in actinometer, 2.—quartz filter, 3.—pressure control, 4.—temperature control, 5.—automatic biaxial solar pointing control, 6.—control block of biaxial pointing control, 7.—commutation and checking block, 8.—recorder of electric quantities, 9.—optical recorder, 10.—power supply.

transmittance is practically constant, e.g. 94 %. In the wavelength range smaller than 0.23 μ the transmittance slowly falls but this does not affect the results as even at the 32—33 km heights the radiation intensity at $\lambda < 0.23$ μ is small (KONDRATYEV, 1965).

The radiation detector is installed into the hermetic shell which is coupled through a flexible vacuum-wire with the controlling device (3) allowing the determination of variations in a fixed pressure value inside the shell from the marks on the recorder band (9). For measuring detector temperature the platinum resistance thermometer (4) is fastened to its back part and through the programme-block (7) switched to the recorder of electrical values (8).

Since the detector sensitivity is dependent on its body (cold junctions) temperature we had to investigate this dependence for a set actinometers. The mean dependence of sensitivity on body (cold junctions) temperature for several instruments is 0.09 % per degree.

The recording of S values on the optical recorder tape (9) was continuously conducted during the entire ascent and drift (up to 3.5 hours). Zero position of the recorder galvanometer (electrical zero) was checked every minute. The optical recorder has thermostabilization.

The actinometers were repeatedly calibrated by the sun, i.e. indirectly checked with the U.S.S.R. reference standard.

The accuracy of absolute S measurements is within the range of 2.5—3 % for 1962—64 flights and about 2 % for 1965—66 flights. Errors in measurements are composed of the errors in the consideration of environmental temperature and pressure influence (for 1962—64 data), nonconsideration of the instrumental selectivity and the errors in the comparison with the standard. It is natural that in the comparison of subsequent vertical profiles of radiative fluxes the errors considerably decrease since in most cases the same measuring instruments are used.

3. Results of measurements

Consider the general peculiarities of vertical profiles of the direct solar radiation in the troposphere and stratosphere from the data of 11 flights (Fig. 2). Soundings were carried out in the middle belt of the European part of the U.S.S.R. The S values were reduced to the mean distance between the earth and the sun.

Variations in S at different heights are chiefly related to the difference in solar elevations (data are not reduced to a certain solar elevation either within the flights or between them) and to that in extinction properties of air masses within the flight period.

Maxima of S in the troposphere and stratosphere up to the heights of 22 km were derived in summer in the noonday (curves 9, 12). The corresponding S profiles are most bent, the drastic growth in the lower troposphere being accompanied by a slight increase in the stratosphere. Profiles 11 and 15, with their minima of S have been obtained at small solar elevations (17° for profile 11 and 20° for profile 15 in the lower troposphere). These profiles are less bent because the change in air mass in the path of a ray occurs more smoothly with ascent.

This variation in S at small solar elevations must lead to higher autumn temperatures in the upper stratosphere and mesosphere (due to absorption of solar radiation), summer temperature at these levels must be much lower than in autumn.

Profile 15 obtained in the morning summer hours with rapidly increasing solar elevation

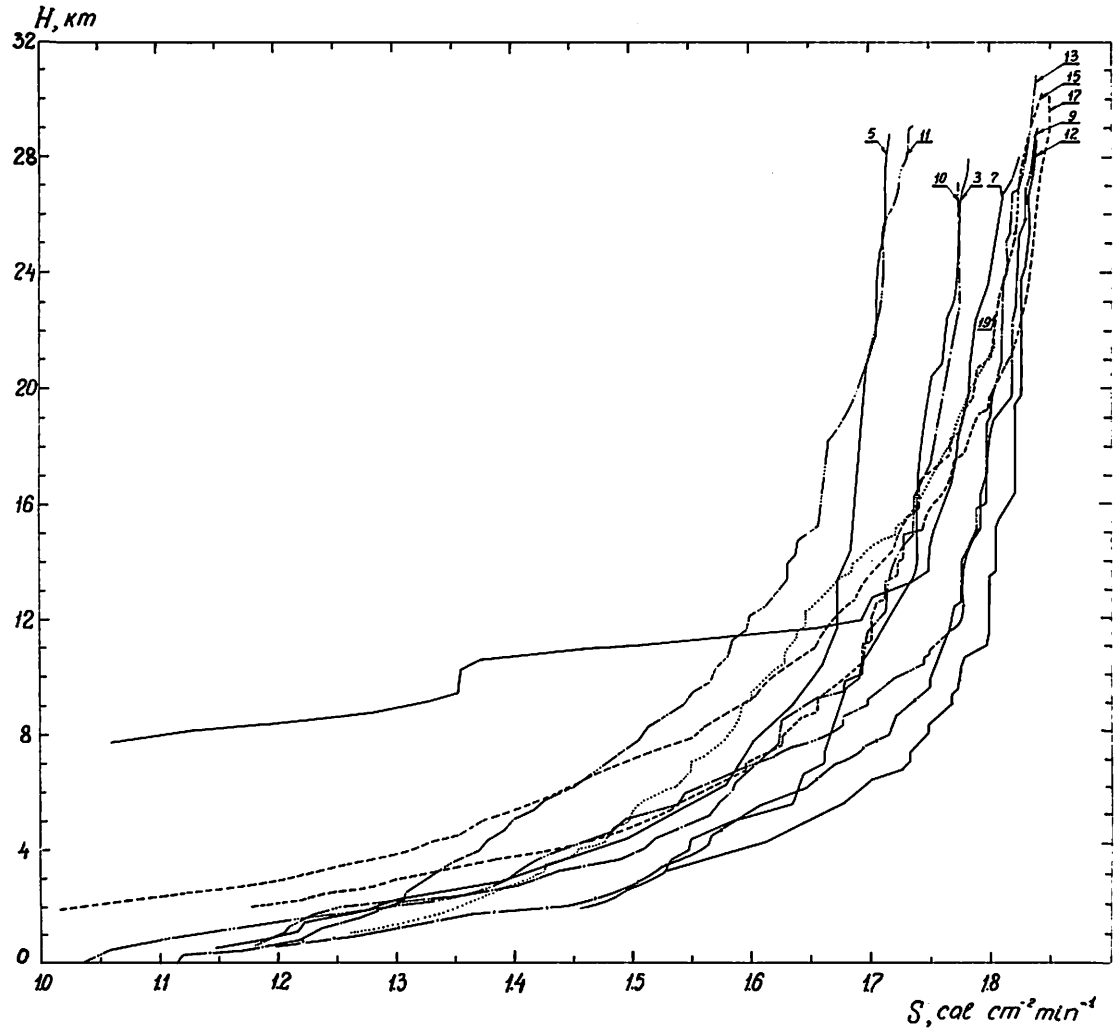

FIG. 2. Vertical profiles of the direct solar radiation fluxes from eleven flights, 1962—65. Flight 3—May 25, 1962, 5—June 5, 1962, 7—June 22, 1962, 9—July 7, 1962, 10—July 12, 1962, 11—Nov. 22, 1962, 12—July 6, 1963, 13—July 19, 1963, 15—July 11, 1964, 17—Oct. 23, 1964, 19—Oct. 21, 1965

indicates the intensive air heating with its subsequent attenuation (in the case of summer season after a sunrise in the upper stratosphere).

Thus in summer, in the stratosphere, the morning heating wave is to be observed shifting to the west, with the sun rising over the horizon.

One should note the peculiarity of the variation in some stratospheric profiles (3, 5, 10 etc.) which is expressed in their distinction from the general variation. The upper branch of the curves (Fig. 2) has the limiting value 1.85 cal/cm²min., the lower one tends to 1.795 cal/cm²min. The occurrence of the lower branch indicates either a decrease in the transparency of the medium between the radiation detector and a source or the change in radiant intensity of the source.

The limiting value of the upper branch (1.85 cal/cm²min) which can be regarded as "normal" for the period under consideration

(1962—66) is far smaller than the calculated value (1.94 cal/cm²min.) therefore, the whole period should be considered anomalous.

M. I. BUDYKO (1966) having compared the annual means of S for 1958—59 and 1964—65 from the data of the U.S.S.R. actinometric stations has found a decrease in annual means by 0.09 cal/cm²min. If the cause of the anomalous phenomena considered is supposed to be the same their appearance should be refered to the end 1959—spring 1962.

In the troposphere profile 7 markedly differs from others. The peculiarity of the variation in this profile is associated with the presence of two-layer semitransparent cloudiness at the heights of 7.5—12 km on the day of sounding. Cloud layers are separated by a transparent interval at the heights of 9.5—10.25 km.

Now, consider summer profiles in greater detail. Profiles 5, 7, 12, 13 were obtained at close solar elevations $h_\odot$ (about 56°), yet, the difference in S at the height of 28 km attains 0.125 cal/cm²min. In the lower stratosphere the discrepancy is also large. Lowered values in flights 3, 5, 10 can be explained only by anomalous attenuation of the direct solar radiation above the level of sounding. In the troposphere the anomalous attenuation is blurred (profiles 3 and 12), at this the inverse phenomenon is possible at which the S values are close at the height of 27—30 km but noticeably differ in the troposphere (curves 12 and 13).

From the S summer profiles as represented in Fig. 2 profile 9 may be considered typical for the 1962—64 period. It characterizes some mean atmospheric condition, whereas profile 12 describes a comparatively pure and cool air mass (above 3 km). The comparison of profile 12 at the levels above 23 km with autumn profile 17 as obtained at $h_\odot = 23°$ shows that the S values are not sufficiently large in flight 12, i.e., that in this period (1963) also exists anomalous attenuation with the source of attenuation situated much higher than the upper point of sounding. Further it will be shown that S values in flight 17 are also smaller than those calculated for a given situation if one proceeds from the solar constant $S_0 = 2.00$ cal/cm²min.

Profile 13 is of interest since it characterizes attenuation properties of a very humid air mass (4.7 cm of precip. water) which reached the height of 16 km and more. Most strong attenuation in this case is marked in the lower 1.5 km tropospheric layer.

All the above-mentioned vertical S profiles possess characteristic step arrangement which is most pronounced at the heights of 8—20 km. Work (KONDRATYEV, NIKOLSKY, and ESIPOVA, 1966) shows that the main part in the stratospheric layer attenuation is played by atmospheric aerosol being arranged in separate layers. From profile 12 one can distinctly see that between the attenuating layers the optically pure air is situated. The presence of the aerosol component in the stratosphere is recorded during the 1962 (3, 9, 10) and 1963—64 flights.

Autumn profiles of the direct solar radiation are reproduced in the Fig. 3. Summer profile 15 as obtained in early morning at small solar elevations (22°42'—38°52') is added to the five autumn profiles. The air mass on that day (July 11, 1964) was comparatively humid (3.57 cm. of precip.water).

During autumn flights the solar elevation varied over a range:

flight N11 Nov. 22, 1962 $h_\odot \approx 16.5°$—17.7°
N17 Oct. 23, 1964 $h_\odot \approx 26.3°$—22.5°
N18 Oct. 1, 1965 $h_\odot \approx 33°$ —35°
N19 Oct. 21, 1965 $h_\odot \approx 27°$ —24.2°
N20 Nov. 15, 1966 $h_\odot \approx 18.6°$—17.5°

The variation in vertical profiles of the direct solar radiation in the troposphere fully reflects the dependence of S attenuation on humidity and turbidity of the air mass on the day of sounding. The smallest values as seen from Fig. 3 were obtained in flight 15 at solar elevations 23°—26°, which is connected with the increased humidity and turbidity of the lower 6 km layer (compare flights 11 and 15). Profile 17 being situated to the right of profile 15 but below the level of 4.5 km, the values of S^{17} are small (compare to profile 11, 17, 19).

Visual aircraft observations and the analysis of the values of shortwave radiation fluxes testify for the strong turbidity of the lower troposphere on Oct. 23, 1964. Profiles 11 ($h_\odot = 16.5°$) and 19 (27°) correspond to the comparatively pure lower troposphere.

It is interesting to compare profiles 17 and 19 as obtained at the same solar elevations but in different years. The difference in S

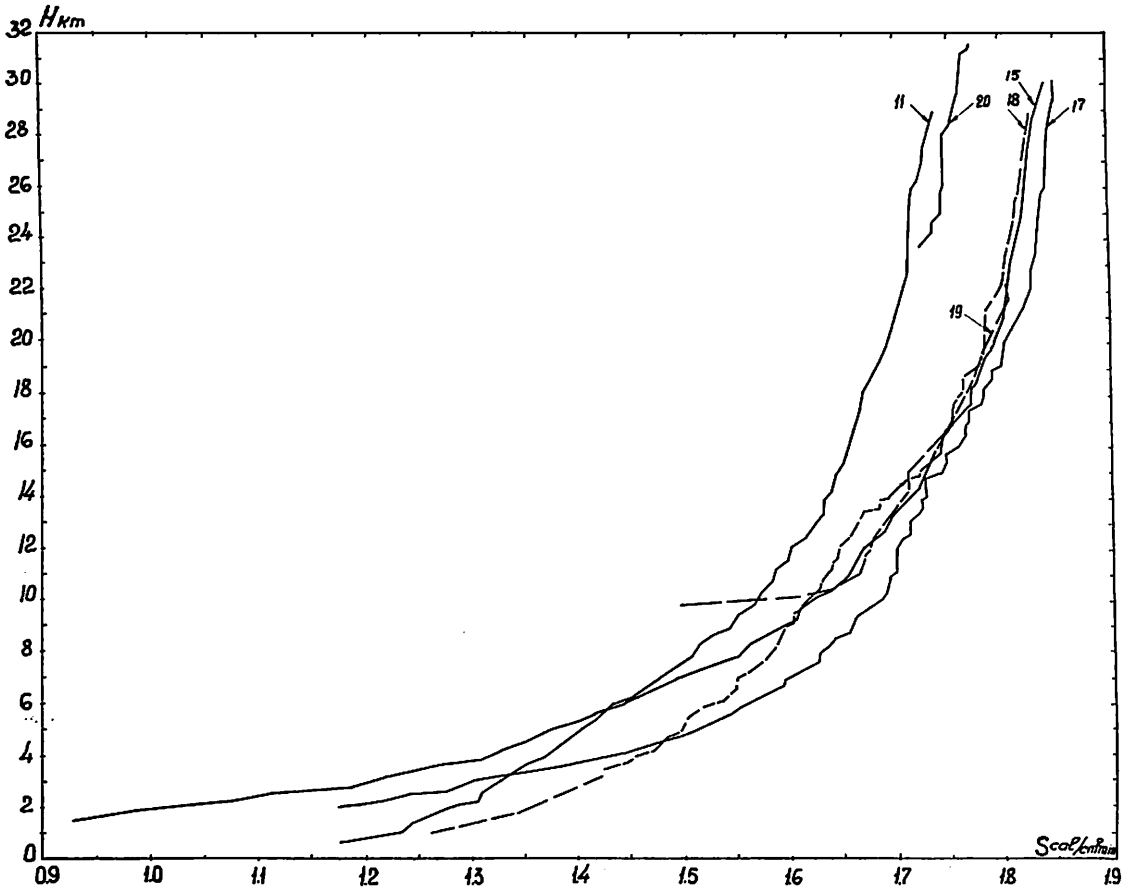

FIG. 3. Vertical profiles of the direct solar radiation fluxes from autumn flights, 1962—66.

corresponding to profiles 17 and 19 in the lower troposphere has been discussed ($S^{17} < S^{19}$). For the upper troposphere we have the reverse picture: $S^{19} < S^{17}$) at the same heights. Such a variation in S for flight 19 is due to the increased attenuation in the 13.5—15 km layer and the decreased S values in the upper troposphere accordingly (redistribution of attenuation).

The general resemblance of stratospheric profiles is, mainly, explained by small solar elevations; their individual peculiarities—by the differences in the attenuating properties of the stratospheric air and the anomalous attenuation in higher atmospheric layers.

The cases described by profiles 11 and 20 (solar elevations are of the order of 17.5°) are characterized by the pure air mass at all the heights of the layer of sounding. The difference in S for the heights of 24—29 km is associated with the additional attenuation in the upper atmosphere characteristic of 1962.

Stratospheric profiles 15, 17, 18 and 19 above 15 km form a compact group, which on the one hand, can indicate the weak dependence of the radiative flux on the solar elevation for $h_\odot > 30°$. If we assume this to be true, then $S^{17}_{29\,\mathrm{km}} = 1.85 \frac{\mathrm{cal}}{\mathrm{cm^2 min}}$ can be regarded as the possible maximum for the heights of 29—30 km. On the other hand, since the $h_\odot$ difference in flights 15, 18 and 19 attains 10° the mentioned proximity of the profiles can be thought to be, to a certain extent, accidental and held as a consequence of the effect

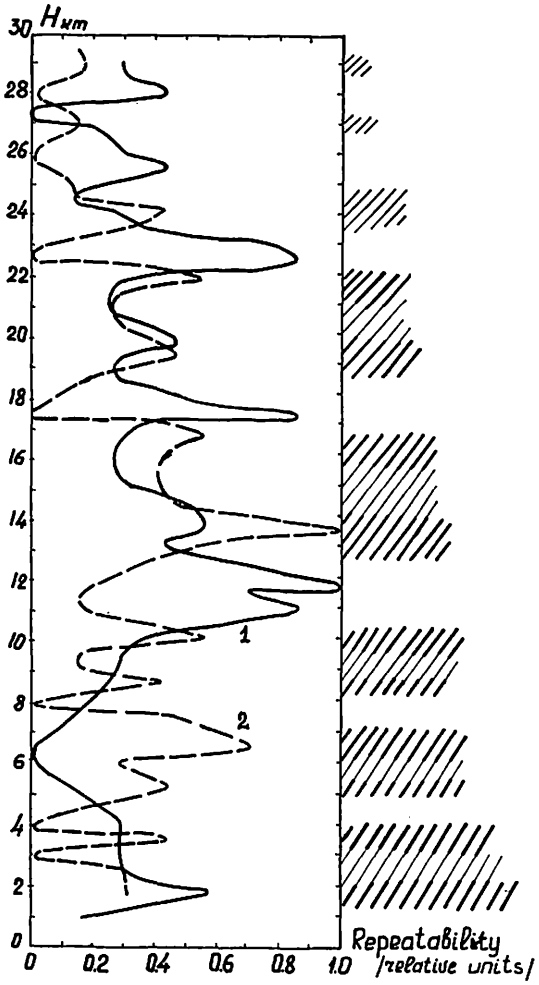

FIG. 4. Comparison for frequencies of attenuating layer and air temperature inversion occurrences at various heights from 16 flights.
1.—curve for frequency of inversion occurrences.
2.—curve for frequency of attenuating layer occurrences.
Zones for most probable occurrence of layers are marked attenuating by slope lines on the right, thickened lines marking central parts of these zones.

of some outer factors variable in time. By the outer factors one can understand both the solar radiation attenuation by the dust matter of the cosmic origin and variations in the solar constant.

The values derived in flight 17 are larger than any other summer values for the height of 23 km and more, and larger than autumn values for the level of 4.5 km and upwards. Further it will be demonstrated that the stratospheric S^{15} and S^{19} values are, at the same heights, larger than those for the 1962—63 flights.

Detailed examination of autumn profiles in the 8—22 km layer shows the presence of stepped (through the layers) attenuation. The change is observed only in the height of the location of the attenuating layers and in their power (the parameter characterizing the vertical layer extension and its turbidity is understood by the power of attenuating layer). Layering is marked not only for the mentioned layer 8—22 km but also for other heights. Yet, the layering structure is most pronounced for 8—22 km.

Through the layers attenuation as represented by profiles 18 and 19 is far stronger than for other flights. From profile 18 one can detect four powerful layers whereas from profile 19—only one 12.5—15 km layer. The occurrence of anomalous attenuation for these two cases is associated with the eruption of the Taal volcano, Sept. 28, 1965. The additional stratospheric attenuation of the direct solar radiation by the volcanic dust on Oct. 1, 1965 was 4.3 % and in 20 days —3.6 %. For flight 17 the layering is rather distinct but the power of layers is markedly smaller (aerosol stratospheric attenuation is less than 1 %).

The comparison of profiles 17 and 19 demonstrates that from the surface observations one can obtain the erroneous idea on the S stratospheric attenuation and miss the anomalous stratospheric turbidity (for example, profile 19) if the information on the aerosol content in the atmosphere and its distribution with altitude is not available.

The least turbid air for the entire layer of sounding was fixed in flight 11 (Nov. 22, 1962), which is confirmed by weakly pronounced stepped arrangement of the profile.

Analysing the peculiarities of the vertical structure for the attenuating layers it is interesting to study its interaction with the specific character of the arrangement of inversion levels. This tropospheric and stratospheric interaction was singled out while comparing the heights of inversion zones with those of the attenuating layers. Aerosol attenuating layers are usually located above

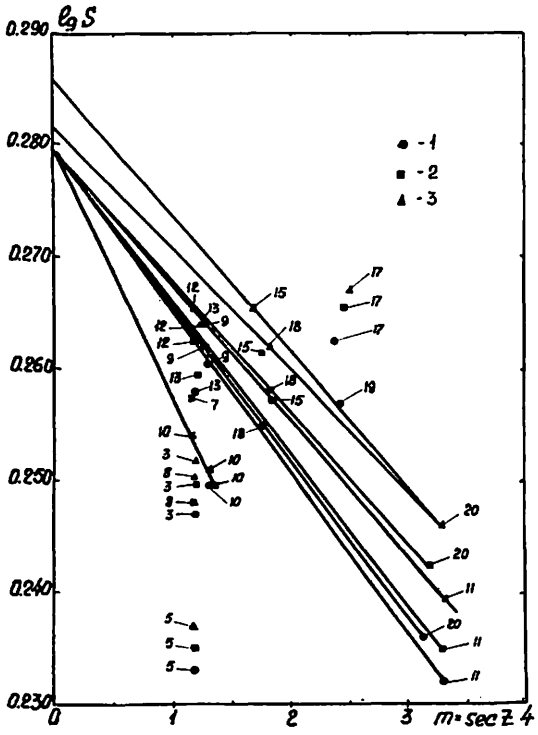

FIG. 5. Logarithmic dependence of the direct solar radiation flux on the atmospheric mass from 1962—66 flights.
1 (○)—data for 22 km.
2 (□)—data for 26 km.
3 (△)—data for 29 km.

or below inversion levels (Fig. 4). Similar location is most pronounced in the upper troposphere and the lower stratosphere. The curve of the probability of the occurrence of aerosol layers at a given height has three basic maxima in the stratosphere and two in the troposphere. Most often aerosol layers arise at the heights of 2—4 km, 6—10 km, 12.3—17 km, 18.6—22.4 km, 23.2—25 km.

The maxima for these zones are situated at the levels of 3.5 km, 6.5 and 10 km, 13.5 and 16.5 km, 19.2 and 21.8 km, 24 km (basic zones possess two centres; the main, over-inversional, is in the lower portion of the zone and the additional, subinversional, is in the upper portion of the zone). Such a structure of aerosol layers suggests the existence of two mechanisms for the particle transfer at these heights: gravitational settling and turbulent diffusion. With this, the turbulent diffusion effect is limited by the local layer boundaries. Mixing in large vertical extensions in the stratosphere does not occur (DYER, 1966). Most flights intended for the analysis of the tropospheric and stratospheric aerosol structure have been conducted in the anticyclonic situation at various stages of the development of this baric formation. The suggested scheme for the layer structure of the upper troposphere and lower stratosphere is directly connected with the dynamical processes in this part of the atmosphere. These problems are treated in greater detail in publication (NIKOLSKY, BADINOV, and LIPATOV, in press).

Atmospheric investigations up to 70 km with a searchlight method by L. ELTERMAN (1966), April—May 1964, showed that the maxima for the aerosol component density are at the heights of 5 and 9 km in the troposphere and of 15.6 (12—23 km layer) and 26 km in the stratosphere.

The comparison of these data with the balloon results shows that the resolution with height in the searchlight stratospheric sounding is not sufficient since the separation of the 12—23 km layer is not fixed. This comparison also permits one to judge on the resemblance of the aerosol structure of the lower stratosphere over two continents.

Let us return to the analysis of the direct solar radiation fluxes and consider the S values dependence at the heights of 22,26 and 29 km on the solar elevation. The heights referred to are chosen in such a manner that one might get rid of local influences while estimating the possible reasons of global changes in the optical properties of the stratosphere. Fig. 5 illustrates the data of most successful flights to establish the dependence of lgS on $m = \sec Z_{\odot}$ and extrapolate the dependence derived beyond the atmosphere. It is seen from this figure that the optical state of the upper atmosphere varies over a large range, which is evident from the different-slopes of the lines. More stable conditions are characteristic of the 1963—66 period as compared with 1962. In 1964—65 the cases of anomalous transparency (17, 19) were noticed as compared with the mean condition of the upper atmospheric transparency

in 1962—66 which, in turn, can be considered much worse if the solar constant is supposed to be $S_0 = 2 cal/cm^2 min$. Data for 1962 are at the level of the means (9, 11), the basic portion of profiles (3, 5, 7, 10) giving the small S values. From 1963 flights (12 and 13) the S values at 29 km are found to be close to means. From 1964—66 flights two give the means of S (18 and 20) and three show the S values at 22, 26 and 29 km to be larger than the means (15, 17 and 19).

In the determination of the dependence of lg S on m, first, the S values for a certain height with close values for the atmospheric mass m have been considered.

The arrangement of S values at 29 km, flights 11 and 20, suggests the lack of any dependence on mass. S values for flight 20 are much larger than for flight 11 which shows the difference in transparency for higher atmospheric layers on these days. Similar conclusion can be made for S values for flights 15 and 18, 17 and 19 (for $H = 22$ km).

The lg S on m dependence can be preliminarily assumed to be linear since at the considered heights for the 0.2—4 μ spectral range the selective absorption (ozone, water vapour, oxygen) is small and the main part of the attenuation is determined by the scattering by air molecules and aerosol particles. The second reason allowing one to state that the lg S on m dependence is close to linear lies in the fact that the linear dependence is "minimizing" from the viewpoint of the obtained values of the solar radiation flux. If one takes into account possible nonlinear dependlence it will be clear that in this case S_0^{extrap} will not exceed 1.95° cal/cm²min (lg $S = 0.29$).

The values for the direct solar radiation flux applied for detecting the lg S on m dependence have been obtained in different seasons and, for most cases, in the noonday. Therefore, the change in solar elevation during the flight is usually small. Various versions of extrapolation have been tested and those leading to real S_0^{extrap} values chosen.

Analyzing the above results one can make certain that the values of the direct solar radiation fluxes as obtained in 1962 attain, at best, some mean level (flights 9, 11) being, for most cases, considerably lowered (flights 3, 5, 6, 8, 10). The reasons of this anomaly are not quite known but one can suppose the anomalous attenuation to be associated with the effect of high-altitude atomic explosions on the upper atmosphere. The comparison of the balloon S data with the time of high-altitude explosions (Willard and Kenney, 1963; Menon, Menon, and Kuroda, 1963) shows the S attenuation to increase after the explosion reaching maximum in five—six days. The value for the additional after explosion attenuation varies from 2 to 8 %. The strongest effect was exerted by the explosion about May 25, 1962 (8 %).

Raghavan and Jadav (1966) from the data of pyrheliometric observations gives the S attenuation values by aerosol component for the years of 1961—65. The increase in radiation attenuation, approximately, as much as 2 times had been observed since April, 1962. The atmospheric turbidity for 1963—65 was much higher as compared with 1961.

Flight 13 demonstrates somewhat lowered values relative to the mean level as determined by flights 9, 11, 12. The lowering might have been caused by the high meteor activity for May—August 1963 (McIntosh and Millman, 1964). The solar radiation attenuation above 29 km for the 1964 flights (15, 17) is less than for previous years. The maximum S values for the entire period of soundings have been derived in flight 17.

The values for the solar radiation flux as obtained in 1965—66 (flights 18, 19, 20) suggest higher turbidity of the upper atmosphere for autumn seasons of this period as compared with 1964. Somewhat lowered S values for flight 18 as compared with flight 19 must have been caused by the eruption of the Taal volcano, Sept. 28, 1965.

The data on the direct solar radiation attenuation and the twilight glow intensity for October 1965 as presented by F. Volz (1966) confirms the dust occurrence in the stratosphere over Europe and the Hawaiian Islands. F. Volz does not single out the October 1965 data (Bergen, Wissenau) seen on the falling branch of the maximum of the twilight glow intensity as fixed at the end of July and August and does not notice the direct connection of European data with

that obtained on Hawaii. Explaining the occurrence of the August maximum by the volcanic dust transfer from the southern hemisphere F. VOLZ suggests that the interchange between the hemispheres occurs only late in summer, whereas our data shows that the stratospheric (16—30 km) meridional transfer from the equator reservoir starts in September proceeding in October.

We believe there is a number of reasons giving rise to an increase in twilight glow. The balloon data shows that the volcanic dust is chiefly concentrated in the lower stratosphere and, consequently, only for some individual cases responsible for the perturbations in twilight glow.

During flight 19 the data only up to 22 km was obtained but even at this height the S values show the atmospheric transparency above 22 km to exceed the mean level, though being somewhat lower as compared with flight 17, Oct. 23, 1964.

$S=1.85$ cal/cm²min being the largest throughout the entire period of the balloon investigations is by 0.09 cal/cm²min smaller than the calculated $S=1.94$ cal/cm²min for the same conditions. $S_0^{extrap}=1.918$ cal/cm²min as derived through extrapolation is by 0.082 cal/cm²min smaller than F. JOHNSON's solar constant. These results permit one to suppose the interplanetary dust in the path of the solar radiation reaching the actinometer to decrease markedly the direct solar radiation flux (about 4 %). The interplanetary dust, probably, makes up the cloud-like formations, the clear space in which sometimes may result in the considerable decrease in attenuation (flights 17 and 19). Similar moments have, evidently, been used (as the best days) by F. JOHNSON, R. STAIR et al. for determining the solar constant. The presence of a substantial amount of very small dust particles in the interplanetary space was reported by papers (HIBBEN, 1966; JAMES, 1967; WOLSTENCCOFT and ROSE, 1967). The size of a dust particle is about 0.5 μ, the concentration being approximately, 100—1000 km^{-3}. The particles, most probably, consist of Fe and SiO_2. The contribution to S attenuation by near the Earth dust cloud, presumably, does not exceed 0.5—0.8 %. Dust particles are situated by the layers of various thickness (20—80 km) at the heights of 70—150 km, 200—280 km, 450 km etc.

The presence of a dust cloud in the upper atmosphere and near the Earth space makes it difficult to take accurate measurements of the solar constant from the Earth's satellites. We think the measurements of solar radiation from the moon's surface with the automatic lunar station or by cosmonauts to be most promising.

Summing up the above-said on the atmospheric optical conditions at the height of 22 km and upwards for the 1962—66 period one should state:

1. Anomalously small S values during the entire 1962—66 period both at the level of 29 km and at the atmospheric boundary (if one regards $S_0=1.98$—2.00 cal/cm²min).
2. The upper atmosphere was most unstable and turbid in 1962.
3. The values for the direct solar radiation flux as obtained in 1963 were close to the 1962 maxima.
4. Attenuation of solar radiation in the stratosphere in 1964—66 relatively decreased despite unfavourable individual phenomena (the Taal volcano eruption).
5. Time coincidence (with one year interval) for two cases of the largest transparency is to be noted (flights 17 and 19) Oct. 23, 1964 and Oct. 21, 1965.

The variation in the anomalous stratospheric turbidity for 1963—64 detected by us is confirmed, in addition to the above results, by the data from other papers. For instance, S. MATSUSHIMA et al. (1966) has investigated the variation in the photometric attenuation coefficient for the visible (β_v) from the Chile and Australia measurements. As seen from these measurements since the middle of May till December, 1963, this coefficient increased as much as 3—4 times. In 1964 β_v was only twice as much as the standard. Towards October 1964 the approach to the standard was observed. A peculiar variation in β_v in the southern hemisphere is due to the eruption of the Agung volcano. As has been stated the effect of the volcanic dust on the stratospheric radiation regime has been noticed from our balloon data, the value of the effect attaining 4.3 %. Yet, we suppose that besides the influence of the volcanic dust largely localiz-

ed in the lower stratosphere other factors are to be taken into account (atomic explosions, mesospheric and ionospheric attenuation by dust particles, space attenuation by dust particles).

To conclude we shall emphasize the preliminary character of the results obtained as well as the necessity for the further improvement of the accuracy of measurements and the ceiling of sounding (up to the heights of the order of several hundreds of kilometres) for more reliable judgement concerning the factors of the direct solar radiation attenuation.

REFERENCES

Budyko, M. I., 1966, Study of the regime of solar radiation from international programmes. Conference on scientific results of IQSY. Moscow, Jan.

Dyer, A. J., 1966, Artificial radio activity, ozone and volcanic dust as atmospheric tracers in the Southern Hemisphere. *Tellus, V. 18, No 2.*

Elterman, L., 1966, Aerosol Measurements in the troposphere and stratosphere. *Applied Optics, V. 5, No. 11.*

Hibben, R. D., 1966, Micrometeorite data challenges theories. *Aviat. Week and Space Technol., V. 85, No. 10.*

James, J. F., 1967, Interplanetary dust and the Zodiacal light. *New scientist, V. 33, No. 535.*

Kondratyev, K. Y., 1965, *Actinometry.* Gidrometeoizdat. Leningrad.

Kondratyev, K. Y., Nikolsky, G. A., Esipova, E. N., 1966, Balloon investigations of radiative fluxes in the free atmosphere. *Izv. Ak. Nauk SSSR. Fisica atm. i okeana. t. 2. N 4.*

Matsushima, S., Zink, J. R., Hansen, J. E., 1966, Atmospheric Extinction by Dust Particles as Determined from Three-Color Photometry of the Lunar Eclipse of 19 December, 1964. *Astronom. Journ., V. 71, No. 2.*

McIntosh, B. A., Millman, P. M., 1964, Radar Meteor Counts: Anomalous Increase during 1963. *Science, V. 146. No. 3650.*

Menon, M. P., Menon, K. K., Kuroda, P. K., 1963, Bomb-produced Cerium isotopes. *J. Geoph. Res. V. 68, No. 15.*

Nikolsky, G. A., Badinov, I. Ya., Lipatov, V. B., in press. On the influence of the synoptic situation on the distribution of optically active components in the lower stratosphere.

Raghavan, S., Jadav, B. R., 1966, Depletion of Solar Radiation by particulate matter in the atmosphere. *Indian J. Meteorol. and Geoph. V. 17, No. 4.*

Volz, F., 1966, Volcanic dust and a global twilight network. *J. Recherches Atmospheriques, V. 11, No. 2—3.*

Willard, R., Kenney, J. F., 1963, Ionospheric effects of high-altitude nuclear tests. *J. Geoph. Res. V. 68, No. 7.*

Wolstencroft, R. D., Rose, L. J., 1967, Observations of the Zodiacal light from a sounding rocket. *Astrophys. Journal, V. 147, No. 1.*

Experiments with automatic interpretation of meteorological forecast charts

By OLOV LÖNNQVIST, *Swedish Meteorological and Hydrological Institute, Stockholm*

ABSTRACT

A method has been tried for automatic translation of the information contained in prognostic charts into weather parameters such as surface wind, surface temperature and precipitation. The method is described and exemplified. Results from two test periods are presented.

1. Introduction

As a result of the use of high speed electronic computers in the weather service the human forecaster is now being furnished with an increasing amount of information in chart form. In addition to forecast charts of surface pressure and upper air topography new kinds of forecast fields are easily prepared by the computer, such as vertical velocity, stability, advection, amount of precipitable water etc. Furthermore, such forecast fields can be presented not only for 24 hours but for validity times as frequent as may be wished, e.g. for 6 hours, 12 hours, 18 hours etc up to 36 hours as is now the practice at the Swedish weather service. This leads to great problems for the forecaster to find time for studying all this information and for extracting out of it a consistent and complete synthesis to form in itself or together with various other information—and experience—the weather forecast to be presented to the various customers.

Automatic interpretation made by a computer and based on climatological information grouped in a convenient and systematic way, would help considerably. The need for this type of climatology was early pointed out by BERGERON (1930), who introduced the term dynamic climatology for this purpose. If the result of such interpretation is presented to the forecaster in a concise and easily readable way, it will make it less vital for the forecaster to study all the forecast charts produced by the computer.

Under certain circumstances the automatic interpretation may be used in its original form as a forecast. Such a procedure might be the only feasible solution for forecasts at remote places or for special purposes.

Computer preparation of forecast fields such as surface pressure and upper air pattern is sometimes misleadingly referred to as numerical weather prediction. This term—if used at all—should of course be reserved for a combined numerical process including real weather forecasting, for instance of the type presented in this paper.

One method for forecast chart interpretation would be the use of regression techniques. In that case the work could be divided in four different steps, viz. (1) search for good predictors, (2) determination of a multitude of possible regression equations, (3) study of the results in order to make a final choice of the equation to be used for each particular element, and (4) introduction of the use of regression equations as a step in the routine computer work, leading to a presentation of forecast suggestions, which could be used either as guidance or as automatic forecasts.

The regression technique, however, does not seem to be very convenient for the problem. The following reasons can be mentioned in favour of this view. Usually one should use more than one predictor for each element and the relation between each such predictor and the element in question is probably not a linear one. That would require quite a lot of predictors in the regression equation, the significance of which would conse-

quently be reduced correspondingly. Furthermore, there is seldom a question of a real functional relationship which means that the equation-form of expressing the relationship is rather artificial. Sometimes, however, a real functional dependence could be expected. A good example is the relation between pressure gradient and wind. In the author's view regression equations should be reserved for such cases.

The alternative to the regression technique would be some sort of weather-type classification technique. If this alternative is choosen the work can be divided as follows:

(1) Historical cases should be classed in weather types by means of a number of predictors; many different classifications should be carried out by varying the number of predictors and by dividing each predictor in a varying amount of classes.
(2) A complete climatology, including mean values and frequencies of various elements, should be worked out for each type as defined by each classification. The quality of each classification should be determined in order to facilitate the final choice.
(3) The results should be studied to make it possible to decide on which classification to use for each element.
(4) The choosen classifications and the established climatology should be used in the routine computer work and the results should be presented in a form suitable to guide the forecaster in his work or, alternatively, in the form asked for by the customer.

At the Swedish weather service experiments with forecast-chart interpretation have been carried out during the last few years. Forecasts of the following elements have been prepared automatically:

surface wind, direction and speed
probability of gale
maximum temperature
minimum temperature
precipitation
precipitation amount
thunder-storm probability
aerodrome weather conditions

In the present paper Section 2 will deal with type classification methods. The next section deals with methods and results of weather-type climatology. The question how to choose the best classification is discussed in Section 4. Aspects on the presentation method are given in Section 5. Finally, in Section 6, results are presented from two test periods. During these tests the automatic forecasts were compared with forecasts specially issued by the ordinary forecaster. All computations reported on in this paper were carried out on the high speed electronic computer Saab D21 at the Swedish meteorological and hydrological institute.

2. Type classification

The surface-pressure configuration is determined by pressure values in five points forming as closely as possible a rectangular cross. A suitable grid size seems to be 150—300 km which corresponds to the grid densities used in numerical forecasting in Sweden. From these five values one can determine four predictors, viz. the pressure in the central point, two components of the pressure gradient (i.e. the west-wind gradient and the south-wind gradient if the surrounding stations are located north, south, east and west of the central point), and the cyclonality determined as the difference between the average pressure in the surrounding points and the pressure in the centre.

Each one of these four predictors can be divided in a number of classes. The division is carried out in such a way that an equal number of cases fall in each class. Now the classification can be characterized by the "classification pattern" i.e. four figures indicating into how many classes each predictor has been divided. The first figure stands for pressure, the second one for west gradient, the third one for south gradient and the fourth one for cyclonality. Thus the pattern 1 4 4 1, indicates that pressure and cyclonality have not been used, while the two components of the pressure gradient have been divided into 4 classes each. In this case the number of types will be equal to 16. In comparison the pattern, 4 4 4 1, means that the number of types has been increased to 64 by also dividing pressure into four classes.

If the predictors are not correlated, each type will contain approximately the same number of cases. If they are correlated (e.g.

pressure and cyclonality) the cases will be unevenly distributed. In most cases this does not seriously effect the usefulness of the classsification method. Other methods could of course be used instead, for instance the descriptive method introduced by HESS and BREZOWSKY (1952). There seems to be certain advantages in using the simple and unprejudiced method described above and choosen for our experiments.

Now, new predictors can be added. We have used relative topography, $\Delta \Phi$, for the layer 1000—500 mb, and vertical velocity, w, both referring to the central point. Persistence predictors like yesterday's temperature at the station have also been used. These predictors are then added to the pattern in such a way that the pattern P, W, S, C, w, $\Delta\Phi$, T_{-1} equal to 1 3 3 1 4 3 4 means that the whole material has been divided into 432 types by splitting the two gradients and the thickness into 3 classes each, and the vertical velocity and yesterday's temperature into 4 classes each. Obviously one has to be somewhat restrictive in carrying out the type classification. A division in a large number of types means a reduction of the number of cases pertaining to each type, which might seriously affect the applicability of the type climatology on a new material. Means to avoid this effect will be discussed later on.

The use of vertical velocity as a predictor involves certain difficulties because of the lack of historical data. For some elements (wind, temperature, surface pressure) historical data might be available for more than fifty years. The use of aerological data reduces our possibilities considerably since homogenious data will scarcely be available for more than fifteen to twenty years. For vertical velocity, historical data may not be available for more than one or two years, since it requires that such data have been determined by routine computer techniques.

The lack of historical vertical-velocity data can to some extent be overcome by sort of guessing the vertical velocity from historical weather maps, using experiences from the few years for which computed data are available. This rather unsatisfactory method has proven to be of some use for improving the accuracy of interpretation.

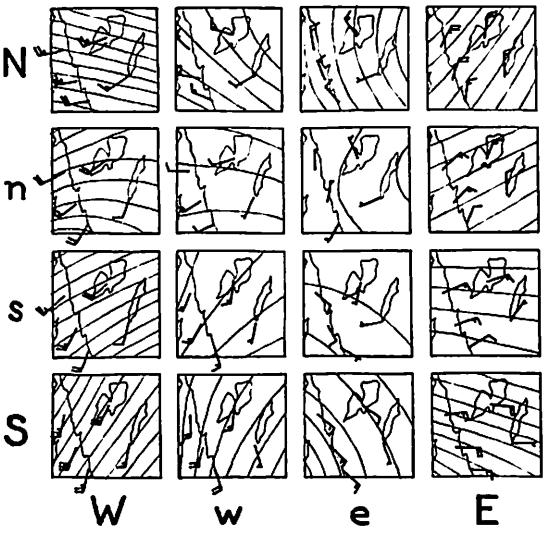

FIG. 1. Average surface pressure distribution and winds in the Swedish westcoast area according to classification 1441, December 1949—1964.

Good results in this respect will not be obtained until there are computed vertical velocity data available for about ten to twenty years.

In the experiments carried out by the author a large number of different classifications have been tried. An example will be given here. Let us take the area around Göteborg at the Swedish west coast and let the stations Hanstholm, Malmö, Oslo and Linköping determine the square within which the atmospheric pressure distribution is studied. Then the grid distance is about 250 km and the coordinate system is orientated approximately in W—E and S—N. Choosing then the classification pattern, 1 4 4 1, we obtain 16 types, which we might refer to as follows, small letters being used for relatively weak gradients:

NW	Nw	Ne	NE
nW	nw	ne	nE
sW	sw	se	sE
SW	Sw	Se	SE

An investigation of data for December 1949—1964 (496 cases), gives for each one of these types the average pressure distribution shown in Fig. 1. The number of cases in each type should be 31, but due to some correlation as well as the random spread of the

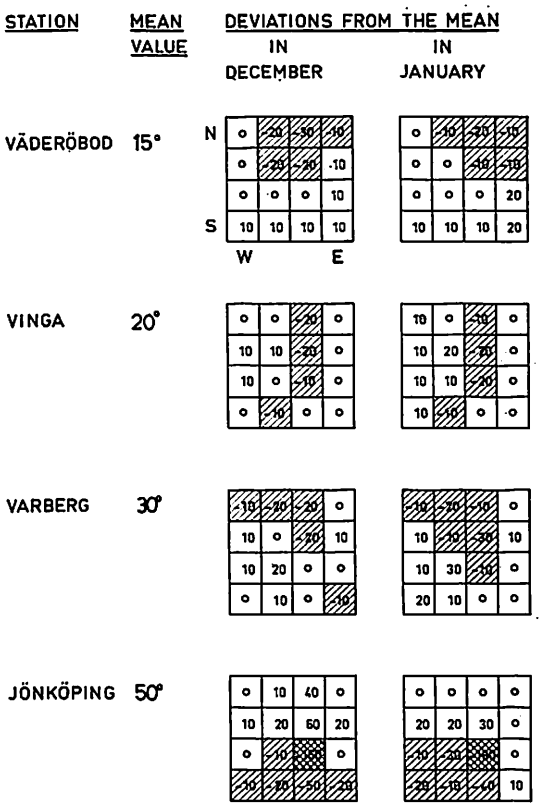

FIG. 2. Mean values of the cross-isobar angle of surface wind, and deviations from the mean value at four Swedish stations. Classification pattern 1441; data from December 1949—1964 and January 1950—1965.

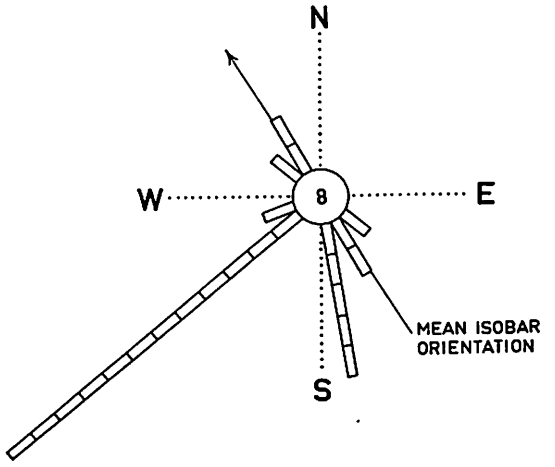

FIG. 3. Frequency of wind directions at Jönköping, December 1949—1964, for surface-pressure distribution of the type "se", according to classification 1441. The mean direction of the isobars is also shown.

relatively small amount of data the number of cases varies in reality from 18 (Type NE) to 48 (Type SE) in December. In January the maximum and minimum amount of cases appear in the same two types. The amount varies from 13 cases (Type NE) to 46 (Type SE), which shows that the distribution is not essentially a random effect.

The example shown in Fig. 1 will be further studied in the following section.

3. Type climatology

Within the area used to define the surface pressure distribution, a type climatology can be determined for any station and for any element.

It is not practicable to present here a full report on all classifications tried so far, nor to discuss in detail all the climatological connections which have been established, as interesting such a discussion could be. We will concentrate on a few striking examples. In order to demonstrate the significance of the results we will compare the findings obtained from the December data (496 cases) with the corresponding results obtained from the January data (496 cases). A certain amount of similarity should be expected. Since the data themselves for these two months are practically unrelated, similarities when obtained prove to a certain extent the significance of the results. The differencies obtained, on the other hand, could either reflect true differencies in the meteorological conditions (e.g. the amount of snow cover and the extent of ice on lakes and sea) or could be random effects due to the limited amount of cases.

(a) *Wind direction*

For each separate case we determine the angle, α, at which the wind crosses the isobars according to the pressure observed at the four surrounding stations. Within each type an "average" cross-isobar angle is determined. It is defined as the value for which the sum of the absolute values of the deviations

from the assumed average is a minimum, no such deviation being counted as more than 180 degrees.

Fig. 2 presents the results, at 06 GMT, for four wind stations, viz. Väderöbod, Vinga and Varberg at the Swedish west coast and Jönköping located in the inland at the southern end of lake Vättern. The mean cross-isobar angles 15, 20 and 30 degrees, respectively, at the coast and 50 degrees in the inland, were obtained from all December and January data taken together (992 cases). The figures in the squares show the deviations from these mean angles obtained in the 16 different types in December and in January. For ease of comparison types showing negative deviations are hatched.

Evidently, the four stations are all different in this respect. For each station the typical main features found from the December data are repeated in the January results. The local exposure, the general orography, and the fetch area could be the reasons for the station characteristics. The strikingly diverging figures for the weak southeasterly type at Jönköping (—160 and —180 degrees) imply cross-isobar angles around —120 degrees, which means that the wind blows from southwest in spite of the weak southeasterly gradient. Fig. 3 shows a polar histogram of the wind directions in this type in December. There are almost no winds crossing the isobar from the right side. The wind direction 230 degrees shows a very high frequency. This is most likely an effect of orography.

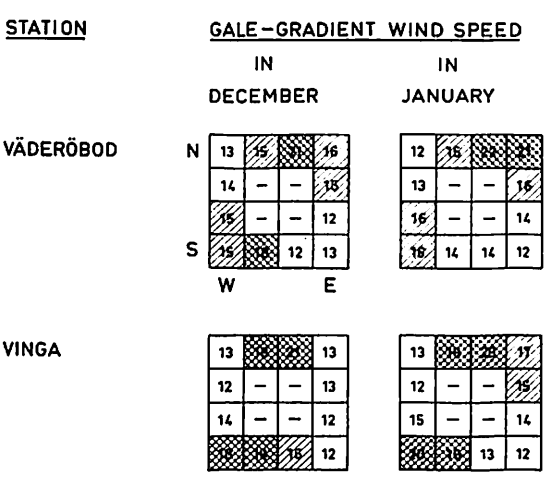

FIG. 4. Wind speeds in m/s at two Swedish stations corresponding to the "gale gradient", 16.3 mb/500 km, according to wind climatology for classification 1441.

(b) *Wind speed*

The wind speed can be expected to be closely related to the isobaric gradient. For this reason a regression equation is determined for each type. As an example, the equation

$$f=3.1+0.66\ G \qquad (1)$$

was found for Vinga in December, when all the cases were taken together, whereas, as an example, the equation

$$f=5.2+0.47\ G \qquad (2)$$

was found to apply for the 18 cases forming the NE-type. Here f is the wind speed in m/s; G is the isobaric gradient in mb measured over 500 km.

Of particular interest is the gradient 16.3 mb/500 km which according to equ. (1) gives $f=13.9$ m/s, i.e. the limit used in Sweden for gale warnings. In Fig. 4 we have investigated which wind speed will be obtained at this particular "gale gradient" according to the regression equation for each type. For obvious reasons the four types in the middle of the square representing weak gradients have been left out. A comparison is given between the results for December and January at the two stations Väderöbod and Vinga. The similarity between the two months is not as striking as for the cross-isobar angle discussed above. Nevertheless there are certain features that repeat themselves, viz. the strong response in wind speed at NNE and SW gradients (it means winds blowing parallel to the coast) and the poor response at NW and SE gradiens. For ease of comparison wind speeds 15—17 m/s are hatched while speeds $\geqslant 18$ m/s are cross-hatched in the figure.

(c) *Amount of precipitation*

In forecasting precipitation one could either forecast the amount or make a qualitative forecast, indicating "yes" or "no" or, going a step further, differentiating between "slight", "moderate" and "heavy", or some other classification. All these possibilities are

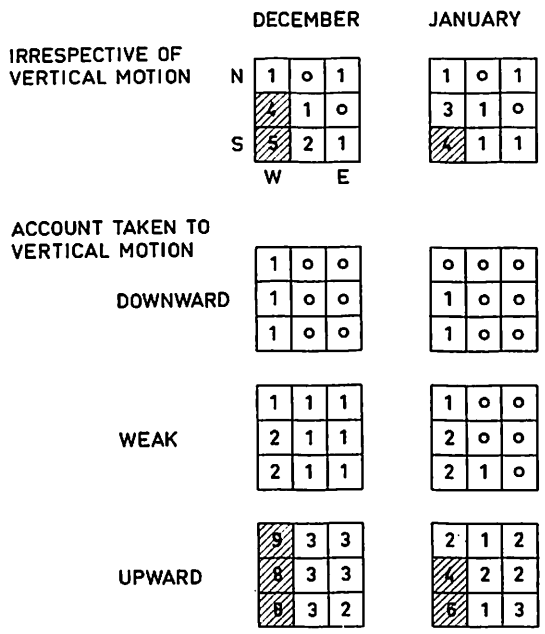

FIG. 5. Amount of preciptation in mm/6 hours at Dalsjöfors according to classification patterns 13311 and 13313, respectively. The figures in the patterns stand for P, W, S, C and w.

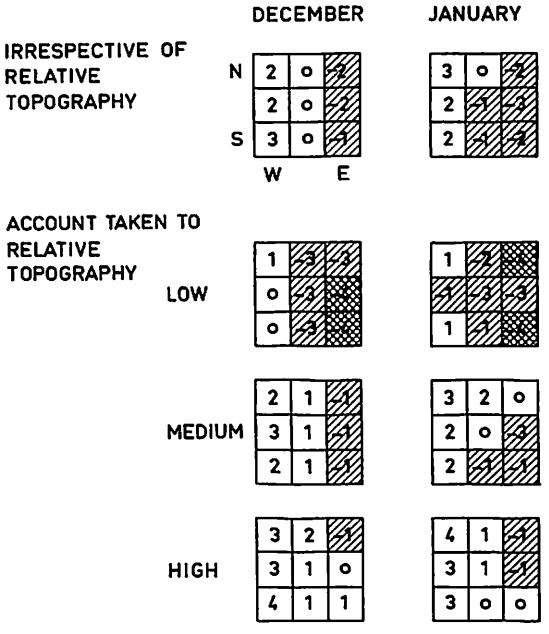

FIG. 6. Maximum-temperature anomalies at Göteborg according to classification patterns 133111 and 133113, respectively. The figures in the patterns stand for P, W, S, C, w and $\Delta\Phi$.

taken care of in the program used by the author for finding the type climatology for precipitation.

We shall deal here with the amount only. Let us choose two different classifications 13311 and 13313, where the five figures stand for pressure, west gradient, south gradient, cyclonality and vertical velocity, respectively. As mentioned already, the classification of the historical data as to vertical velocity was made by a subjective method.

Fig. 5 shows the average amount of precipitation at Dalsjöfors, 65 km east of Göteborg, for the 9 types according to the classification 13311, and for the 27 types according to 13313. A comparison is made for December and January.

The figure shows that the westerly and southwesterly types are characterized by relatively large amounts of precipitation. The introduction of vertical velocity as a third predictor improves the quality of the description.

Taking into account the fact that the amount of precipitation is a very difficult element to forecast due to its very large variability, the lack of agreement between December and January for large amounts in particular, is not too serious and might moreover partly be attributed to real differences.

(*d*) *Maximum temperature*

For the maximum temperature at Göteborg Fig. 6 shows the deviations from the normal value (+1° C in December; —3° C in January) for the 9 types according to classification 133111, and for the 27 types according to 133113, where the last figure indicates that the relative topography $\Delta\Phi$ between 1000 mb and 500 mb is divided into 3 classes. The agreement between the two winter months is very good although there are of course certain differencies, whether real or caused by random effects might be difficult to know from this very first experiment. Evidently both the west gradient and the thickness are good predictors for the maximum temperature whereas the effect

TABLE 1. *Flight-weather classification*

Class	Description	Visibility not below	Cloud base not below	Further condition
A	good	4.8 km	300 m	—
B	rather good	1.6 km	150 m	A not applicable
C	rather bad	0.8 km	60 m	A or B not applicable
D	bad	—	—	A, B or C not applicable

of differences in the south gradient is very small. Consequently another combination including some other predictor would be preferable. As mentioned in Section 4, yesterday's temperature would be one such predictor.

(e) Flight weather

In weather forecasting at aerodromes there are two elements which are of particular interest, visibility and base of low clouds. In the experiments with automatic forecasts of flight weather, the author has so far concentrated on forecasting a combination of these elements. In doing so the flight weather is divided into four classes *A*, *B*, *C* and *D* according to its seriousness to aviation. The classes are defined in Table 1.

Because of the disparity between the classes as far as interval size is concerned, the decision as to which of the classes should be forecast in each type cannot simply be determined by the mode or the average. Some sort of weight factor should be used instead.

In doing so for the airport Göteborg/Torslanda in December, and dividing the data into 200 classes, according to the pattern 155118, we obtain the results shown in Fig. 7. The question whether it is wise to divide the 496 cases in as many as 200 classes will be further discussed in next sub-section. Studying Fig. 7 we should only notice that in spite of the very few cases in each type, there is a large amount of consistency when we go step by step from low values to high values

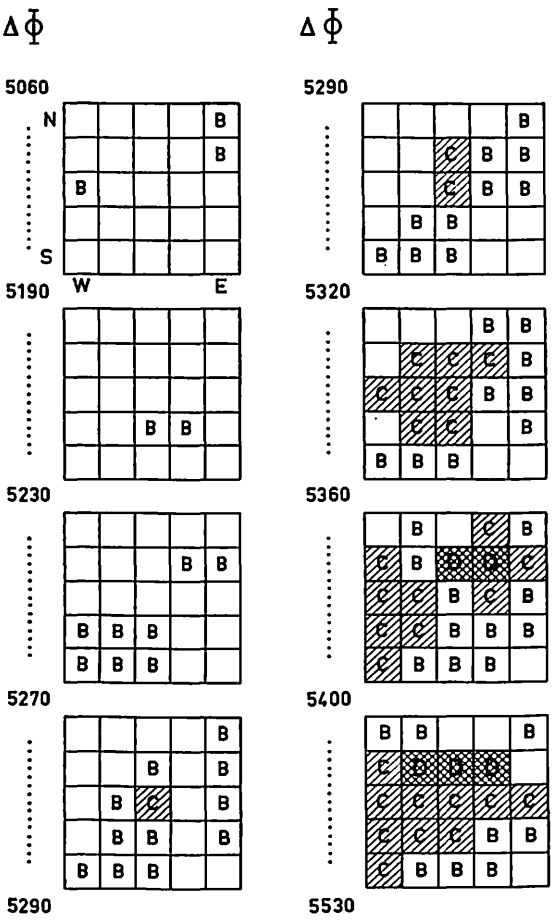

FIG. 7. Flight weather at Göteborg—Torslanda according to classification pattern 155118. Data from December 1949—1963. In types where good flight-weather, A, should be forecast no entry is made. B, C and D stand for rather good, rather bad, and bad weather, respectively.

of relative topography. There is also a certain consistency from the point of view of surface-pressure configuration as shown within each square. Obviously the seriousness of flight weather in Göteborg is strongly related to the relative topography. Maximum seriousness seems to occur in cases with weak northerly gradients.

When formulating an aerodrome forecast the ordinary forecaster is entitled to indicate not only the most probable weather but also a second or even a third weather with lower probability. The same can be done when formulating forecasts automatically. This

will be further exemplified in the last section of this paper.

(f) Smoothing

When the number of cases is limited and when the division into types is carried very far, as for instance in the example mentioned above under (e), the number of cases within each type might be reduced to very low values, even zero. In order to avoid obtaining results which would be insignificant it is advisable to introduce some sort of smoothing. This can be done in various ways. The author has choosen to give each case in the type under study a weight factor equal to the number of cases in the type. Cases in adjacent types are given a factor equal to one. The effect of the smoothing then can be demonstrated as follows. If three predictors are used, a type is usually surrounded by six adjacent types. In that case the adjacent types jointly modify an anomaly in the type value by ten per cent if the number of cases in each type is equal to 60. If instead the number of cases per type is equal to 6 the average obtained from the adjacent types jointly have the same weight as the average obtained within the type itself.

The effect of smoothing on the significance of the result is under study. The results of the study will be presented in a separate paper.

4. Selection of classifications

It is impossible to know at an early stage in the investigations which combination of predictors will give for each element and at each station the best possible description of the typical conditions. When a regression technique is used the selection can be based on the variance reduction achieved. In doing so one has to consider as well the significance of the result, in order not to incorporate predictors the influence of which is almost negligible. The same holds for type classification.

Each classification for which a complete climatology has been established has to be tested and its quality has to be indicated by a figure, e.g. the variance reduction. The goodness of a classification can be judged, however, in different ways. It is difficult to know which mark-setting does best reflect the opinion of the user, or, rather, his economical benefit. For that reason more than one set of quality marks should be used.

In Table 2 you will find a summary of the combinations tried by the author for the minimum temperature at Göteborg in December. The quality marks used are the RMS

TABLE 2. *Comparison of classifications concerning Minimum temperature at Göteborg in December*

Classification pattern P W S C$\Delta\Phi T_{-1}$	Number of types	RMS Error (°C)	Variance reduction (%)	Rate of success (%)
1 1 1 1 1 1	1	4.56	0.0	50.0
Pressure only				
1 2 2 1 1 1	4	3.88	27.6	71.0
1 3 3 1 1 1	9	3.88	27.6	70.8
1 4 4 1 1 1	16	3.75	32.3	73.2
1 5 5 1 1 1	25	3.79	31.0	74.0
Thickness only				
1 1 1 1 3 1	3	3.56	39.0	71.3
1 1 1 1 4 1	4	3.48	41.8	71.6
1 1 1 1 5 1	5	3.41	44.1	72.1
1 1 1 1 8 1	8	3.32	47.0	72.8
Pressure and thickness				
3 1 1 1 4 1	12	3.19	51.1	77.8
1 3 1 1 4 1	12*	3.14	52.5	78.0
1 1 3 1 4 1	12	3.45	42.8	72.2
1 1 1 3 4 1	12	3.41	44.1	74.5
3 3 1 1 3 1	27*	3.06	55.0	80.2
3 1 3 1 3 1	27	3.25	49.1	76.6
1 3 3 1 3 1	27	3.10	53.8	79.7
Persistence only				
1 1 1 1 1 4	4	3.16	52.0	80.7
1 1 1 1 1 8	8	3.02	56.1	81.4
All combined				
1 1 1 1 3 4	12	2.54	69.0	84.7
1 1 1 1 3 8	24	2.44	71.4	85.6
3 1 1 1 3 3	27	2.59	67.7	84.0
1 3 1 1 3 3	27*	2.39	72.5	87.3
1 1 3 1 3 3	27	2.62	67.0	83.3
3 1 1 1 3 8	72	2.32	74.1	87.4
1 3 1 1 3 8	72*	2.16	77.5	89.3
3 3 1 1 3 4	108	2.16	77.5	89.6

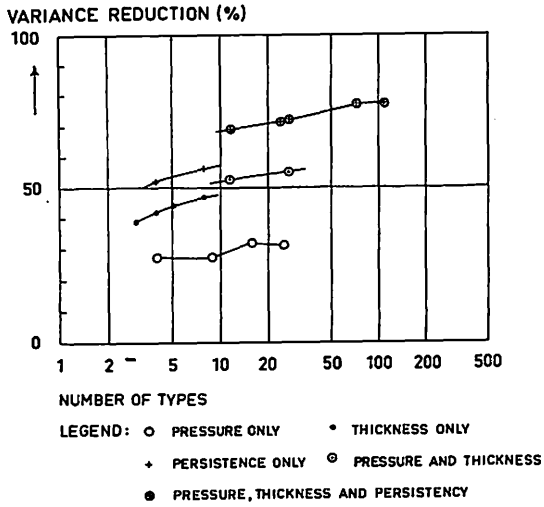

FIG. 8. The goodness of type classification of minimum temperature at Göteborg in December, given in terms of the relative variance reduction, as a function of the number of types used for the classification.

error and the "rate of success". For evaluating the rate of success we have divided the temperature values into eight classes and we have applied a score table constructed in such a way that random forecasts give the figure 50 %. From the RMS errors we have computed the relative variance reduction. The table shows that yesterday's temperature is the best predictor. Then comes the relative topography. By combining these two predictors with surface pressure predictors, the variance can be reduced considerably. This is seen even more clearly from Fig. 8, were the variance reduction is plotted as a function of the number of types (on a logarithmic scale). Where the table contains a group of classifications giving the same amount of types, only the best one, indicated by an asterisk, is plotted in the figure.

5. Presentation methods

When the classification climatology has been established and the final selection made from the point of quality and reliability, an extraction and presentation program has to be put into operation as an integral part of the daily computer work.

The question how to present this guidance to the forecaster is very important. Different methods have been tried at the Swedish weather service. On this point an agreement has to be reached between the programmer and the forecaster. A few aspects on the presentation problem will be given here.

One way of presentation is to prepare a weather-type climatological atlas. In that case the daily computer work is limited to carrying out a classification from the available forecast fields, thus indicating for the next 6, 12, 18, 24, 30 and 36 hours the appropriate figure for the expected weather type over various parts of the area of interest to the forecaster.

Another possibility wolud be some sort of tabulation. It can be carried out either element by element and station by station as follows:

Winds:

Vinga: 06 GMT NNE 6 m/s
12 GMT N 8 m/s
18 GMT NNW 12 m/s etc.

Or it can be done hour by hour in the following way:

06 GMT:

Vinga: NNE 6 Moderate rain Temperature +6
Göteborg: N 3 Heavy rain Temperature +3
etc.

A third possibility—not too difficult to achieve—would be to use the interpreted values of wind, precipitation and temperature for automatic plotting of forecast "observations" on the forecast charts in the same way as actual observations are plotted on ordinary weather maps.

Another question to be agreed between the programmer and the forecaster would be whether the interpretation should be presented in words ready for use in the written forecast, or numerically in tabular form, including additional information available in the type climatology such as probabilities and alternatives.

The forecaster should be aware of the fact that, given the climatological interpretation, almost any form of presentation can be produced by the computer through proper programming.

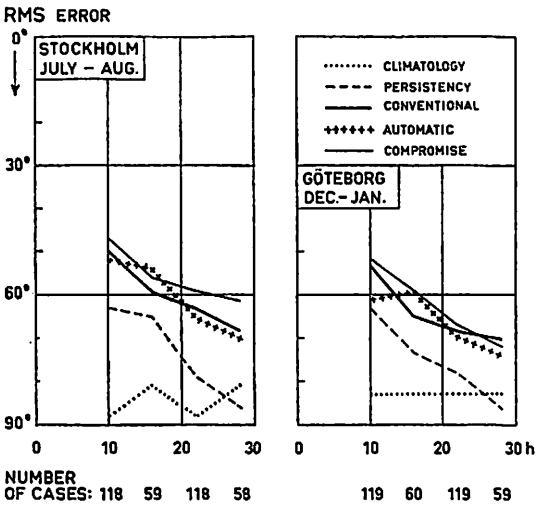

FIG. 9. Accuracy in forecasting wind direction (RMS error in degrees) during test periods given as a function of time. Dotted line shows simple climatological forecast. Broken line shows persistence forecast. Full line shows conventional forecast. Cross-dotted line shows automatic forecast. Thin line shows 50—50 % compromise between conventional and automatic forecasts.

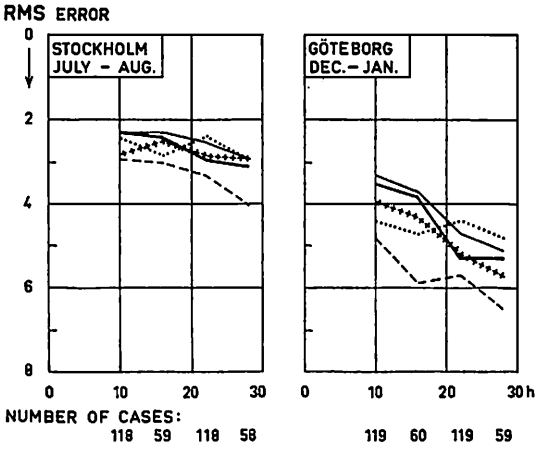

FIG. 10. Accuracy in forecasting wind speed (RMS error in m/s) during test periods. For legend, see Fig. 9.

6. Results from two test periods

At the Swedish weather service arrangements were made during December 1966, and January, July and August 1967 for a comparison between automatically produced forecasts and special forecasts made at

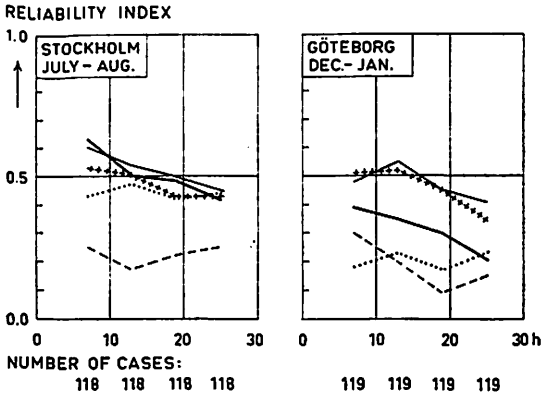

FIG. 11. Accuracy in forecasting precipitation (reliability index) during test periods. For legend, see Fig. 9.

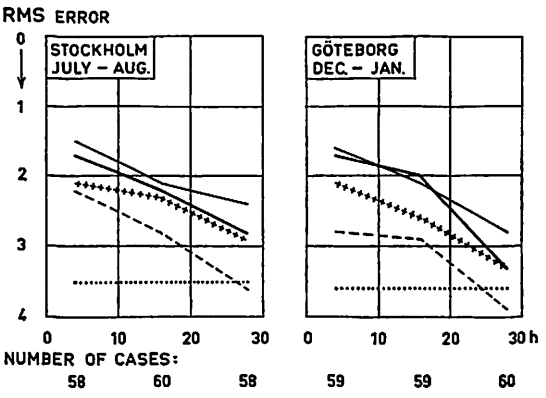

FIG. 12. Accuracy in forecasting maximum temperature (RMS error in ° C) during test periods. For legend, see Fig. 9.

approximately the same times and under the same conditions by the forecaster on duty.

During the winter period the forecasts concerned Göteborg, during the summer they concerned Stockholm. A brief summary of the results are given in Fig. 9—14. The figures would speak for themselves, but it is necessary to notice that, although the amount of cases is fairly high, a two-month test period is much too short for drawing any safe conclusions. Unfortunately none of the test periods were particularly typical. During the summer test, for instance, low pressure situations did not occur at all while anticyclonic high pressure situations were clearly overrepresented.

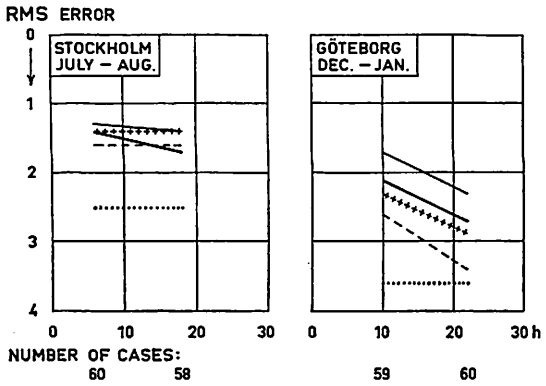

FIG. 13. Accuracy in forecasting minimum temperature (RMS error in ° C) during test periods. For legend, see Fig. 9.

It is worth noticing that in almost all cases a compromise (50—50 %) between the conventional and the automatic forecast is better than any one of the forecasts themselves. This indicates that automatic forecasts could, at least, be used as a valuable tool.

As an explanation to Fig. 14 it should be mentioned that the flight-weather test was carried out in December only, The curve at the top of the figure and the cross sign closely behind represent a test in which the alternative weather forecasts are taken into consideration according to the rules used in Scandinavia for conventional testing of aerodrome forecasts. The other curves in the figure refer to the case when only the main forecast is taken into consideration. An example showing a very good automatic flight-weather forecast is reproduced in Table 3. Alternatives when issued are shown in brackets.

In conclusion, our experiments in automatic forecasting are most promising and the work will continue. We have found that it is relatively easy to produce forecasts automatically which are almost as good as the conventional ones. It is much more dificult to really surpass them in quality, and much work has still to be done in order to find, if possible, better combinations of predictors than those tried so far. At the same time work is spent on improving the quality of the forecast charts as to their capability of catching both the large-scale development and the detailed structure. This is a very important work, since—of course—interpretation forecasts should never be expected to be any better than the prognostic charts on which they are based.

TABLE 3. *Aerodrome forecasts for Göteborg-Torslanda issued 29 December 1966 and based on observations for 12 GMT (Alternatives in brackets)*

Time of validity	Ordinary forecast	Automatic forecast	Weather observed
18 GMT	B (C)	B (C)	B
00 GMT	B (D)	B (C)	C
06 GMT	B (C)	C (D, A)	D
12 GMT	B	A	A
18 GMT	A (B)	A	A

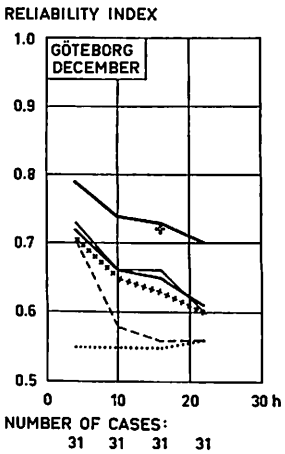

FIG. 14. Accuracy in forecasting aerodrome weather at Göteborg—Torslanda during December 1966. For legend, see Fig. 9. The line at the top (conventional) and the cross closely below (automatic) show the results obtained when alternative forecasts are taken into account in the test procedure.

REFERENCES

BERGERON, T., 1930, Richtlinien einer dynamischen Klimatologie. *Met. Zeitschr., 47*, pp. 246—262.

HESS, P., and BREZOWSKY, H., 1952, Katalog der Grosswetterlagen Europas. *Ber. Deutschen Wetterdienst, U.S. Zon, 33*, 33 pp.

Some observations of snow melt

By ALF NYBERG

Swedish Meteorological and Hydrological Institute, Stockholm

ABSTRACT

By use of a recording snow melt-meter the hourly amount of melt water has been studied in relation to meteorological factors. In general there is a good agreement between theoretical and observed values. However, during strong isolation deviations have been found which call for further studies. The amount of liquid water in the melting snow is found to be only a few per cent of the mass of the snow layer when there is free drainage whereas in laboratory experiments without free drainage a percentage of 30 % or more can be obtained.

1. Introduction

In a previous paper (NYBERG, 1965) was described an instrument for recording evaporation from a snow surface. In principle it consists of a balance. On a rotating drum a pen is recording the level of a vessel filled with snow. This vessel is moving upwards without hindrance of the surrounding snow when snow is evaporating. As this instrument functioned in a satisfactory way when properly treated, it was thought that a similar idea could be used for the design of a snow melt-meter. Such a meter has thus been constructed and it has been used during a melting period in the Swedish mountains.

A schematic picture of the instrument is shown in fig. 1. It consists to a large extent of the same parts as the evaporimeter, but instead of a movable snow-filled vessel there is a funnel manufactured of transparent plastic material filled with snow and ending in a pipe from which melt water runs down into a bottle placed on a movable platform. The movements of this platform is recorded on the drum. The thickness of the snow was kept as close as possible to 30 cm and the area of the funnel was 1000 cm².

The melt-meter was placed at Ljusnedal (Lat. 62° 33′*N*, Long. 12° 36′*E*, 585 m above m.s.l.). Most of the time the observations were made by non professionals living close by the observation site. Due to lack of complete instructions and some instrumental shortages the record fell out during several short periods. None the less useful results were obtained and they will be discussed below. At the same time an evaporimeter was placed close to the melt-meter. However, this functioned in a completely satisfactory way during short periods only. Other recording instruments were giving temperature and relative humidity in a normal screen and wind speed. Temperatures were also given by ventilated thermometers on a mast in the levels 0.6 m, 2.2 m and 8 m. The net incoming (or outgoing) radiation was recorded with a radiation balance meter.

2. Theoretical relations

Already in 1918 ÅNGSTRÖM discussed the heat exchange at the snow surface and gave the equation of the heat balance, which in a modified form is given by equation (1). The amount of snow melting in one time-unit, S, depends upon various meteorological factors namely the net radiation Q, the flux of heat from the air through convection W, the evaporation E and the heat conducted to (or from) deeper layers of the snow, G. M and L are the latent heat of melting and of evaporation respectively, and P the heat from precipitation.

The following equation is valid

$$M \cdot S + L \cdot E = Q + W + G + P \qquad (1)$$

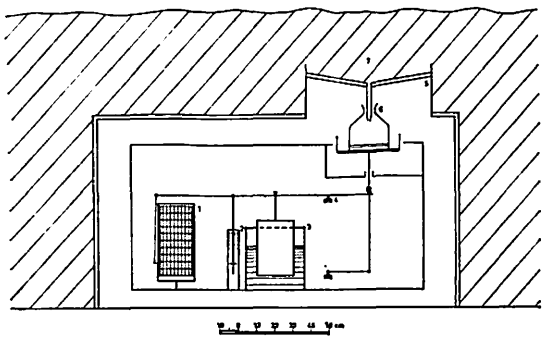

FIG. 1. Diagram showing the melt meter. 1, Recording drum. 2 and 3, Damping arrangements. 4, Edge of balance. 5, Vessel (area 1000 cm²) with pipe. 6, Bottle for collection of melt water. 7, Snow.

We have $E = A_z \cdot \varrho \cdot \frac{5}{8} \cdot \frac{1}{p} \cdot \frac{\partial e_z}{\partial z}$

where A_z is the coefficient for eddy exchange of water vapour at the level z, p is the air pressure, ϱ the density of the air and e_z the vapour pressure at the level z. We also have

$$W = A'_z \cdot c_p \cdot \varrho \cdot \frac{\partial T_z}{\partial z}$$

where A'_z is the eddy conductivity, c_p the specific heat of air and T_z the temperature at the level z. All temperatures are in degrees Celsius.

We assume that $A_z = A'_z$ and substitute $\varrho \cdot A_z \cdot \frac{\partial e_z}{\partial z}$ and $\varrho \cdot A_z \cdot \frac{\partial T_z}{\partial z}$ by $\frac{(A'+B'u)(e_s-e_a)}{z}$ and $\frac{(A'+B'u)(T_a-T_s)}{z}$

where u is the observed wind velocity, e_s, T_s are the values of vapour pressure and temperature at the snow surface and e_a and T_a are the corresponding values as measured in the observation screen at the level $z = 1.5$ m.

P is generally small and no case with rain has been studied here. It is therefore neglected.

If the snow sheet has a uniform temperature of 0° the term G is also zero. A special case when G is not zero will be briefly discussed later.

We put $\frac{A'+B'u}{z} = A + Bu$

Equation (1) may then be written

$$\frac{M \cdot S - Q}{c_p (T_a - T_s) - L \cdot \frac{5\,(e_s - e_a)}{8 \cdot p}} = (A + Bu) \quad (2)$$

3. Data

In Table 1 is given observed values of S, Q, T_a, e_s and e_a for 44 cases, when the instruments all functioned well. Values of $(A+Bu)$ have been computed from equation (2) and they are shown in fig. 2. A line of best fit to these values has been drawn giving $A = 5$ and $B = 1.2$ and from this line values of S have been computed and these are also shown in Table 1. It is remarkable that the value of B i.e. the increase of the eddy conductivity with the wind is small.

4. Discussion of errors

Before discussing the results a discussion of the errors of observation of various elements seems approriate.

a) *The amount of hourly melt water S*

The values of S are in general rather accurate. The percentage error does not normally exceed 10. However, certain errors are due to the fact that melting snow can hold some water as droplets between crystals or films of water on crystals. There seems to exist a maximum amount of water held and when this stage is reached the snow is said to be saturated (DE QUERVAIN, 1948). The amount of water in the saturated stage is given by various investigators as from 1 % to 30 % or even more. GERDEL (1954) says that the water holding capacity during a study of many individual cases with free drainage varied between 0.7 and 5.5 % with the majority of cases less than 2 %. It is also possible that the snow may be oversaturated for a shorter time when melting is very rapid. However, if melting then decreases more water will run off than the amount corresponding to actual melting and the normal saturation stage will be reached again within about one hour (GERDEL, 1945).

b) *The net radiation Q*

The values of Q are fairly reliable. However, in some cases the instrument gave too small values due to rime deposit. At some occasions the sky was cloudy and thus the radiation varied rapidly with time. It is then uncertain over which period mean values should be computed.

c) *Temperature values*

The temperature in the screen is following the air temperature with a certain lag. This lag, however, was not very large at 11^h and 14^h when most of the observations used were obtained but could be of importance at other hours. Another cause of error was the heating of the screen by radiation. By comparison between the screen temperature with that of the ventilated thermometers it appears that the difference may amount to as much as 0.5°—1° during light winds.

The temperature of the snow is sometimes uncertain. Radiation errors of the thermometer on the snow surface are unavoidable and not easily determined. The first assumption was that during snow melt the snow surface temperature was zero. However, this is not correct. In some cases the wet bulb temperature of the air is considerably below zero as well as the measured snow surface temperature. During such cases melting may take place below the surface where incoming radiation is absorbed but no outgoing radiation losses and no evaporation occur. That happened e.g. on 5 May at 8^h and on 9 May at 11^h. Melting of snow at lower levels when the surface temperature is below 0° has been described by DE QUERVAIN (1948) and HOECK (1952). The exact temperature of the snow surface is very difficult to determine in such cases.

There are also cases when it appears that the temperature of the snow or rather the water film on the snow is above 0°. I have not in the literature found any observations or discussions of such cases. However, a certain positive temperature in the melt water must obviously exist. The question is what temperatures we can get. The absorption of incoming rays of solar energy by passage through a film of 0.1 mm thickness is very small. However, it has been mentioned by HOECK (1952) that wet snow is absorbing more radiation than dry snow. It is conceivable that repeated reflexion and absorption can take place in water films and droplets thus lengthening the path considerably and thereby increasing the absorption. This question has to be studied further.

Another possibility is that by pollution of the snow strong local absorption of short wave radiation may increase the snow melt temperature. It is, however, not feasible to decide upon this question from the data available.

d) *The evaporation E*

The computed evaporation depends upon the temperature observations in the screen and at the snow surface. An increase of the screen temperature would increase the computed value of the saturated vapour pressure but on the other hand this would be partly compensated by lower relative humidity in the screen than in the free air. Values of e_a are therefore considered to be fairly correct.

The vapour pressure over the snow is more depending on the snow temperature. Surface temperature errors may therefore cause considerable errors in e_s.

5. Results

In the first phase of melting at the surface the water pouring down into deeper and cold layers will freeze again and no run off will be observed. Therefore there was no melting recorded during the period 8—9 April or during 19—22 April although the maximum temperature was well above 0°. However, during most of these days the outgoing radiation prevented any melting (in accordance with equation (2). On 20 April in the afternoon there was probably some melting (estimated to about 1.5 mm) but the water froze again in the cold deeper snow and no melting was recorded. The amount would have been sufficient to heat the snow layer by 5° which would not have raised the temperature to 0° in this case. A similar situation occurred on 22 April. Some melting took place but there was no melt recorded. On

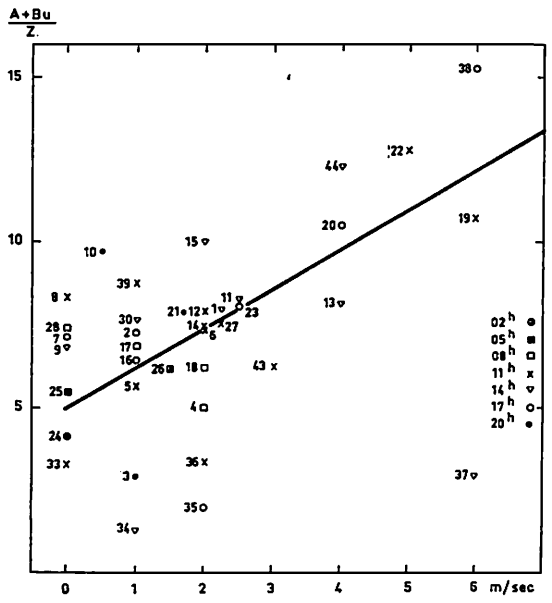

FIG. 2. Values of $(A+Bu)$ as function of u. The figures indicate the same numbers as in Table 1. The equation is $(A+Bu)=5+1.2$ u.

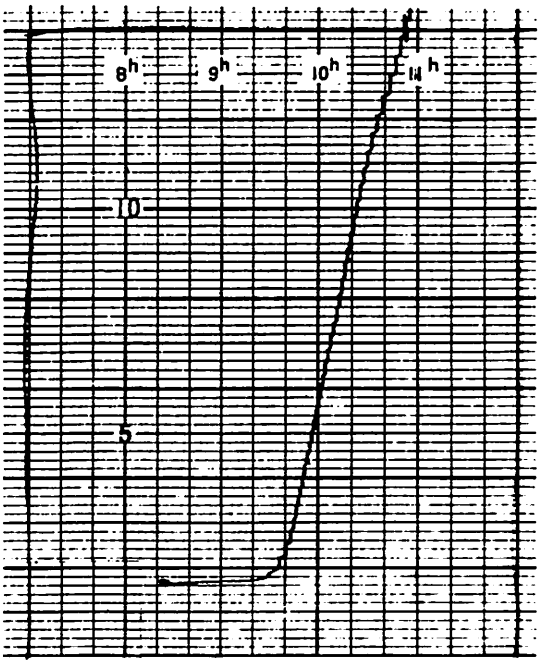

FIG. 3. Recorded melt water on 3 May in the morning. The distance between two horizontal lines corresponds to 0.04 mm water.

24 April the air temperature reached the 0° level a few minutes after 8^h. However, it was not until 14.30 that run off was recorded. With the aid of equation (2) and the regression line in fig. 2 the amount of melted snow until 14.30 has been estimated to be 2.75 mm. About a quarter of this was used for heating the snow by refreezing melt water and the rest for saturating it with liquid water. The content of liquid water was then about 4 % of the snow mass.

In this study we have tried to avoid cases when the snow was being heated or when the snow was not yet saturated. It is possible that in some cases at the end of the day when the snow was supersaturated more water was running off than the simultaneously melted amount. However, no clear indications of such a process have been found.

When snow is melting the water is not running down into the snow quite uniformly but channels are formed in the snow and in these channels water with a temperature slightly above 0° can reach the bottom even before the whole layer has been heated to 0°. Fig. 3 shows such a situation. It is a record of the melt on 3 May. The temperature during the night was below 0° during 6 hours. The minimum temperature was about —2° and the temperature rose to 0° at about 4 o'clock but there was outgoing radiation. At 8 a.m. the air temperature was +2.6° and the snow temperature probably close to 0° and melting started but the run off was very small indeed. Only at 9.20 it started to increase and reached an expected value at about 9.40.

From the equation (2) one can compute the melting from 8^h to 9.40. We get the value 1.20 mm whereas the amount recorded was 0.16 mm. The difference or 1.04 mm was therefore used for saturating the snow. The liquid water content was less then 3 % of the total mass of snow above the melt meter. This is of course only an estimate as the density of the snow was not measured. Further the cloudiness varied so that the radiation value is somewhat uncertain but still it is clear that there was not a large percentage liquid water held by the snow.

Observations of fresh snow in a cold laboratory with a temperature a few degrees

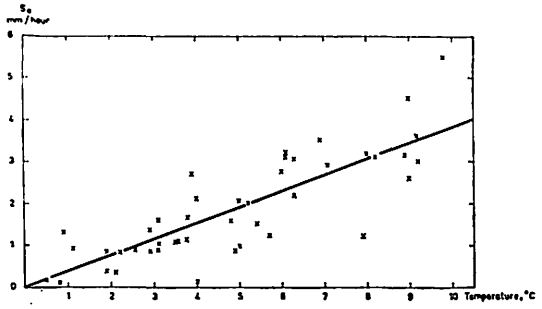

FIG. 4. Hourly water melt and air temperature.

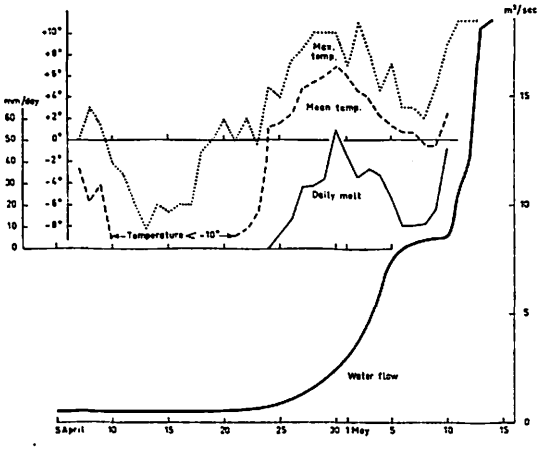

FIG. 5. Daily maximum and mean temperatures, measured melt water and run off in the river Ljusnan.

below 0° and a radiating lamp giving an energy of 0.9 cal/cm²/min gave similar results. In these cases the temperature of the snow was measured in various levels below the snow surface and the density of the snow was also measured. The liquid water content in a layer of large ice particles was found to be 1.5 % and in light snow 6 to 12 %. On a piece of melting solid ice hanging on a string in a warm room was formed a film of water with a mean thickness of 0.05 mm or 1.5 % of the mass. Another experiment with a snowball hanging on a string in a warm room gave a liquid water content of 38 %, that is to say all the space between the crystals was filled with water. In this latter case there was no free drainage but water fell out in drops at the bottom of the ball.

The maximum hourly value of snow melt amounted to 4.5 mm/hour at 11^h on 11 May. Actually the last observed value, No 44, amounts even to 5.6 mm/hr but this is higher than the computed value and may have been influenced by absorption of energy at the bottom of the vessel as the snow thickness rapidly decreased. This value is therefore not considered reliable. The total daily melt was recorded by the melt-meter but also by the evaporimeter. There was good agreement between the two meters. In general the difference of daily values did not surmount 15 % and the mean difference was 4 %, the evaporimeter giving the higher values. The largest amount, measured on 29 April, was 5.5 liter/1000 cm² day=55 mm/day or with a density of 0.4 a layer of 14 cm snow/day. These values are somewhat higher than those obtained by FORSMAN (1963) in Northern Sweden near the Polar circle by means of hourly observations of the run off from vessels of an area=1 m². That maximum hourly value was 3.6 mm water and the maximum daily value was 29 mm water.

In fig. 2 we see that in spite of a considerable spreading of values there is an increase of $(A+Bu)$ with the wind velocity. Some values are extremely large and deviating very much from the mean line. In some cases No. 29, 32, 34 and 35, this could depend upon the fact that the convective heat flux and the heat used for evaporation were about equal. They balanced each other so that we got undetermined values. In some other cases, No. 36 and 37, the $(A+Bu)$ values are too small. The snow temperature was assumed to be zero but the wet bulb temperature was below zero. If the values of the wet bulb thermometer were to be accepted as valid for the snow surface the $(A+Bu)$ values would be quite in line with the other observations.

In some other cases the values of $(A+Bu)$ are very low and even negative. In these cases reasonable values would have been obtained if the snow or water film temperature had been 1 or 2 degrees above zero.

If we study Table 1 and take the difference between observed and computed melt values we find another expression of this result. Positive values are in general small. The largest one is No. 44 which may be explained

TABLE 1. *Meteorological parameters are*

Q, the net radiation given as read off values which multiplied by 11.1 give the value in cal/cm²hr.

T_a, the air temperature in degrees Celsius measured in the thermometer screen.

$(e_s - e_a)$, the difference between vapour pressure in mb at the snow surfade e_s and in the thermometer screen e_a.

S_o, observed amount of melted snow in mm water per hour.

S_c, computed value of melted snow derived from average values of $(A+Bu)=5+1.2$ u obtained from fig. 2

No.	Date	Hour	Q	T_a	u	(e_s-e_a)	S_o	S_c	S_o-S_c	$(A+Bu)$
1	24.4	14	+0.2	+3.6	2	0.4i	1.10	1.09	0.01	7.91
2		17	—0.2	+4.9	1	0.27	0.75	0.60	0.15	7.29
3		20	—0.2	+4.0	1	—0.13	0.11	0.42	—0.31	2.93
4	25.4	09	+0.2	+2.6i	2	—0.80i	0.88	1.12	—0.24	5.02
5		11	+0.2	+3.7	1	—0.73	1.14	1.25	—0.09	5.63
6	26.4	11	+0.8	+6.3	2	0.56	2.20	2.22	—0.02	7.32
7		17	+0.2	+5.7	0	0.78	1.24	1.00	+0.24	7.15
8	27.4	11	+1.0	+7.1	0	0.76	2.90	2.50	+0.40	8.39
9		14	+1.0	+8.9	0	0.29	3.16	3.33	—0.17	6.82
10		19.30	—0.05	+5.0	0.5	—0.30i	0.96	0.63	+0.33i	9.75
11	28.4	13	+0.3	+9.0	2.5	0.35i	2.60	2.52	+0.08	8.32
12	29.4	11	+1.0	+8.0	2	0.54	3.16	3.03	+0.13	7.94
13		14	+1.0	+9.2	4	0.62	3.62	3.71	—0.09	8.17
14	30.4	11	+1.1	+8.2	2	1.21	3.10	3.07	+0.03	7.47
15		14.40	+0.4	+9.2i	2	0.90	3.00	2.33	+0.67i	10.04
16		17	+0.0	+7.9	1	1.03	1.22	1.31	—0.09	6.45
17	1.5	06.30	+0.8i	+3.8	1	—1.5i	1.64	1.46	+0.18	6.91
18		08	+1.2	+6.1	2	—1.12	3.20	3.51	—0.31	6.20
19		11	+0.4	+6.9	6	—1.15	3.50	3.89	—0.39	10.72
20		17	+0.2	+5.2	4	—0.82	2.00	2.15	—0.15	10.51
21	2.5	20	—0.2	+2.9	2	—0.95	0.84	0.76	+0.08	7.90
22	3.5	11	+1.0	+4.0	5	1.26	2.14	2.03	+0.11	12.80
23		16	+1.0i	+6.0i	2.5i	1.51	2.76	1.88	+0.40	8.11
24	4.5	02	0.0	+0.8	0	—0.08	0.12	0.15	—0.03	4.13
25		05	0.0	+0.5	0	—0.18	0.19	0.13	+0.06	5.50
26		08	+0.3	+3.1	1	—0.08	1.04	1.04	±0.00	6.20
27		11	+1.0	+3.9	2	—0.30	2.68	2.68	±0.00	7.55
28	5.5	09	+1.1	+2.2	0	3.02	0.86	1.08	—0.22	7.43
29		11	+1.8	+4.8	1	2.89	1.61	2.49	—0.88	470.00*
30		14	+1.8	+6.3	1	2.35	3.05	2.96	+0.09	7.69
31	6.5	11	+1.8	+3.1	2	1.78	1.60	3.33	—1.63	neg.*
32		14	+0.9	+2.9	4	1.68	1.32	1.25	+0.07	43.80*
33	7.5	11	+0.6	+3.5	0	0.55	1.10	0.98	+0.12	3.34
34		14	+0.6	+3.1	1	1.09	0.88	1.06	—0.18	1.32
35		17	+0.2	+2.1	2	0.54	0.34	0.56	—0.22	1.97
36	8.5	11	+1.1	+0.9	2	1.57	1.30	0.97	+0.37	3.35
37		14	+0.8	+1.1	6	1.97	0.90	0.26	+0.63	2.97
38		17	+1.2	+1.9	6	2.13	0.85	1.16	—0.31	15.30
39	9.5	11	+0.8	+1.9	1	2.58	0.38	0.65	—0.27	8.82
40		14	+2.3	+5.0	3	1.80	2.06	3.78	—1.72	neg.*
41		17	+1.5	+5.4	3	1.37	1.50	2.91	—1.41	neg.*
42	10.5	11	+2.6	+6.1	3	1.61	3.20	4.51	—1.31	neg.*
43	11.5	11	+2.5i	+9.0i	3	1.68	4.50	4.93	—0.43	6.25
44		14	+1.3	+9.8	4	1.95	(5.55)	3.84	(+1.71)	(12.30)

* values not plotted in fig. 2.

by the fact that at the time of this observation so much snow had melted that there was a considerable heating from below. Some negative values are rather large. They all occur when the net radiation was large and some could be explained as resulting from too high values of Q. However, Q was always below 0.43 cal/cm²min which is not unlikely high and the instrument in general functioned well. A moderate decrease of Q would anyway not lead to a reasonable value of the computed snow melt S_c.

On the other hand it does not seem likely that the temperature of the water film on the snow crystals would raise to as much as 2°. There are also cases with relatively strong incoming radiation especially in the beginning of the melting period, where the assumption of increased surface temperature would lead to larger discrepancies between measured and computed melt values. We have assumed that $A_z = A'_z$ i.e. that the "Austausch" values for heat and water vapour are identical. If this is not correct a part of the discrepancies may be explained as resulting from that assumption. Further studies will have to be undertaken.

Fig. 4 shows the correlation between hourly values of mean air temperature and melt water. When rough estimates of the daily run off are wanted the maximum temperature or the sum of hourly positive temperature values may be used. The correlation will of course vary with local conditions like latitude, height above the sea, snow depth and density, cloudiness and winds but the method may be appreciated for its simplicity.

As can be seen from fig. 5 the run off in the river Ljusnan close by the "melt station" shows a slow increase already before the air temperature rose to 0°. This may be explained by melting of ice in the river by radiation as the water reflects less than the snow. There is a clear increase in the flow when melting starts to be recorded in the meter and this increase continues until the melt in the meter reaches its maximum on 30 April and still a few more days. Then the melt decreases considerably until 7—8 May and during this time the flow in the river is almost stationary. The 9 May the melt is again increasing and the 11 May the water flow increases again. There is a lag of 2—4 days from melt recorded in the meter to the occurence of an appreciable effect on the flow.

Acknowledgement

Mr. Helge Björklund has assisted in a valuable way in preparation of the field study and in carrying out the laboratory experiments.

REFERENCES

Forsman, A., 1963. Snösmältning och avrinning. *Not. och prelim. rapporter. Ser. Hydrologi Nr 2.* Sveriges Met. och Hydr. Inst. Stockholm (in Swedish).

Gerdel, R. W., 1954. The transmission of water through snow. *Transact. Amer. Geoph. Union.*

Hoeck, E., 1952. Der Einfluss der Strahlung und der Temperatur auf den Schmelzprozess der Schneedecke. *Beiträge zur Geologie der Schweiz. Geotechn. Ser. Hydrologie. Lief. 8.* p. 1—36.

Nyberg, A., 1965. A Study of the Evaporation and the Condensation at a Snow Surface. *Ark. f. Geophys. Bd.* 4 *nr* 30.

de Quervain, M., 1948. Über den Abbau der Alpinen Schneedecke. Union Geod. et Geophys. Int. ass. hydr. Sc. *Procès-verbaux. Assemblée Générale d'Oslo Vol.* 2. p. 55—68.

Ångström, A., 1918. On the Radiation and Temperature of Snow and the Convection of the Air at its Surface. *Ark. f. Mat. Astr. och Fys. Vol.* 13. *Nr* 21.

The radiation balance of earth-atmosphere system over both polar regions obtained from radiation measurements of the Nimbus II meteorological satellite

By

EHRHARD RASCHKE[1] *Laboratory for Atmospheric and Biological Sciences, Goddard Space Flight Center, Greenbelt, Maryland*

FRITZ MÖLLER, *Meteorologisches Institut der Universität München, Germany*

WILLIAM R. BANDEEN, *Laboratory for Atmospheric and Biological Sciences, Goddard Space Flight Center, Greenbelt, Maryland*

ABSTRACT

Measurements of the outgoing emitted longwave radiation and the reflected solar radiation were obtained for the first time over the entire globe from the Nimbus II meteorological satellite. These data were obtained during the period 16 May—28 July, 1966 and covered the onset and development of the summer and winter seasons in the Northern and Southern hemispheres, respectively.

Nimbus II carried a five-channel medium resolution radiometer, two channels of which received longwave radiation and reflected solar radiation in wideband spectral intervals from 5.0 to 30.0 microns and 0.2 to 4.0 microns, respectively. From these "filtered beam" measurements the outgoing "unfiltered" radiation fluxes were calculated using empirical integration techniques. The method of WARK et al. (1962) was applied in principle to compute the outgoing flux of emitted longwave radiation. The flux of reflected solar radiation was computed, utilizing empirically derived models of the dependence of the reflection properties of the earth-atmosphere system on the zenith angles of the sun and the measured beam and on the relative azimuth between the two.

The results of the outgoing longwave radiation, the albedo, and the radiation balance of the earth-atmosphere system were obtained as averages for five subperiods, each of a half month's length. As an example, results obtained for the period 1—15 July, 1966 over both polar regions are presented and discussed in the form of maps in this paper.

The albedo over the central Arctic north of 80° N diminished continuously from May to the end of July from 68 % to 50 % due to the melting of ice and snow surfaces. The radiation balance only during the first half of July became slightly positive (+0.012 cal cm^{-2} min^{-1}) there. During all other subperiods, it resulted in a net radiation flux toward space.

Over the Antarctic during this season the radiation balance is almost entirely determined by the outgoing longwave radiation flux.

The global albedo for all five subperiods was found to be about 30 %. This value is considerably less than earlier accepted values ranging between 33 % and 43 %. The radiation balance over the entire globe resulted in a slight energy gain of +0.002 cal cm^{-2} cm^{-1} during the second half of May and a deficit between —0.003 and —0.007 cal cm^{-2} min^{-1} during the other four subperiods.

1. Introduction

The radiation balance of the earth-atmosphere system over each geographic location describes the energy gain or loss of the system resulting from two processes: "absorption" of incoming solar electromagnetic radiation and emission of longwave thermal radiation. Absorption, reflection and scattering of incident solar radiation and the emission of longwave radiation to space takes place mainly at the surface and in atmospheric layers up to a height of about 50 km. Therefore, the radiation balance deter-

[1] On leave from the University of Munich, Germany, as a National Academy of Sciences Post-Doctoral Resident Research Associate.

mines primarily the net radiation flux at the level of about 50 km, and should be closely related to all atmospheric processes below that level.

Earlier investigations (ALT 1929; BAUR and PHILLIPPS, 1934, 1937; BUDYKO, 1963; HOUGHTON, 1954; LONDON, 1957; SIMPSON, 1929; VOWINKEL and ORVIG 1964) showed clearly that in the annual average, energy is gained at low latitudes and lost at high latitudes. This forms a thermal gradient requiring an energy exchange between low and high latitudes by the atmospheric circulation and also by ocean currents. These investigations, however, were based on observations whose reliability was not very satisfactory over both polar regions and over oceanic areas (ÅNGSTRÖM, 1925). Moreover, the computations of the fluxes of absorbed and emitted radiation, could take into account only in very simplified models all physical processes taking part in the radiative transfer within the atmosphere and at the ground. Thus widely differing results were obtained.

Radiometric measurements of reflected solar radiation and of emitted thermal radiation from artificial satellites should provide an ideal basis to observe steadily and very accurately the radiation balance on a global scale. Such measurements were carried out beginning with the launching of the first meteorological satellite Explorer VII and continuing with different instruments from several TIROS satellites (BANDEEN, HALEV and STRANGE, 1965; HOUSE, 1965; RASOOL and PRABHAKARA, 1966). These satellites however, "observed" the earth no farther poleward than 60° N and 60° S. Nimbus II, launched on May 15, 1966 and the succeeding satellites ESSA 3 and ESSA 5 performed the first radiation measurements over the entire globe. Considerable computational efforts are necessary to determine from the filtered beam measurements of the radiometer the desired quantities, namely the outgoing fluxes of reflected solar radiation and of longwave thermal radiation, leaving the atmosphere to space.

It is the purpose of this paper to discuss the results of the radiation balance and related quantities, which were obtained from Nimbus II measurements during the period 16 May to 28 July, 1966 over both polar regions. This period was divided into 5 smaller intervals each of a half month's duration, of which one was chosen here (1—15 July, 1966) to demonstrate our calculation methods and the results. All other results and the computation methods in more detail will be described in a final report on this research (RASCHKE and PASTERNAK, 1968).

2. The Nimbus II measurement

The satellite Nimbus II was launched on May 15, 1966 into a sun-synchronous, nearly polar orbit (NORDBERG, MCCULLOCH, FOSHEE, and BANDEEN, 1966). At a mean height of 1140 km above the earth's surface it crossed the equator in the northward direction at around local noon and in the southward direction on the opposite side of the earth at around local midnight. Its orbital period of 107 minutes and its height provided that generally each area element on the earth was observed at least once in the daytime and once in the nighttime within a 24 hr interval. But difficulties in the data acquisition from orbit did not allow the recording of all data, thus causing gaps in observational coverage of the globe.

A scanning five-channel medium resolution radiometer aboard Nimbus II measured the reflected solar radiation in the spectral range from 0.2—4.0 microns and the emitted thermal radiation in the spectral range from 5.0 to 30.0 microns. In a third channel infrared radiation between 10 and 11 microns, a measure of the temperature of the underlying surface (clouds and/or ground), was received. The instantaneous angular field of view of the radiometer of about 2.5 degrees enabled a spatial resolution on the earth's surface from about 50 km (at the subsatellite point) to about 110 km (at a nadir angle of 40 degrees). A calibration source aboard Nimbus II provided for correcting the measurements of infrared radiation for changes in the instrumental response. The measurements of reflected solar radiation were checked by comparison of all measurements obtained over cloudless portions of the Sahara. No changes in the instrumental response could be observed in these measurements.

3. Method of computation

The net radiation flux or radiation balance Q at a surface element, whose geographic coordinates on the earth's surface are λ and Φ is defined as the algebraic sum of all radiation fluxes crossing it:

$$Q(\lambda,\Phi,\ d)=S(\lambda,\Phi,\ d)-R(\lambda,\Phi,\ d)-E(\lambda,\Phi,\ d). \quad (1)$$

In Equation (1) S, R and E are the fluxes of incoming and reflected solar radiation and of emitted longwave radiation, respectively. The letter d designates that day, for which Equation (1) applies. The reference area is assumed to be perpendicular to the earth's radius vector passing through it.

The fluxes R and E outgoing from an observed element on the earth's surface have been computed by integrating the radiance N over the hemisphere above that surface:

$$\text{Flux}=\int_0^{2\pi}\int_0^{\pi/2} N(\theta,\psi)\sin\theta\cos\theta\,d\theta\,d\psi. \quad (2)$$

In this general equation θ and ψ are the zenith angle and the relative azimuth angle (with respect to the vector of incident solar radiation) of a measurement by the Nimbus II radiometer.

The computational procedure presumes the geometric generalization that the atmosphere and surface of the earth form the surface of an imaginary sphere, having the mean radius of the earth (6371 km), but still having the same physical properties as the actual earth-atmosphere system. The computational procedures of both outgoing radiation fluxes required further generalized assumptions to convert the measured "filtered" radiances into the "unfiltered" radiances and to perform the integration over the upward hemisphere.

According to the method of WARK et. al. (1962) the unfiltered radiance of longwave thermal radiation was computed from the measured "filtered" radiance using a relation, which was found from calculated values of the outgoing radiance from a large set of atmospheric profiles (LIENESCH, 1966). Figure 1 shows as dots calculated radiances in the vertical direction. Encircled points mark results computed for a zenith angle $\theta=78.5°$. These results show a nearly linear relation between the "filtered" and "unfiltered" radiances due to the wide filter range (5.0—30.0 microns) of the channel used for the measurements.

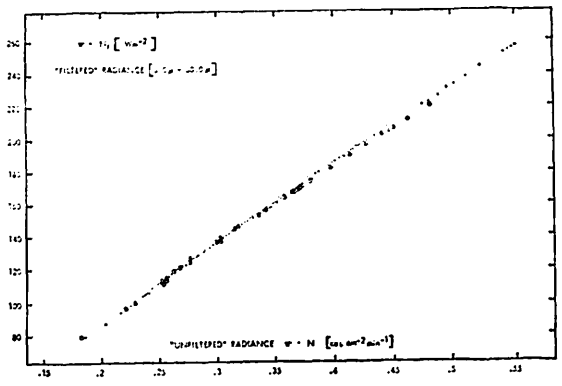

FIG. 1. Nimbus II: Relation between the "filtered" (5.0—30.0 microns) and "unfiltered" radiance of outgoing longwave radiation.

A relation which desribes the dependence of N on the zenith angle was determined statistically by LIENESCH and WARK (1967) from radiation data of TIROS satellites. An assumption of symmetry of emitted longwave radiation with respect to the azimuth angle ψ was made in this study.

The thermal radiation outgoing from an area is strongly correlated with the temperature of the underlying surface (MÖLLER and RASCHKE, 1964); thus it is largely dependent on daily changes of the cloudiness and on the temperature at the ground. Over most regions of the earth Nimbus II measured longwave radiation twice a day, close to local midnight and local noon. It has been assumed that these measured values are mean values for nighttime and daytime conditions, respectively. The daily mean of the flux then was calculated by weighting each of both values according to the duration of the daytime and nighttime periods, respectively.

The calculation of the reflected flux of solar radiation during a day from an "observed area" is more complicated, since the reflection properties of the earth-atmosphere system show clearly a strong dependence on both the zenith and azimuthal angles (θ and ψ) of the measurements and on the sun's elevation above the horizon (e.g. ARKING, 1965; BARTMAN, 1967; COULSON, 1959; HEGER,

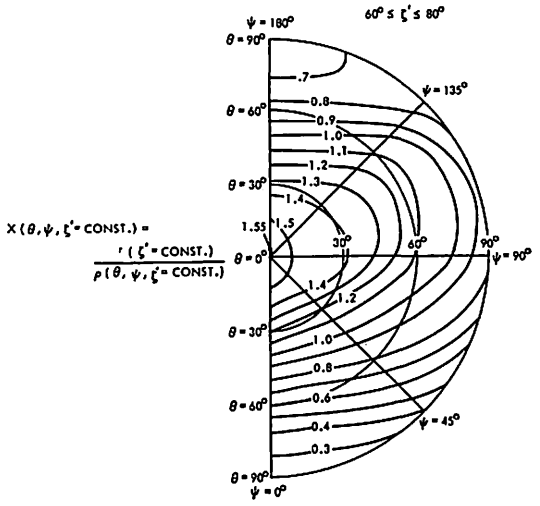

FIG. 2. Dependence of the ratio $X = r/\varrho$ on the angles θ and ψ of the measurement at very low sun ($60 < \zeta' < 80°$).

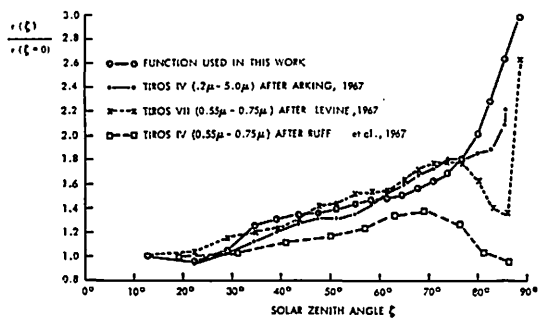

FIG. 3. The relative change of the directional reflectance, r, of the earth-atmosphere system with the sun's zenith angle, ζ'.

1966). This required, as mentioned above, the determination of the solar radiation reflected into the upward hemisphere from the measured beam radiance N and an extrapolation from the moment of measurement to the interval from sunrise to sunset over the same area. The simplifying assumption of a Lambertian surface, as was done in the past by several authors (BANDEEN, HALEV and STRANGE, 1965; MÖLLER, 1967; RASOOL and PRABHAKARA, 1966; WINSTON, 1967) probably caused an underestimation of the reflection properties of the earth-atmosphere system, especially at very low solar elevation angles.

The method of calculating the flux of reflected solar radiation between sunrise and sunset is only briefly outlined here. From the measured "filtered" radiance N_f the bidirectional reflectance ϱ_f' is obtained by means of Equation (3):

$$\varrho_f'(\theta, \psi, \zeta') = \frac{N_f(\theta, \psi)}{S_f(d) \cos \zeta'} [sr^{-1}]. \qquad (3)$$

Here ζ' is the solar zenith angle at the moment of measurement. The "filtered" irradiance S_f of incoming solar radiation is obtained by integrating the product of the extraterrestrial spectral irradiance of solar radiation (JOHNSON, 1954) and the filter function of the instrument over all wavelengths. Because of the wide range (0.2—4.0 micron) of that filter it was assumed that ϱ_f' in Equation (3), which refers to the "filtered" radiation only, is equal to the mean reflectance ϱ' over the entire spectrum.

To determine the ratio r between the radiation reflected into the entire hemisphere and the incident solar irradiance at the zenith angle ξ' an integration is needed over θ and ψ analogous to Equation (2). Therefore diagrams were derived from many measurements of reflected solar radiation (ARKING, 1965; BARTMAN, 1967; CHERRIX and SPARKMAN, 1965; SALOMONSON, 1966) showing the ratio $X = r/\varrho$ (where $\varrho = \pi \cdot \varrho'$) versus θ and ψ. One of these diagrams, which were drawn for only three ranges of the sun's zenith angle ξ' (viz., 0°—35°, 35°—60°, 60°—80°), is shown in Figure 2. It demonstrates that at low sun ($60° < \zeta' < 80°$) the ratio r/ϱ is very small for ψ but large θ, corresponding to a bright horizon in the direction of the sun and also a relatively high radiance of backscattered radiation for values of ψ near 180°. The reflectance $\varrho = \pi \cdot \varrho'$ is small in the nadir and larger towards all points of the horizon. The integral of r/ϱ over the hemisphere is π. The ratio r, often called the directional reflectance (BARTMAN, 1967), is still a function of the sun's zenith angle. Thus for the computation of the outgoing flux of solar radiation reflected to space from an area between sunrise and sunset, a statistical relation, obtained from the above mentioned measurements, was used. In Figure 3 this relation is compared with results recently

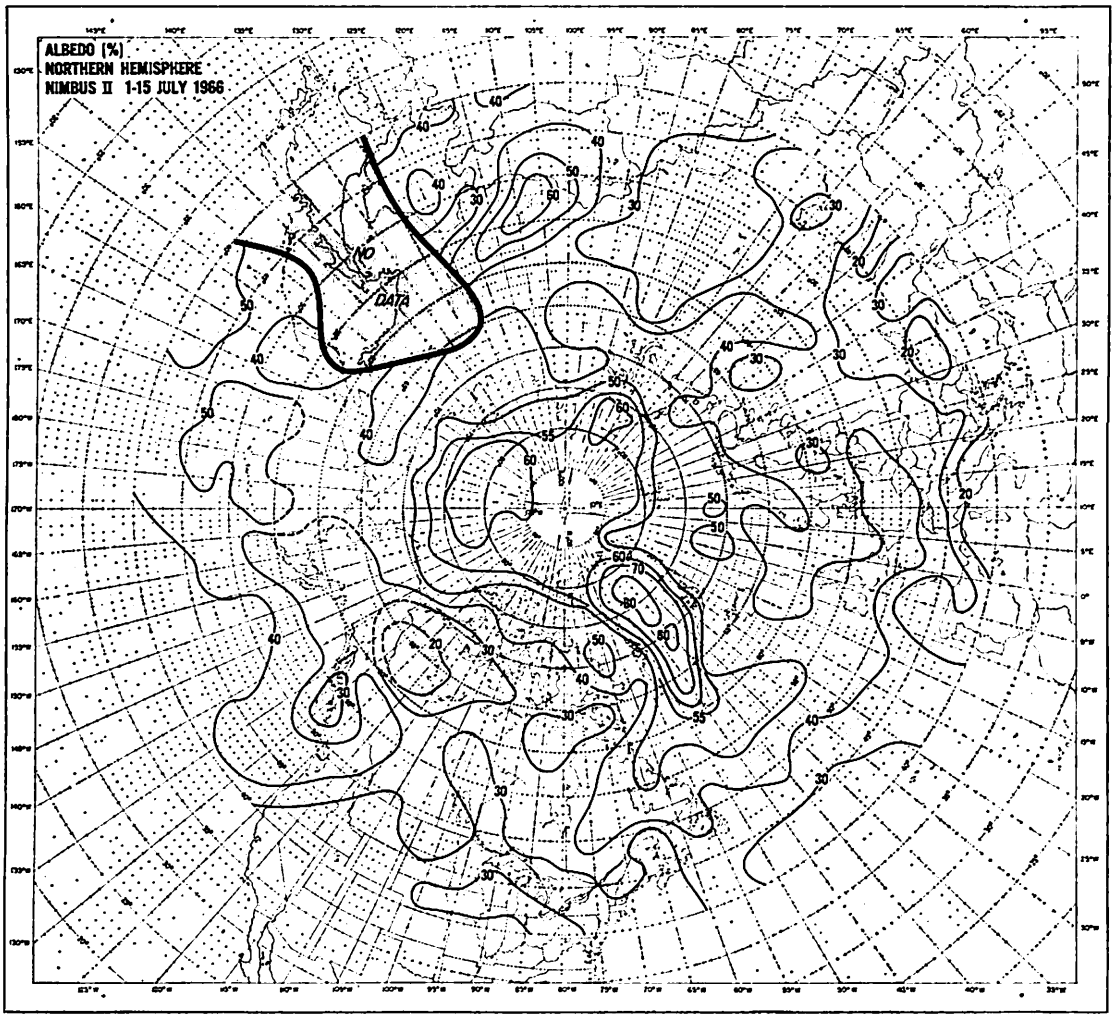

FIG. 4. Nimbus II: Albedo [%] of the earth atmosphere system over the northern hemisphere during the period 1—15 July, 1966.

obtained statistically by several authors from TIROS measurements.

In a further step the mean daily albedo, which is the ratio between daily reflected and daily incident solar radiation, was obtained from a single measurement of r by integrating over all solar elevations during the day from sunrise to sunset. With a simple model (Table IX in BAUR, 1953) a mean refraction of solar radiation in the atmosphere was taken into account in calculations of both the incoming and the reflected flux of solar radiation. The solar constant S_0 was assumed to be 2.0 cal cm^{-2} min^{-1} although recently Drummond et al. (1967) found from airplane measurements a lower value of 1.95 cal cm^{-2} min^{-1}.

All single results were averaged within grid fields of the size of 5 degrees of longitude and 2 to 5 degrees of latitude. Measurements in both spectral ranges obtained at zenith angles larger than 45 degrees were omitted to avoid excessive limb effects in the results. The albedo of an observed area was then

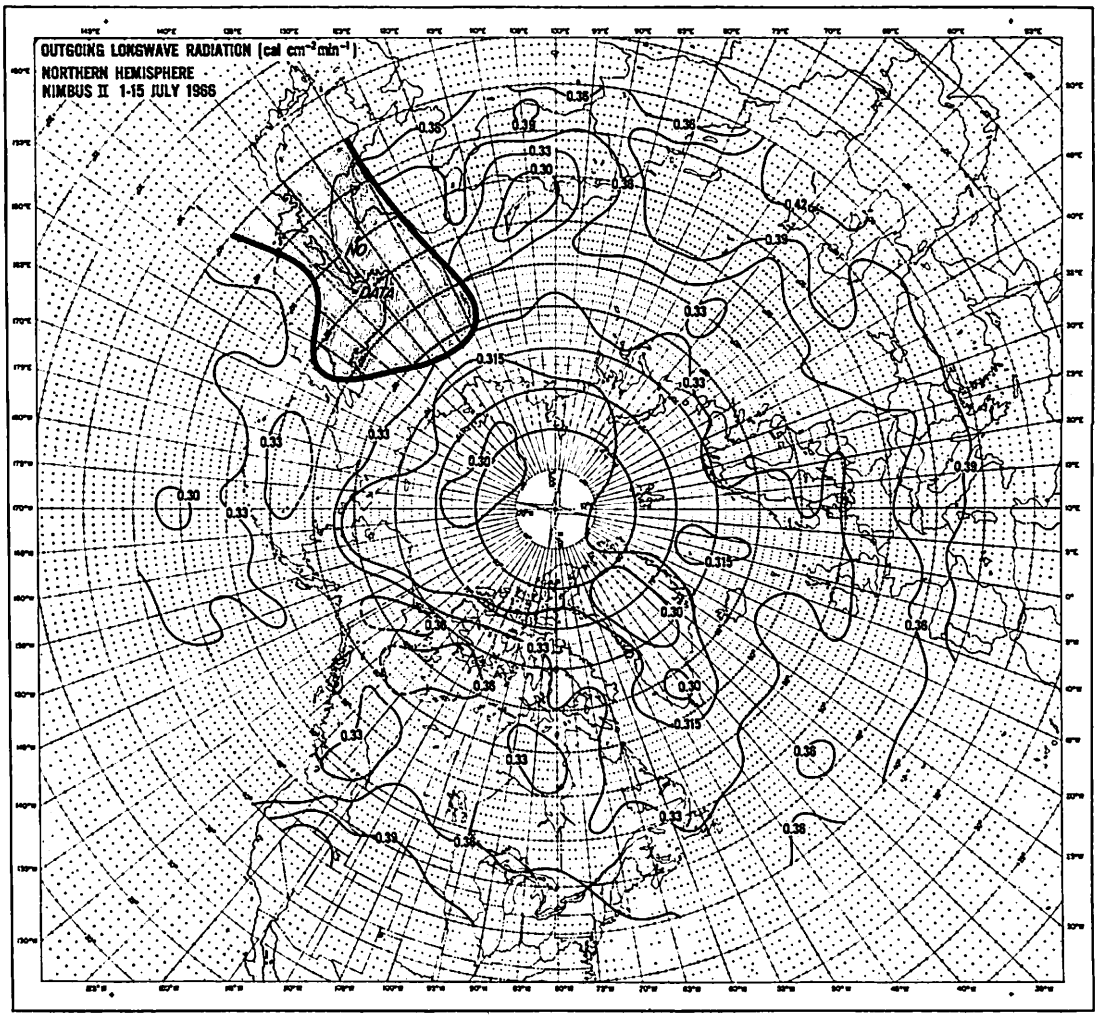

FIG. 5. Nimbus II: Total outgoing longwave radiation flux [cal $cm^{-2}min^{-1}$] over the northern hemisphere during the period 1—15 July, 1966.

defined to be the ratio of R over S. The difference between S and R simply describes the absorbed amount of solar radiation.

These simplified models, indeed, may cause considerable errors in the results, if used for specific geographic areas and meteorological conditions such as cloudless, partially cloudy, and overcast cases. In investigations of the radiation balance over smaller geographic locations more sophisticated models should be used. These however have not been derived so far, due to the lack of observational data. It is believed, however, that such errors are averaged out in these investigations on a global scale.

4. Radiation balance over the arctic basin

During that time when data of the Nimbus II medium resolution radiometer were available the sun's declination ranged between +19 and +23 degrees. Thus, the earth-atmosphere system over the North-Pole received during a 24 hour interval even more solar radiation than regions in the northern subtropics. But ice and snow surfaces and a

TABLE 1. *Zonal averages of the incoming (S) and absorbed (S—R) solar radiation, the emitted longwave radiation (E), the radiation balance (Q) and the albedo (R/S) over the northern hemisphere. Periods 1—5 are listed in Table II.*

Latitude	Period	R/S %	S	S—R	E	Q
			All in cal cm^{-2} min^{-1}			
85° N	1	66.3	0.682	0.230	0.284	—0.054
	2	65.7	0.746	0.256	0.296	—0.040
	3	61.9	0.762	0.290	0.312	—0.012
	4	56.6	0.738	0.320	0.308	+0.012
	5	55.2	0.670	0.300	0.310	—0.010
80° N	1	68.9	0.675	0.210	0.282	—0.072
	2	67.9	0.736	0.236	0.296	—0.060
	3	61.6	0.756	0.290	0.310	—0.020
	4	57.7	0.728	0.308	0.309	—0.001
	5	56.1	0.660	0.290	0.312	—0.022
75° N	1	67.7	0.662	0.214	0.286	—0.072
	2	64.6	0.724	0.256	0.300	—0.044
	3	58.9	0.740	0.304	0.306	—0.002
	4	55.8	0.715	0.316	0.310	+0.006
	5	48.8	0.648	0.332	0.310	+0.022
70° N	1	60.3	0.650	0.258	0.296	—0.038
	2	52.3	0.705	0.336	0.312	+0.024
	3	47.2	0.720	0.380	0.315	+0.065
	4	45.7	0.696	0.378	0.320	+0.058
	5	44.9	0.635	0.350	0.315	+0.045
65° N	1	47.8	0.644	0.336	0.305	+0.031
	2	39.9	0.690	0.415	0.327	+0.088
	3	39.3	0.700	0.425	0.322	+0.103
	4	41.1	0.680	0.400	0.327	+0.073
	5	40.7	0.632	0.375	0.327	+0.048

mean cloud coverage of 6/10 to 10/10[1] caused more than 50 % of the incoming radiation to be reflected back to space. Figure 4 illustrates this for the period 1—15 July, 1966.

In Figure 4 the 50 % isoline follows (except south of Greenland) closely the climatological boundary of a mean ice coverage of 0.8—1.0 of the arctic ocean during this period (U.S. NAVY HYDROGRAPHIC OFFICE, 1958). The same position of that boundary is confirmed by the Nimbus II AVCS photographs of the same period. The albedo over the Norwegian Sea and over the Barents Sea, which were icefree but also covered with 6/10 to 10/10 of clouds, is remarkably less than over the aforementioned areas, demonstrating the high influence of the reflectance of the ice surface on the total albedo and, therefore, also on the radiation budget of the earth-atmosphere system. Since the ocean water has a reflectance of less than 10 % the albedo of the cloud-ocean surface system is strongly diminished even over dense cloud covers. The reflectance of the ground contributes much to the amount of shortwave radiation flux emerging from the upper surface of the clouds.

The albedo over Greenland sharply rises from the coastline to the interior from 60 % to more than 80 %. This corresponds to the surface albedoes of 71 % to 79 % measured by KASTEN (1963) over the Greenland ice

[1] Maps of the mean cloud coverage over the Northern hemisphere were obtained for the same periods of Nimbus II measurements through the courtesy of the USAF Environmental Technical Applications Center, Washington, D.C.

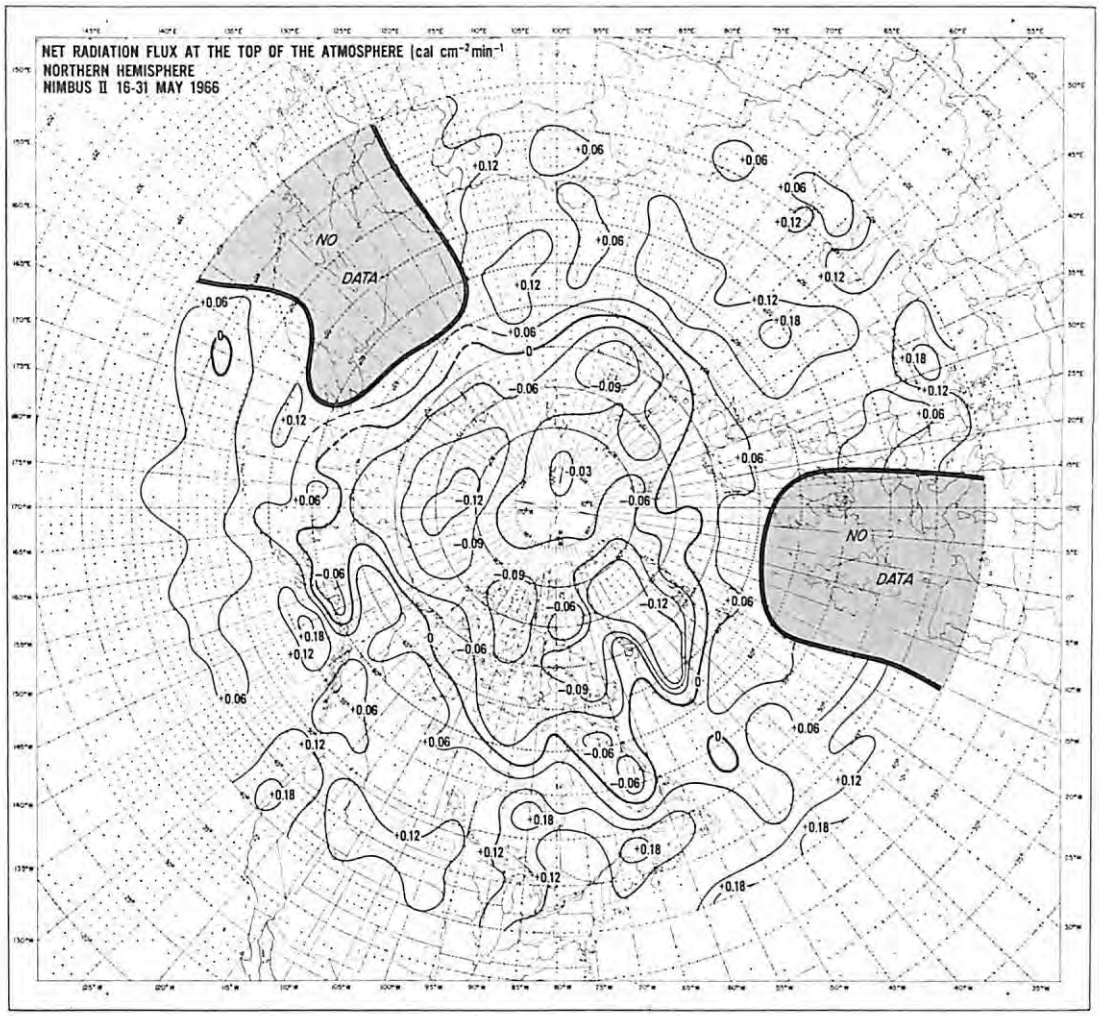

FIG. 6. Nimbus II: Radiation balance of the earth atmosphere system over the northern hemisphere during the period 16—31 May, 1966.

cap. The albedo as measured from space over Greenland remains nearly constant (from May to July), while the average albedo of the northern hemisphere (as shown in Table I) decreases due to melting of ice and snow surfaces. This decrease of the albedo and the very high sun during the end of June and the first half of July causes the amount of absorbed solar radiation to exceed the radiation loss by outgoing longwave radiation over the pole during the first half of July.

Figure 5 shows the field of outgoing longwave radiation for the same period. Due to a cloud cover with mostly stratocumulus, altostratus. and stratus this field is nearly uniform. Only over the high inland ice of Greenland and over the thick ice mantle on the East Siberian Sea areas of lower emission occur. As Table I shows the outgoing longwave radiation increases only slowly during the beginning of the northern summer until June, then remains constant during July (period 4 and 5). This holds also for the mean temperature of the earth-atmosphere system. Thus changes in the amount of the incoming solar radiation

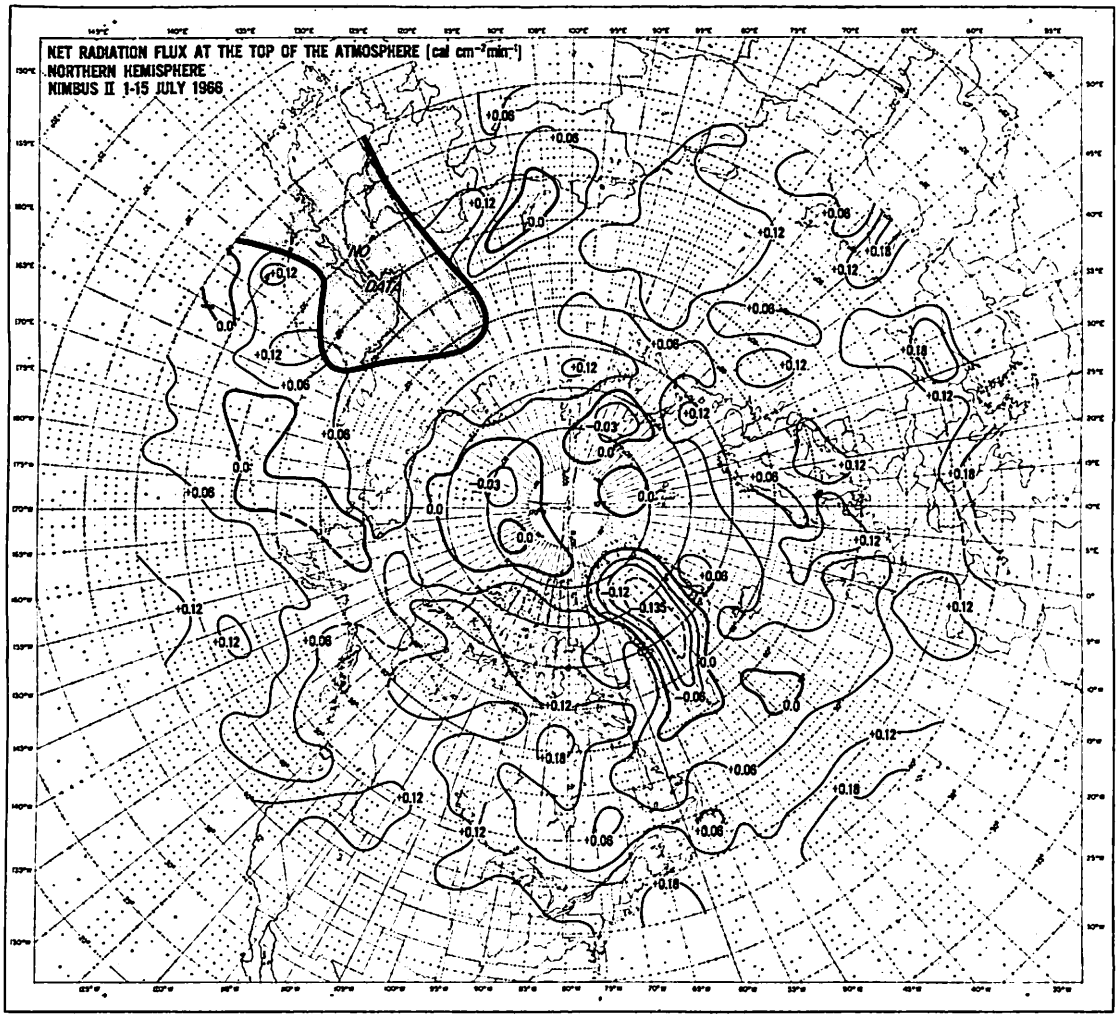

FIG. 7. Nimbus II: Radiation balance of the earth atmosphere system over the northern hemisphere during the period 1—15 July, 1966.

as well as changes in the albedo during this time of the year solely influence the radiation balance of the Arctic.

Figures 6 and 7 show maps of the radiation balance (i.e., the net radiation flux at the top of the atmosphere) for two periods. During the second half of May (Figure 6) the radiation balance north of 70° N is everywhere negative except over the Norwegian Sea, where lower albedoes occur over the icefree sea surface. Here clearly the influence of the polar ice cap on the radiation budget is demonstrated. This subject has been discussed by several authors (FLETCHER, 1965; VOWINKEL and ORVIG, 1964). Maxima of the deficit occur over Greenland and over the East Siberian Sea. They remain deficit areas even during the first half of July, when over all other areas the amount of absorbed solar radiation slightly exceeds the emitted radiation (Figure 7). Zonal averages in Table I show that the radiation balance becomes negative towards the end of July north of 75° N due to decreasing elevation of the sun

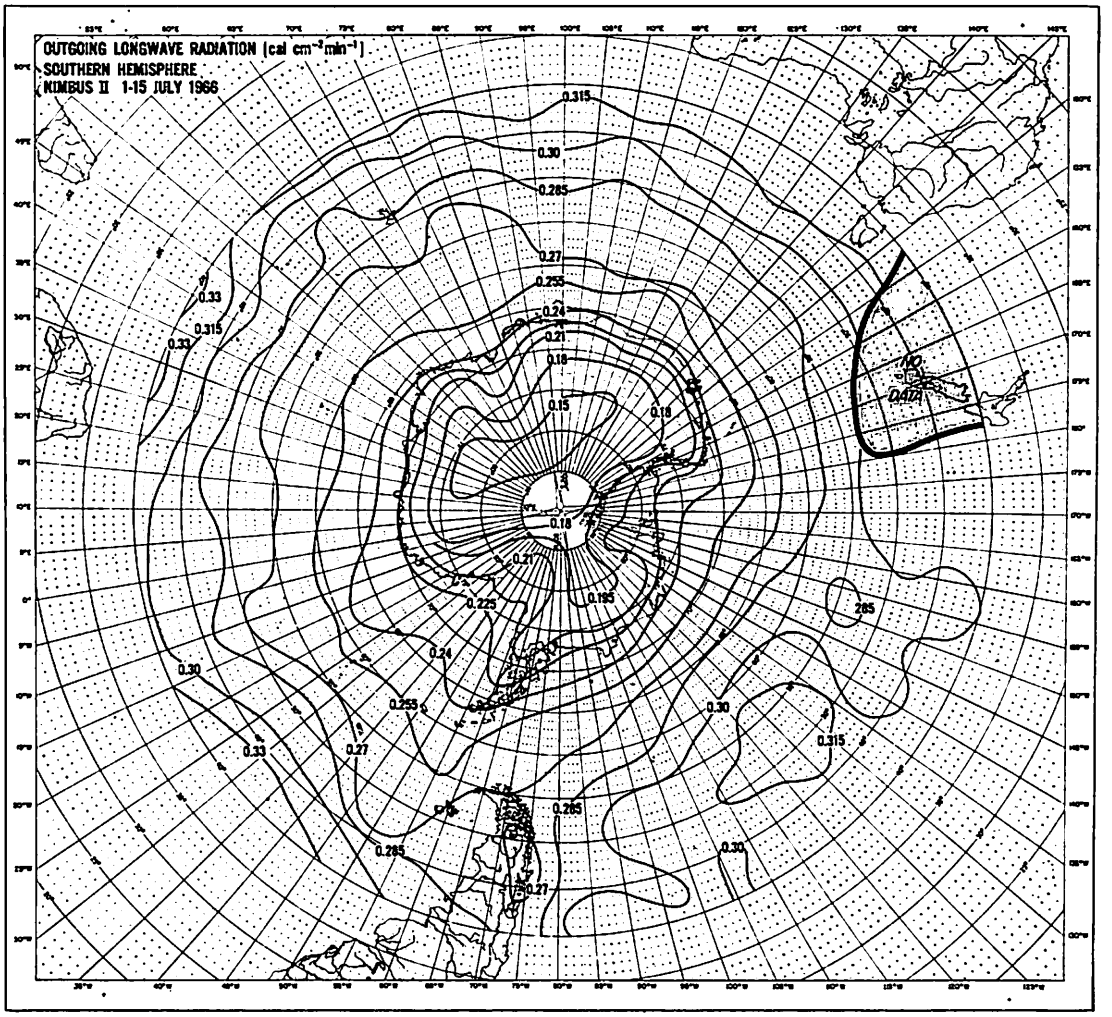

FIG. 8. Nimbus II: Total outgoing longwave radiation flux [cal cm^{-2}min^{-1}] over the southern hemisphere during the period 1—15 July, 1966.

above the horizon. These results do not agree with studies of other authors. VOWINKEL and ORVIÜ (1964) found positive values for the radiation balance over the central arctic in their very detailed analyses only for June, while FLETCHER (Figure 10 in (FLETCHER, 1965)) has obtained a positive balance also for the months May and July. VOWINKEL and ORVIG (1964), perhaps might have underestimated the cloud cover in upper layers of the atmosphere (HENDERSON, 1967).

5. Radiation balance over the antarctic

The Antarctic continent south of 71° S did not receive any solar radiation from May to July. Thus the radiation balance during this period consists entirely of the loss of radiative energy by emission of thermal radiation. Figures 8 and 9 show the fields of outgoing longwave radiation and of the equivalent blackbody temperature of infrared radiation between 10 and 11 microns, which

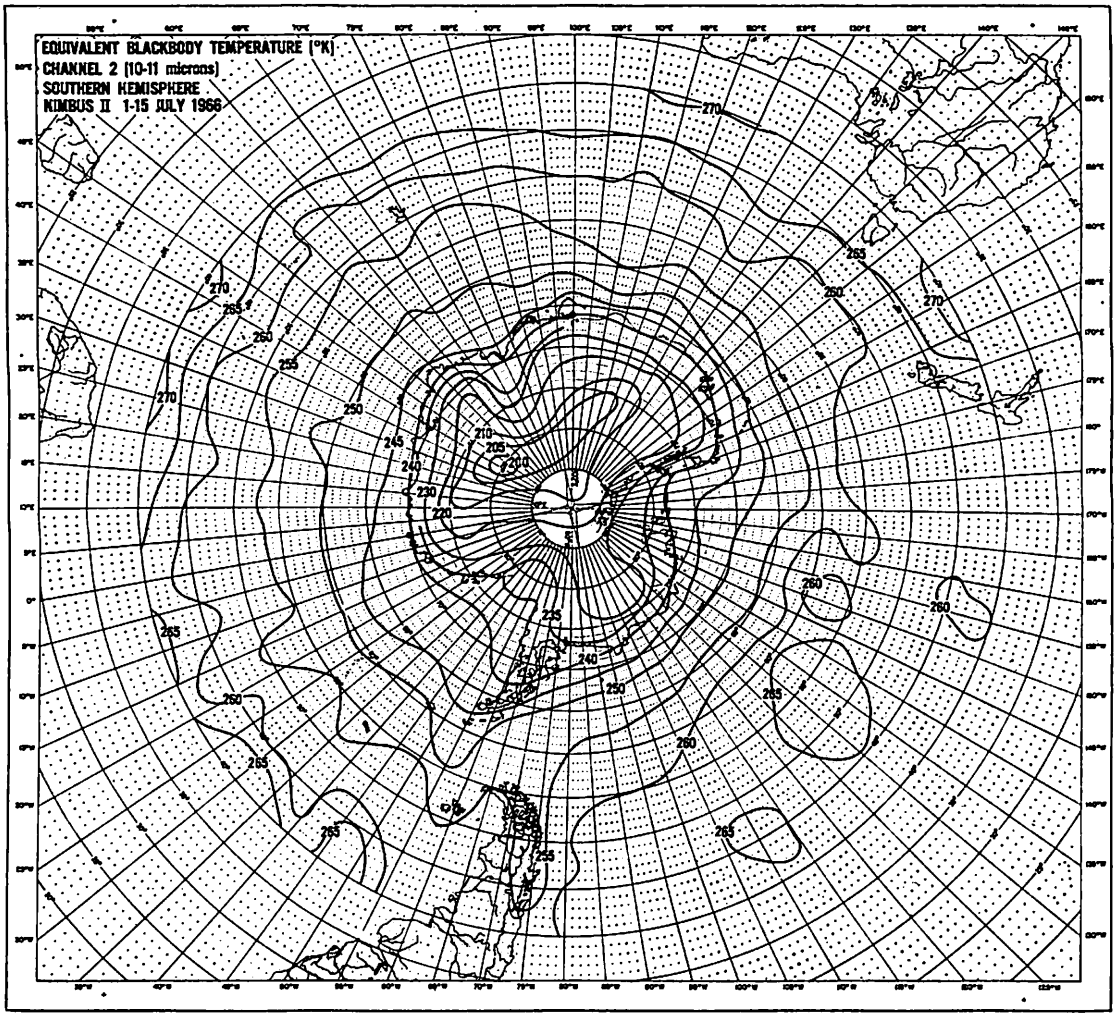

FIG. 9. Nimbus II: Equivalent blackbody temperature [°K] of infrared radiation in the spectral range 10—11 microns emerging over the southern hemisphere during the period 1—15 July, 1966.

is very close to the temperature of the underlying surface. The pattern of both fields over the southern oceanic areas is almost zonal. The 250° K isotherm in Figure 9 closely follows the mean climatological pack-ice boundary during July (U.S. NAVY HYDROGRAPHIC OFFICE, 1957). Over the continent the isolines follow more or less the geographic contours. At the Soviet Plateau close to Queen Maud Land with elevations of more than 3500 meters above sea level, surface temperatures of less than 210° K (see also Figure 77 in ATLAS OF THE ANTARCTIC, 1966) cause a minimum in the field of outgoing longwave radiation. High cloud surfaces over the west coast of South America and east of the Antarctic Peninsula are clearly associated with areas of low temperature in Figure 9 and therefore with lower emitting areas in Figure 8.

Solar radiation is available only north of 71° S to compensate for the loss of radiative energy. Because of the minimum of longwave emission in the central antarctic continent and of the increase of emission toward lower latitudes the radiation balance shows a

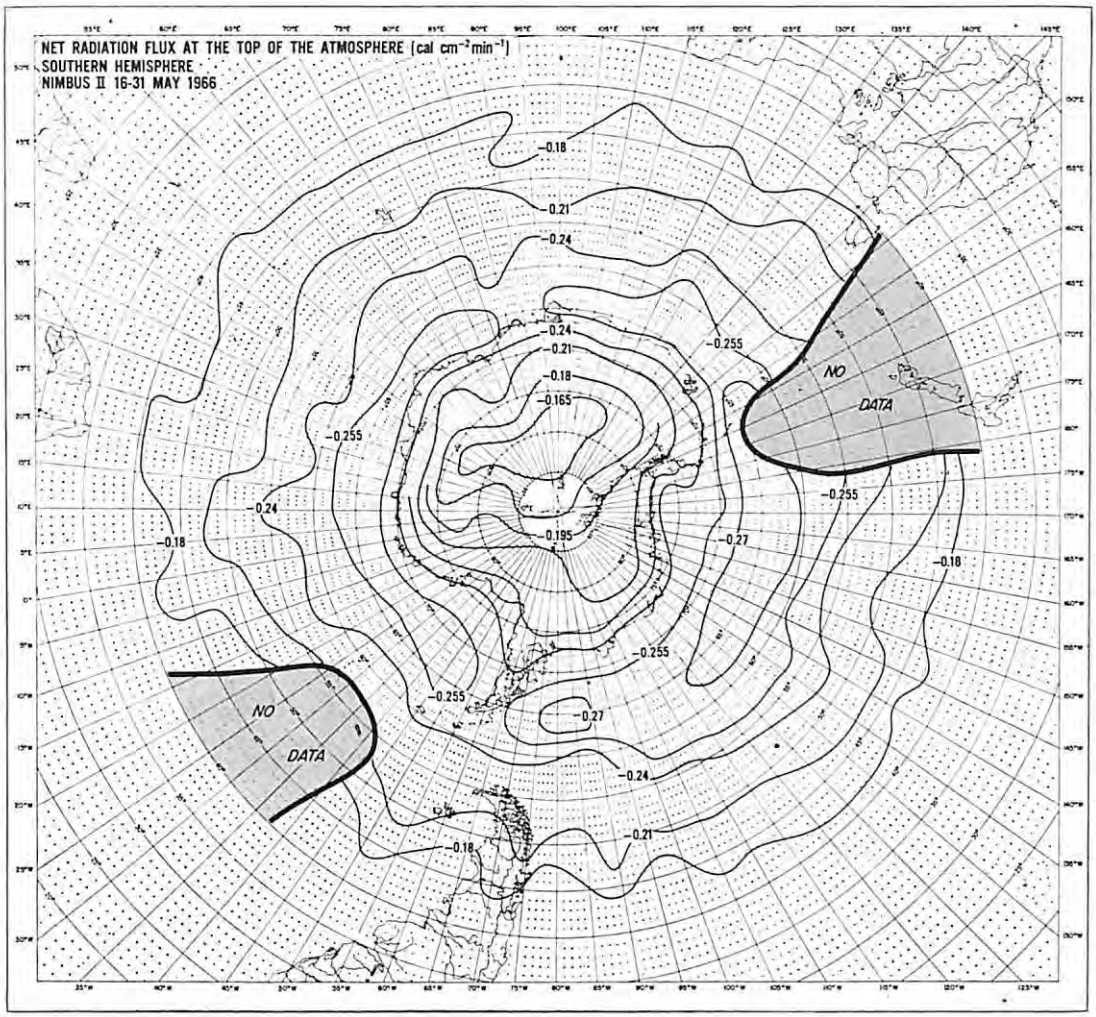

FIG. 10. Nimbus II: Radiation balance of the earth atmosphere system over the southern hemisphere during the period 16—31 May, 1966.

maximum radiation deficit of more than 0.24 cal. cm^{-2} min^{-1} in a zonal ring between 55° and 70° S during May (Figure 10). This ring expands slightly during the first half of June, but becomes smaller toward July (Figure 11) due to decreasing temperatures by radiative cooling and the equatorward expansion of the pack ice at its southern boundary and an increase of incoming solar radiation at its northern boundary.

Zonal averages of the radiation balance for all five periods (Table II) show clearly a rapid cooling of the inner Antarctic from May to the end of June with a reduced rate during July. At 70°—80° S the cooling is nearly compensated for in July by advection. At lower latitudes the maximum of the radiation deficit occurs at the end of June at lowest elevations of the sun above the horizon.

GABITES' (in DWYER, 1960) and SIMPSON'S (1929) results on the radiation balance of the earth-atmosphere system are added for comparison in Table II. Gabites, who used observational material from the IGY (1957—1958), obtained the closest agreement with

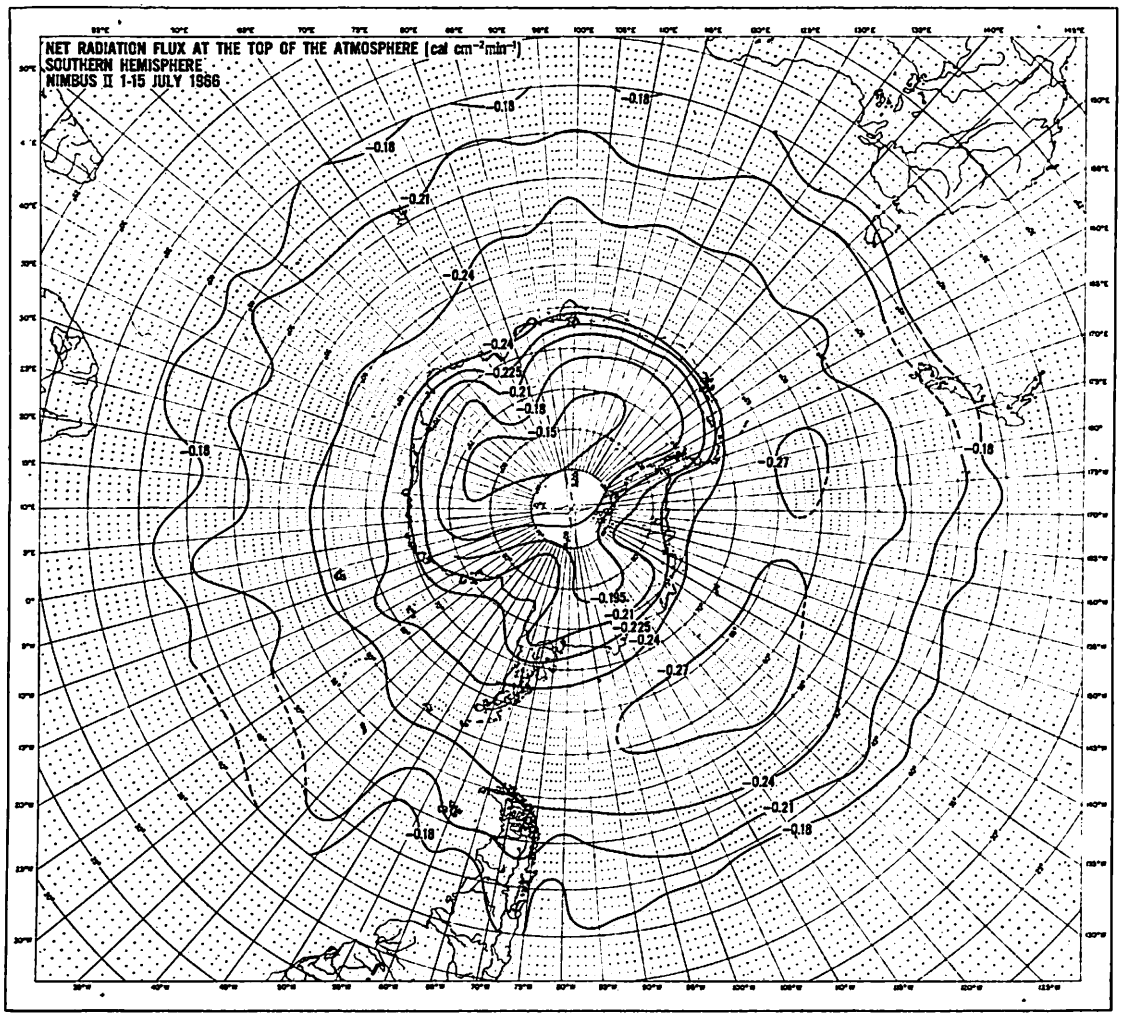

FIG. 11. Nimbus II: Radiation balance of the earth atmosphere system over the southern hemisphere during the period 1—15 July, 1966.

our results at 60° S and 65° S. Simpson's values over the Antarctic continent show a radiation loss which is too high, since he derived the temperatures there by extrapolation from lower latitudes.

6. Global radiation balance

The geographic distribution of the radiation balance during the first half of July over the entire globe is shown in Figure 12. During this time an energy surplus of absorbed solar radiation over emitted longwave radiation is found nearly everywhere north of 10° S. Maxima of energy gain occur over the relatively cloudless northern subtropical oceans. The large desert areas of North Africa and Arabia in contrast show a deficit, which has been predicted by BUDYKO (1963) for the annual average. This deficit is caused by the high values of the albedo (30 % to 40 %) and by the high surface temperature of those areas. Over the entire southern hemisphere south of 10° S the radiation balance everywhere is negative. The deficit over land was found to be somewhat higher

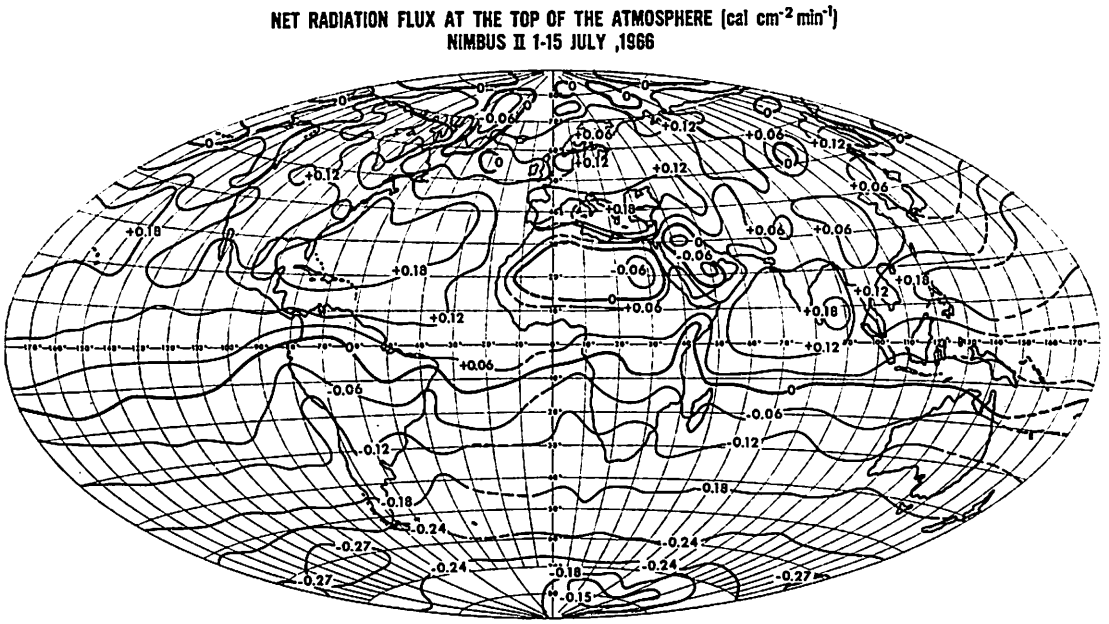

FIG. 12. Nimbus II: Radiation balance of the earth atmosphere system over the entire earth during the period 1—15 July, 1966. The deficit over Greenland exceeds 0.12 cal cm^{-2} min^{-1}.

than over the surrounding oceanic areas at the same latitude.

The numerical values in Figure 12 clearly differ from the figures obtained by MÖLLER (1967) in a preliminary study, mainly due to the fact that the careful corrections we have developed in section 3 were not applied in his investigations of Nimbus II measurements during the same period.

Table III summarizes the global averages, of the albedo, of the absorbed solar radiation, of the emitted longwave radiation, and of the radiation balance. These values in contrast to the zonal averages shown in Tables I and II show no significant changes with time indicating that the entire globe changes its radiation budget, if at all, only over a longer period than that of these satellite measurements. The global albedo was found to be only 29—30 % which is considerably less than all values be-

TABLE II. *Zonal averages of the radiation balance over the southern hemisphere. Values in cal cm^{-2} min^{-1}.*

	Period	85° S	80° S	75° S	70° S	65° S	60° S	55° S
Nimbus II	16—31 May	—0.190	—0.194	—0.208	—0.238	—0.250	—0.248	—0.234
	1—15 June	—0.185	—0.195	—0.204	—0.233	—0.250	—0.256	—0.245
	16—30 June	—0.180	—0.185	—0.195	—0.228	—0.252	—0.256	—0.250
	1—15 July	—0.176	—0.183	—0.193	—0.222	—0.240	—0.245	—0.238
	16—28 July	—0.170	—0.183	—0.193	—0.218	—0.238	—0.240	—0.225
Gabites	June	—0.186	—0.200	—0.225	—0.240	—0.250	—0.247	—0.233
(in DWYER, 1960)	July	—0.180	—0.195	—0.225	—0.235	—0.250	—0.243	—0.230
SIMPSON	June	—0.253		—0.254		—0.245		—0.226
(1928)	July	—0.253		—0.253		—0.240		—0.213

TABLE III. *Global Radiation Balance from Nimbus II Measurements.*

	Albedo %	Absorbed Solar Radiation	Outgoing Long-wave Radiation	Radiation Balance
		all in cal cm^{-2} min^{-1}		
May 16—31	30.1	0.341	0.339	+0.002
June 1—15	30.6	0.337	0.342	—0.005
June 16—30	30.1	0.338	0.345	—0.007
July 1—15	29.1	0.343	0.346	—0.003
July 16—28	29.5	0.342	0.345	—0.003

tween 33 % and 43 % obtained by several authors in earlier studies (ALDRICH, 1919; BAUR and PHILLIPPS, 1934; 1937; FRITZ, 1949; SIMPSON, 1929; ÅNGSTRÖM, 1962). The global average of the radiation balance was slightly positive at the end of May, and ranged between —0.003 cal cm^{-2} min^{-1} and —0.007 cal $cm^{-2}min^{-1}$ during all other periods. This slight radiation deficit was earlier suggested by SIMPSON (1929) for the same season. But due to uncertainties in our computational methods as well as due to the incertainties in the true value of the solar constant, these values do not allow definite conclusions about the heat budget of the earth-atmosphere system. They indicate, however, that a revision of the hitherto-given models of the budget of solar and terrestrial radiation appears necessary. Unfortunately, the period of available radiation measurements from the Nimbus II satellite was too short to correlate our results on the radiation balance with indices describing typical features of the circulation (HUSCHKE, FLETCHER and RAPP, 1967).

Acknowledgements

The authors should like to express their appreciation to Mr. Robert Hite and Mr. Hugh Powell for their extensive efforts in the computer processing of the vast amount of satellite radiation measurements utilized in this study.

REFERENCES

ALDRICH, L. B., 1919, The Reflecting Power of Clouds, *Smithsonian Miscellaneous Collections 69, No. 10.*

ALT, E., 1929, Der Stand des Meteorologischen Strahlungsproblems. *Meteor. Zeitschrift, 46,* pp. 504—513.

ARKING, A., 1965, The Angular Distribution of Scattered Solar Radiation and the Earth Albedo as observed from TIROS. *Institute for Space Studies, New York, Research Reports,* July 1, 1964—June 30, 1965, pp. 47—67.

ATLAS OF THE ANTARCTIC (ATLAS ANTARKTIKI), 1966, Moscow-Leningrad.

BANDEEN, W. R., M. HALEV, and I. STRANGE, 1965, A Radiation Climatology in the Visible and Infrared from a TIROS Meteorological Satellite. NASA Technical Note D-2534, 30 pp.

BARTMAN, F. L., 1967, The Reflectance and Scattering of Solar Radiation by the Earth. Technical Report, 257 pp, University of Michigan, Contr. NASr-54(03).

BAUR, F., ed. *Linke's Taschenbuch der Meteorologie.* Neue Ausgabe, Vol. II. Leipzig, 1953.

BAUR, F. and H. PHILIPPS, 1934, 1937, Der Wärmehaushalt der Lufthülle der Nordhalbkugel in Januar und Juli and zur Zeit der Äquinoktien und Solstitien. *Gerl. Beitr. Geophys., 42,* pp. 160—207; *45,* pp. 82—132.

BUDYKO, M. I., ed., 1963, *Atlas of the Heat Balance of the Earth* (Atlas Teplovogo Balansa Zemnogo Shara), Moscow.

COULSON, K. L., 1959, Characteristics of the Radiation Emerging from the Top of a Rayleigh Atmosphere, *Planet, Space Sci., 1,* pp. 265—284.

CHERRIX, T., and B. SPARKMAN, 1965, A Preliminary Report on Bidirectional Reflectances of Stratocumulus Clouds Measured with Airborne Medium Resolution Radiometer. *NASA X-622-76-48,* Goddard Space Flight Center.

DRUMMOND, A. J., J. R. HICKEY, W. J. SCHOLES, and E. G. LAUE, Multichannel Radiometer Measurement of Solar Irradiance, 1967. *The Eppley Laboratory Inc., Reprint Series No. 33,* Paper presented at the AIAA Meeting, Jan. 23—26, 1967, in New York.

DWYER, L. J., ed., 1960, *Antarctic Meteorology*—Proceedings of the Symposium held in Melbourne, Febr. 1959, Pergamon Press.

FLETCHER, J. O., 1956, The Heat Budget of the Arctic Basin and Its Relation to Climate. *The RAND Corporation, R-444-PR.*

FRITZ, S., 1949, The Albedo of the Planet Earth and of Clouds. *Journ. Meteor., 6,* pp. 277—282.

HEGER, K., 1966, Die von der getrübten Atmophäre nach aussen gestreute Strahlung. *Beitr. z. Physik d. Atm., 39,* pp. 12—36.

HENDERSON, P., 1967, Cloud Conditions over the Beaufort Sea. Publ. in *Meteorology, No. 86, Dept. of Meteor., McGill University,* Montreal, Canada.

HOUGHTON, H. G., 1954, On the Annual Heat Ba-

lance of the Northern Hemisphere. *Journ. Meteor. 11*, pp. 3—9.

HOUSE, F. B., 1965, The Radiation Balance of the Earth from a Satellite. Ph. D. Thesis, Dept.of Meteor., The University of Wisconsin.

HUSCHKE, R. E., J. O. FLETCHER, and R. P. RAPP, An Apparent Statistical Relationship Between Polar Heat Budget and Zonal Circulation. Contr. No. NASr-21-(07), January 1967, RM-5234-NASA, *The RAND Corporation*, Santa Monica, Calif.

JOHNSON, F. S., 1954, The Solar Constant. *Journ. Meteor., 11*, pp. 431—439.

KASTEN, F., 1963, Meteorologisch-Optische Untersuchungen auf dem grönländischen Inlandeis. *Polarforsch, 5*, pp. 202—207.

LEVINE, J. S., 1967, The Planetary Albedo Based on Satellite Measurements Taking into Account the Anisotropic Nature of the Reflected and Backscattered Solar Radiation. Masters Thesis, Graduate School of Arts and Sciences, New York University, New York, N.Y.

LIENESCH, J. H., 1966, private communication.

LIENESCH, J. H., and D. Q. WARK, 1967, Infrared Limb Darkening of the Earth from Statistical Analyses of TIROS data. *Journ. Appl. Meteor., 6*, pp. 674—682.

LONDON, J., 1957, A Study of the Atmospheric Heat Balance. Final Report, Contract AF 19(122)-165, Research Division, College of Engineering, New York University, New York.

MÖLLER, F., 1967, Eine Karte der Strahlungsbilanz des Systems Erde-Atmosphäre für einen 14-tägigen Zeitraum. *Meteor. Rundschau, 20*, pp. 97—98.

MÖLLER, F., and E. RASCHKE, 1964, Evaluation of TIROS III Radiation Data. NASA Contractor Report—112 (Grant NsG-305 with University of Munich, Germany).

NORDBERG, W., A. W. MCCOLLOCH, L. L. FOSHEE, and W. R. BANDEEN, 1966, Preliminary Results from Nimbus II. *Bull. Am. Meteor. Soc., 47*, pp. 857—872.

RASCHKE, E. and M. PASTERNAK, 1969, The Global Radiation Balance of the Earth-Atmosphere System from Radiation Measurements of the Nimbus 2 Meteorological Satellite. NASA Technical Report (in preparation), see also NASA-X-622-67-383, Aug. 1967.

RASOOL, S. I., and C. PRABHAKARA, 1966, *Heat Budget of the Souhern Hemisphere.* Problems in Atmospheric Circulation, ed. by Garcia and Malone, Spartan Books, Wash., D.C., 76—92.

RUFF, I., KOFFLER, R., FRITZ, S., WINSTON, J. S., and RAO, P. K., 1967, Angular Distribution of Solar Radiation Reflected from Clouds as Determined from TIROS IV Radiometer Measurements. *ESSA Technical Report, NESC-38*, Washington, D.C.

SALOMONSON, V., 1966, Anisotropy of Reflected Solar Radiation from Various Surfaces as Measured with an Aircraft-Mounted Radiometer. Research Report, Contract NASr-147, Colorado State University, 29 pp.

SIMPSON, G. C., 1929, The Distribution of Terrestrial Radiation. *Memoirs of the Royal Meteor. Soc., 3, No. 23.*

U.S. NAVY HYDROGRAPHIC OFFICE, 1957, 1958, *Oceanographic Atlas of the Polar Seas.* Part I: Antarctic, Part II: Arctic. Washington, D.C., H.O. Pub. No. 705.

VOWINKEL, E., and S. ORVIG, 1964, Radiation Balance of the Troposphere and of the Earth-Atmosphere System in the Arctic. Sci. Rep. No. 9; Contract AF 19(604)-7415, Dept. of Meteor., Montreal.

WARK, D. Q., G. YAMAMOTO, and J. H. LIENESCH, 1962, Methods of Estimating Infrared Flux and Surface Temperature from Meteorological Satellites. *Journ. Atm. Sci., 19*, pp. 369—384.

WINSTON, J. S., 1967, Planetary Scale Characteristics of Monthly Mean Long-Wave Radiation and Albedo and Some Year-to-Year Variations. *Monthly Wea. Rev., 95*, pp. 235—256.

ÅNGSTRÖM, A., 1925, The Albedo of Various Surfaces of Ground. *Geografiska Annaler, 36*, pp. 323—342.

ÅNGSTRÖM, A., 1962, Atmospheric Turbidity, Global Illumination and Planetary Albedo of the Earth. *Tellus, 14*, pp. 435—450.

Transmission of solar radiation in the spectral region 0.55 to 0.64 μm and the Ångström turbidity coefficient

By G. D. ROBINSON. *Meteorological Office, Bracknell, Berks England*

ABSTRACT

Some hitherto unpublished measurements of solar radiation in the yellow—orange region of the spectrum, made in 1947/48/49 at Kew Observatory are examined in relation to the extinction by atmospheric aerosol, the Ångström turbidity coefficient, the visibility and the scale height of the aerosol distribution.

1. In the years 1947 to 1949 measurements of the intensity of direct solar radiation in certain wave-length regions were made on a continuous basis at Kew Observatory (51° .05° N; 00.3° W). Results of these measurements have been used in various studies, but they have never been published in detail. The observing site is situated about 10 miles to the west (prevailing wind westerly) of the centre of the London urban area and the atmospheric pollution there is typical of that in the outer suburbs of a very large city, i.e. typical of the conditions in which millions of people live. Because of this, and because the nature of the atmospheric pollution in many areas, including London, has changed in recent years with changes in fuel usage it seems useful to put on record some of the radiation data in a way which readily allows comparison with other observations of atmospheric transmission. The turbidity coefficient, introduced by A. Ångström (1929, 1930) provides a very convenient way of doing this. The Kew results were expressed as the fraction of radiation in a limited spectral range transmitted by the atmosphere—a satisfactory statistic, but one which, unlike the turbidity coefficient, allows comparison with data for other sites and other periods only if the same spectral range is always used. This note records some of the measurements and the corresponding newly computed Ångström turbidity coefficients.

2. The instruments used were Moll-type thermopiles set normal to the solar beam and held there by a heliostat. The collection angle was limited by diaphragms; the diameter of the limiting aperture subtended an angle of 10° at the centre of the thermopile. Two of the thermopiles were equipped with glass filters—Chance OY2 and Chance OR1. The transmission properties of the filters were determined by spectrophotometer after completion of the measurements. The data refer to the spectral region defined by the difference between the pass-bands of the two filters. The computed equivalent sharp cut-off wavelengths of the filters were 0.553 μm and 0.641 μm and within this band the ratio of incident to transmitted energy was 1.13. This factor can be shown to vary only negligibly for all reasonable spectral distributions of the incident light. The thermopiles were standardised in sunlight against Ångström compensation pyrheliometers on the uncorrected Ångström scale. The measurements have not been converted to the subsequently introduced I.P.S. 1956 since the uncertainty of the solar constant is comparable with the difference between the scales.

3. The Ångström turbidity coefficient β is defined in the following way. The intensity of the solar beam measured by an instrument sensitive to wavelengths in the range λ_1 to λ_2 is

$$I=\int_{\lambda_1}^{\lambda_2} I_O(\lambda) \exp. m[-a_R(\lambda)-a_G(\lambda)-a_D(\lambda)]d\lambda$$

where I_O is the intensity outside the atmosphere—the solar constant multiplied by the correction for solar distance, m is the air mass traversed by the radiation, $a_R(\lambda)$ is the extinction coefficient for Rayleigh scattering by molecules, $a_G(\lambda)$ is the extinction coefficient for gaseous absorption and $a_D(\lambda)$ is

TABLE I. *Transmission of the Direct Solar Radiation in Wave Length Range λλ 0.55 μm—0.64 μm at Kew.*

Sine of Solar Altitude	No. of Occasions Examined	Frequency of transmission in range 0.89—1.00	0.79—0.88	0.69—0.78	0.59—0.68	0.49—0.58	0.39—0.48	0.29—0.38	0.19—0.28	0.09—0.18	0.00—0.08	Median Transmission
0.1—0.2	70	—	—	—	—	.03	.12	.26	.40	.09	.01	.26
0.2—0.3	117	—	—	—	.03	.20	.20	.20	.21	.14	.01	.37
0.3—0.4	100	—	—	.03	.15	.25	.20	.12	.15	.04	—	.45
0.4—0.5	83	—	.01	.10	.22	.27	.18	.08	.12	.01	—	.52
0.5—0.6	99	.01	.04	.21	.25	.20	.14	.08	.06	—	—	.57
0.6—0.7	84	.01	.12	.24	.25	.19	.13	.05	.01	—	—	.62
0.7—0.8	78	.01	.24	.33	.22	.09	.09	.01	—	—	—	.70
>0.8	59	—	.34	.41	.08	.05	.08	.02	.02	—	—	.71

the extinction coefficient for dust. Ångström then defined β by

$$a_D(\lambda)=\beta\lambda^{-1.3}$$

where λ is expressed in units of 1 μm so that for a measurement of I in the range λ_1 to λ_2 at air mass m we have

$$I=\int_{\lambda_1}^{\lambda_2} I_O \cdot T(m,\lambda) \exp.(-m\beta\lambda^{-1.3})d\lambda$$

where $T(m,\lambda)$ is the transmission of air mass m of clean atmosphere. In the case of the Kew observations the factor

$$\overline{T(m)}=\int_{0.553}^{0.641} I_O(\lambda)T(m,\lambda)d\lambda / \int_{0.553}^{0.641} I_O(\lambda)d\lambda$$

had been computed for the appropriate $I_O(\lambda)$ and m, assuming NICOLET's (1951) distribution of the extraterrestrial radiation, a solar constant of 1.38 kWm^{-2}, a total ozone content of 0.2 cm, CRAIG's (1950) values of the absorption coefficients in the Chappuis band of ozone, and Rayleigh scattering according to the Smithsonian Meteorological Tables. Making the simplifying approximation

$$\int_{0.553}^{0.641}\lambda^{-1.3}d\lambda/0.088 \approx 0.6^{-1.3} \approx 1.95$$

we have

$$\exp.(-1.95m\beta)=I/I_O \cdot \overline{T(m)} \qquad (1)$$

4. Table I sets out the Kew observations in terms of a frequency distribution of fractional transmission for various values of air mass. It must be emphasised that this Table does not give an unbiassed assessment of the atmospheric transmission properties at Kew in 1947—1949. The fact that an observation is included in the Table implies a period of at least 30 minutes with no cloud within 5° of the sun. Furthermore for low solar elevations (air mass > 3) occasions of very high turbidity were necessarily excluded as the transmitted radiation was then so small that reasonably accurate measurement of the ratio I/I_O was impracticable—at least in the conditions of routine recording. The occasions of highest turbidity are thus excluded. The Table is however reasonably representative of atmospheric transmission on occasions with broken cloud and solar elevation $>\sin^{-1}0.3$.

Table II sets out the values of β corresponding to various values of I/I_O in the wave-

TABLE 2. *Ångström's turbidity coefficient β for various solar elevation angles (h) and fractional transmissions in the wavelength range 0.55 μm to 0.64 μm (I/Io), assuming Nicolet's extraterrestrial solar spectrum and 0.2 cm O_3*

	I/I₀							
Sin h	.8	.7	.6	.5	.4	.3	.2	.1
.8	.04	.10	.17	.24	.33	.45	.62	.90
.7	.04	.09	.15	.23	.31	.44	.59	.86
.6	.03	.07	.11	.17	.24	.33	.45	.67
.5	.02	.04	.09	.14	.19	.27	.37	.55
.4	(.003)	.01	.06	.10	.15	.20	.29	.43
.3	—	—	.02	.06	.10	.14	.20	.32
.2	—	—	—	.02	.05	.08	.12	.19
.1	—	—	—	—	—	.01	.03	.06

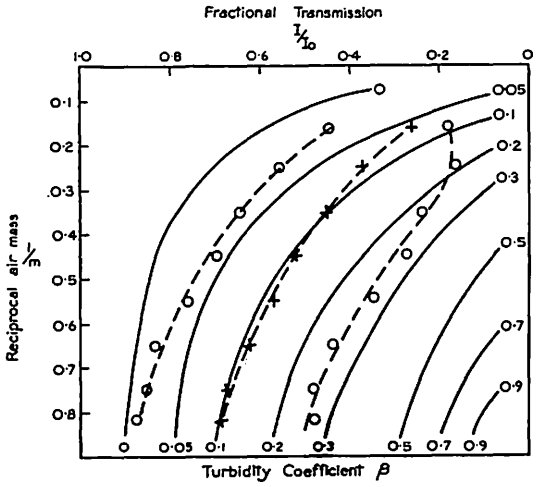

FIG. 1. Transmission of solar radiation in the range $0.553\mu m < \lambda < 0.641\ \mu m$, and Ångström's turbidity coefficient β, with observations at Kew Observatory in 1947/49. The crosses mark the median of the observations, the circles enclose 80 per cent of all the observations.

length range $0.553\ \mu m < \lambda < 0.641\ \mu m$ as computed from Eq (I). The value of $T(m)$ i.e. I/I_O for $\beta = 0$, is also included, the entry for $m = 10$ being a graphical extrapolation.

Fig. 1 combines the results of the two Tables, showing the median and first and ninth deciles of the observed distribution of fractional transmission plotted on a background of β values. This diagram confirms that the observations probably cover a representative sample of turbidity conditions with broken cloud except for the exclusion of occasions of high turbidity with $m > 3$.

5. Radiation observations from which β can be computed are still comparatively rare: the only universally made observation related to atmospheric turbidity is the visibility (or meteorological optical range). Visibility depends on atmospheric extinction by scattering; if α is the scattering coefficient, and if we make the usual assumption that the smallest detectable relative brightness difference is 0.02 it can be shown that

$$\text{visibility } (V) = 4/\alpha$$

If the turbidity is entirely due to scattering we may replace α by $\beta\lambda^{-1.3}$ (i.e. 1.95 β for the wavelength range 0.55 μm to 0.64 μm) remembering that β is now in units of (air mass)$^{-1}$ so that the expression

$$V = 4/1.95\beta$$

will express the visibility in units of the scale height of the scattering medium. We see from Fig. 1 that for solar elevation $> \sin^{-1} 0.3$ the median β for Kew can be taken as 0.1 with 80 per cent of occasions having β between 0.025 and 0.25. The corresponding visibilities are 80R 20R and 8R, R being the appropriate scale height of the dust layer. No direct comparison can be made with observed visibility, but the median visibility at Kew at noon in July over a period of years covering the observations of β was between 10 km add 20 km and at noon in December between 3 km and 6 km so that a scale length for the scattering layer of 0.5 km to 1 km is indicated. This is a very rough estimate for various reasons, one being that the extinction of the solar beam by dust almost certainly includes a component of absorption as well as scattering (e.g. ROBINSON, 1966). Nevertheless it is quite a reasonable value for the scale height of the dust layer at Kew; use of the same method at other sites might give some information on the height distribution of atmospheric dust content.

6. This note is published by permission of the Director-General of the Meteorological Office, Bracknell, Berks. England.

REFERENCES

CRAIG, R. A. 1950, Observations and photochemistry of atmospheric ozone and their meteorological significance. *Met. Monog. Amer Met Soc, 1, No. 2.*

NICOLET, M., 1951, Sur la détermination du flux énergétique du rayonnement extraterrestre du soleil. *Arch. Met. Geophys Biokl, B3,* pp. 209—219.

ROBINSON, G. D., 1966, Some determinations of atmospheric absorption by measurement of solar radiation from aircraft and at the surface. *Q.J. R. Met. Soc., 92,* pp. 263—269.

ÅNGSTRÖM, A., 1929, On the atmospheric transmission of sun radiation and on dust in the air. *Geogr. Ann. 11,* pp. 156—

— 1930, On the atmospheric transmission of sun radiation II *Geogr. Ann. V., 12,* pp. 131—

Studies on the effect of lake regulation on local climate

By BERTIL RODHE

Swedish Meteorological and Hydrological Institute, Stockholm

ABSTRACT

This is a brief report on the essential results achieved at the investigations which during the past twenty years have been performed by the Swedish Meteorological and Hydrological Institute on the subject mentioned in the heading. The temperature and humidity conditions are discussed. The most outstanding effect is the increase of fog frequency in winter when ice formation is prevented in the river because of increased stream velocity.

1. Introduction

Since the nineteenforties, the water flow of a great deal of the rivers in the northern part of Sweden has been modified for electric power production.

The natural annual maximum of river water which is primarily due to melting snow, secondly related to summer rains, is collected in a lot of lakes in the upper parts of rivers. The lake areas are considerably enlarged by mean of dams at the outlets and the water level ranges artificially between an uppermost and a lowermost limit, the altitude difference between these being approved by a special Swedish court (vattendomstol). In some lakes the altitude difference is up to 20 m or even more. The lake water is discharged during the cold season. The water level is generally found at the lowermost limit at the end of the winter.

Storing water in the mountain lakes implies that the river springflood is cut off and that the winter flow, which under natural conditions is the annual minimum, is considerably increased and in some rivers reversed to the annual maximum.

Because the water has to pass the power station at the very moment the electricity is consumed, the discharge must be modified in short-range periods, too. This second type of water flow modification is mostly applied at the dams of the power stations. The water is released during working days and spared during holidays and during the nights. Consequently, the water level varies in the storage behind the dams between day and night and between working days and holidays. The altitude variation may be up to a metre or even more. Downstream, the river flow varies in a corresponding way between maximum on working days and minimum on holidays and during the nights.

A great many people in northern Sweden live alongside the lakes and the rivers, and they are aware of, and sometimes troubled by, natural variations as well as annual and short-range modifications of the water level. That is why no artificial change of the water conditions in lakes and rivers is allowed without being approved by the special court mentioned above. The companies of water power production are bound to indemnify property-holders along the lakes and the rivers for any injury involved.

Local climate is an effect of the merging of atmosphere, ground surface and vegetation as well as water surface in lakes and rivers. Human habitation and farming alongside the lakes and the rivers greatly depend on the particular type of climate which prevails there. Any modification of water level and river flow which may have an effect upon the above-mentioned merging of atmosphere and surface and thus may change the climatic conditions, is a matter of

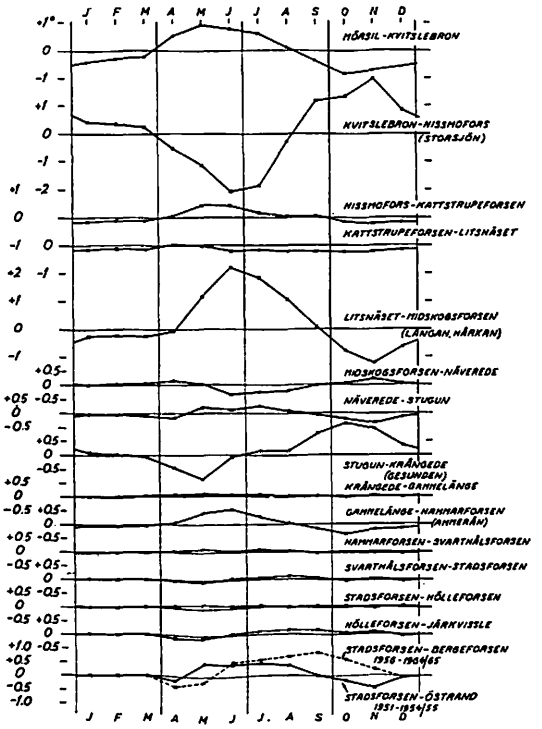

FIG. 1. The annual variation of the water temperature along a river (Indalsälven). Postive differences involve a downstream increase of temperature.

vital interest. A paragraph in the special Swedish law, which concerns rivers and lakes, prohibits any artificial change of the prevailing water conditions if this has an injurious effect upon climate. However, up to now no court has put this paragraph into practice but a lot of compensation claims are raised by inhabitants who live alongside rivers and lakes where the discharge is modified.

Since the nineteenforties, the Swedish Meteorological and Hydrological Institute has been requested by the special courts in question to act as an expert on these matters. The problem has been studied for nearly twenty years and a report submitted in May 1967. A brief review of the essential points and conclusions in this report will be given in the following.

2. The effect of discharge modification on water temperature

The annual variation of the water temperature along a river is seen in Fig. 1, where the conditions of Indalsälven are shown. The curves of the diagrams join points of monthly mean temperature differences between a station of water temperature measurement and the next downstream station. The values are positive if there is a downstream increase of temperature.

We see that there is generally a downstream increase of temperature from spring time in April—May until late summer or autumn. (E.g. Mörsil—Kvitslebron, Hissmofors—Kattstrupeforsen etc.).

When the river passes through a lake, the outlet is cooler than the inlet from the time of the thaw in spring until August (Kvitslebron—Hissmofors at the lake of Storsjön, and Stugun—Krångede at the lake of Gesunden). This matter is obviously due to the deep water-mass of the lake which is more resistant to temperature changes than the turbulent flow of the shallow river.

Beginning in September, the lake thus forms a storage of relatively warm water and consequently, the outlet is warmer than the inlet. Downstream the outlet, the water of the river gets successively cooler (e.g. Hissmofors—Kattstrupeforsen—Litsnäset). In winter there is a region of ice-free water next to the outlet, the length of which depends upon the temperature of the outlet water, velocity of the stream and the weather conditions.

The effect of water storage upon the temperature of a stream flow passing through is similar to that of a lake. This is obvious because the storage is more resistant to temperature variations than the river itself. The date of shift between the seasons of cooling and heating, depends on the magnitude of the water-mass stored. When a deep storage has a low maximum temperature in summer the shift comes rather late in the season between summer and autumn.

In the most downstream part of the river Indalsälven, a power station (Bergeforsen) was started in 1955. Before that year, the temperature variation along the river (Stadsforsen—Östrand) followed the features described above with downstream rising temperature in summer an falling in autumn. The water temperature in the downstream part of the storage area is nowadays, in autumn about a degree Centigrade higher than in the

days before the power station was established.

An affluent joining a main stream, generally raises the water temperature of the latter in summer and cools the main flow in autumn. The reason is, obviously, that the smaller the river, the higher the water temperature in summer and the lower in autumn. (E.g. Litsnäset—Midskogsforsen where the affluents are Långan and Hårkan, Gammelänge—Hammarforsen where the affluent is Ammerån).

3. The net loss of total heat from a water surface

The heat loss from a water surface depends upon the temperature difference between the water surface and the air. A mean rise of the surface water temperature results in an increase of the net heat loss. A rough estimate of the magnitude of the increase of heat loss caused by such a rise in temperature, is the purpose of the study in the following section.

The study is based upon temperature and water measuremens made during 1945—65 at two electric power stations downstream Storsjön in Indalsälven. The stations are Hissmofors and Kattstrupeforsen. The distance between them is about 6 km. There is no significant affluent adding water to the river between the stations. The difference between the water temperatures at the stations is therefore mainly caused by the heat transfer between the water and the atmosphere.

Knowing the water mass passing through the station and the temperature difference, we easily compute the total heat transferred from the water mass to the air. Since we are mostly interested in heat loss, our study is concentrated upon the months September, October and November.

The dots in the diagrams of the Figs 2 a—c show the relation between mean values of net heat loss and mean temperature differences between the water surface (T_w) and the air (T_a). All mean values cover periods of five days. The correlation coefficient is 0.67 ± 0.06 in September, 0.75 ± 0.04 in October and 0.81 ± 0.04 in November. The relationship is obvious. It increases during the autumn.

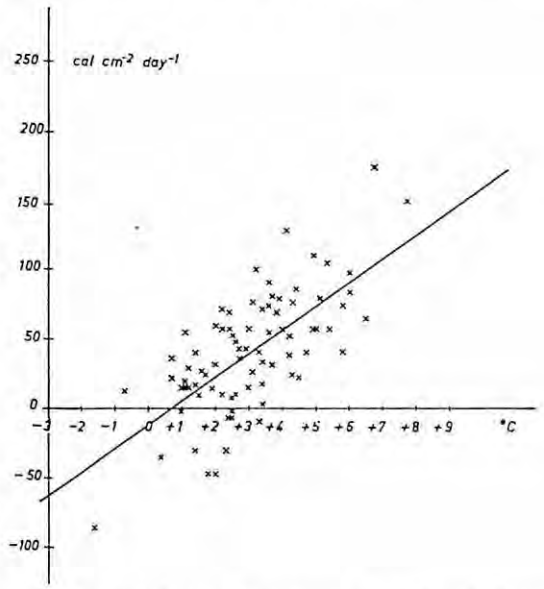

FIG. 2 a. The relation between the net loss of heat from a river and the difference between the temperatures of the water surface and the atmosphere. The dots refer to five-day mean values. Locality: Hissmofors—Kattstrupeforsen, Indalsälven. September 1945—1965.

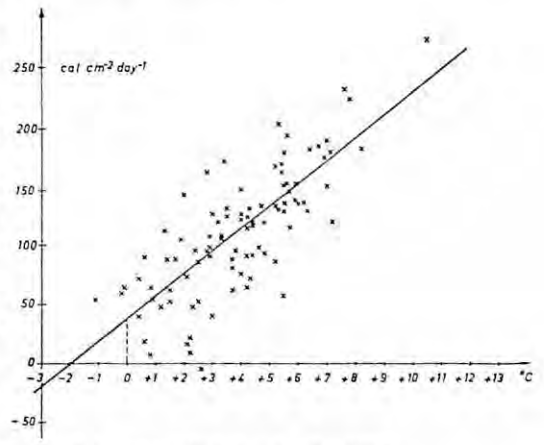

FIG. 2 b. Ditto. October 1945—1965.

The lines of regression are drawn in the diagrams. Their equations are

in September

$$Q = 17.3(T_w - T_a) - 13.0 \text{ cal cm}^{-2} \text{ day}^{-1}$$

in October

$$Q = 18.7(T_w - T_a) + 38.9 \text{ cal cm}^{-2} \text{ day}^{-1}$$

in November

$$Q = 19.2(T_w - T_a) + 33.1 \text{ cal cm}^{-2} \text{ day}^{-1}$$

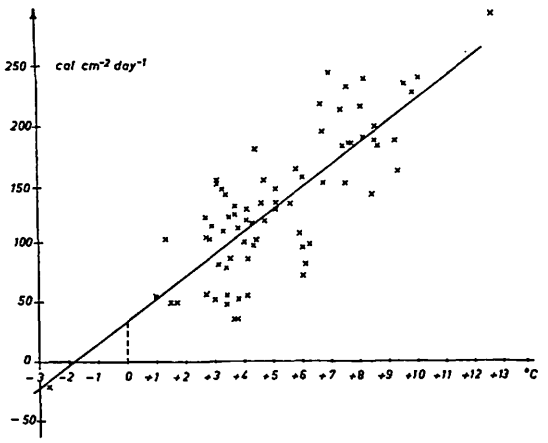

FIG. 2 c. Ditto. November 1945—1965.

The dispersion of the dots around the lines of regression is surely caused by the following matters.

1. There is a short-range modification of stream flow passing the area so that the water masses entering and leaving are not equal in every moment. At times, water is either stored or discharged. However, the storage within the area is small and the modifications mostly cover short ranges. Thus, the mean values extending over five-day periods are expected to be almost unaffected.

2. The subject of the present investigation was not in sight twenty years ago, and it is not before now when the data of water temperature were studied that the possibility of getting the results reviewed here became obvious. So, the measurements were indeed not arranged for the purpose of the actual investigation and therefore, they do not completely meet the accuracy required. In some years, the measurements are obviously fallacious, and such periods are excluded from the study.

The climate station (Östersund) referred to for air temperature readings is not so close to the river area as desirable. The distance is 20 km. Since five-day periods are used, the error of applying the Östersund temperature readings to the area is mostly a systematic one, and the true position of the zero point on the horizontal axis of the diagrams is unknown.

3. The convective transfer of heat from the water surface to the atmosphere depends in parts on the wind conditions. We have disregarded the wind effect. The five-day period is assumed to be long enough to keep the error so introduced in the mean values to a minimum.

4. The water mass receives heat by shortwave radiation. According to records during 1957—65 at Östersund (Frösön), the average total of sun and sky radiation received by a horizontal surface is in September 196, in October 79 and in November 20 cal cm^{-2} day^{-1}.

The dispersion of the dots in the diagrams is surely in parts due to variations of the shortwave radiation about the quoted mean values.

5. A part of the total heat loss is due to longwave radiation. It depends upon the water temperature as well as the air temperature. No measurements are available in the area. An estimate is done by means of the following formula which is based upon the well-known suggestion made by ÅNGSTRÖM (1916). The constants are those used by GEIGER(1961).

$$Q_s = 0.97\,\sigma T_w^4 - \sigma T_a^4 (1 + kN^2)\,(0.820 - 0.250 \cdot 10^{0.0945\,e})\quad (2)$$

where σ = Stefan-Boltzman's constant,
k = a factor depending upon cloud conditions,
N = cloud amount, 0.0—1.0,
e = vapour pressure in mbs.

At the monthly mean conditions of temperature, humidity and cloud amount at Östersund, the formula gives the following approximate values of net heat loss by longwave radiation, in September 125, in October 149 and in November 159 cal cm^{-2} day^{-1}.

The dipersion of dots in the diagrams is surely in parts due to variations of the longwave radiation around these mean values.

Now, suppose the mean water temperature is increased by lake regulation, say one degree centigrade. According to the regression lines, this would involve a net increase of the heat transferred from the water to the atmosphere, in September 17, in October and November 19 cal cm^{-2} day^{-1}.

A part of this increase is an effect of longwave radiation, i.e.

$$\frac{dQ_s}{dT_w} = 0.97 \cdot 4\,\sigma\,T_w^3.$$

The rest is related to convection and evaporation. According to our estimations this rest is in September 7, in October 8 and in November 9 cal cm^{-2} day^{-1} per centigrade increase of water temperature.

4. The evaporation from a water surface

The relation between the transfers of sensible heat and latent heat (evaporation) by convection is commonly referred to as the BOWEN ratio. The ratio may be computed in a theoretical way as follows, giving the relation between the total heat of convection and the amount of evaporation in mm.

Say, an eddy mass of air gets in touch with the water surface and attains its temperature as well as its saturation vapour pressure conditions. The total heat so transferred to a unit mass of air is

$$A = \int_{T_v}^{T_w} \left[c_p + T \frac{\partial}{\partial T} \left(\frac{Lr}{T} \right) \right] dT \qquad (3)$$

where T_w = the water surface temperature,
T_v = the wet-bulb temperature of the air,
r = the saturation vapour mixing ratio at temperature T,
c_p = the specific heat of air at constant pressure,
L = the latent heat of evaporation.

Simultaneously, the following amount of vapour is added to a unit mass of dry air in the eddy,

$$B = r_w - 0.01\, R\, r_a \qquad (4)$$

R is the relative humidity originally found in eddy. The subscripts w and a indicate that the saturation vapour mixing ratio r refers to the temperatures T_w and T_a respectively, T_a being the original dry bulb temperature of the eddy.

May be, only a fraction of (A) is transferred to the eddy. We may assume that the evaporation (B) is then reduced to the same degree. So, the ratio between evaporation and total heat of convection nevertheless reads B/A.

The well-known *Bowen* ratio is based on the ratio of sensible and latent heats transferred, and a constant k is applied:

$$\frac{A}{BL} - 1 = k \frac{T_w - T_a}{e_w - e_a} \qquad (5)$$

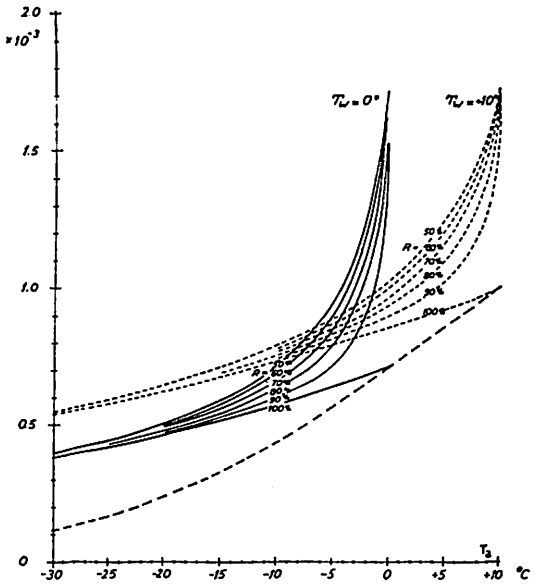

FIG. 3. The variation of B/A, see (3) and (4). Two examples, a) $T_w = +10°$, b) $T_w = 0°$ C.

Here e is the vapour pressure in mbs with subscripts referring to water surface and atmosphere.

Theoretical values so computed are found in the Tables 1 and 2. In Fig. 3, a diagram gives two examples of the variation of the ratio B/A with the temperatures T_w, T_a and relative humidity R. The coefficient k varies about 0.5 to 0.65. It is the smaller, the higher T_w and the smaller the difference between T_w and T_a. BOWEN (1926) derived $k = 0.61$.

Our investigation in the preceding section has shown that when the mean water temperature is increased by one degree centigrade, then the net loss heat by convection and evaporation in average increases about 7 to 9 cal cm^{-2} day^{-1} in September to November. Applying the normal values of B/A in Östersund, this increase indicates that the monthly evaporation increases 2 to 3 mm.

WALLÉN (1966) has computed the evaporation by means of PENMAN's formula with reference to a grass surface. He found for September and October the average totals 38 and 9 mm respectively. NYBERG (1965) has found that the evaporation from a snow surface may be in March during 23 days

TABLE 1. *The ratio B/A, A in cal g⁻¹*

$T_w - T_a$	R	$T_w = +20°$	$T_w = +10°$	$T_w = 0°$
+5°	90 %	$1.28 \cdot 10^{-3}$	$1.02 \cdot 10^{-3}$	$0.72 \cdot 10^{-3}$
	70 %	$1.39 \cdot 10^{-3}$	$1.15 \cdot 10^{-3}$	$0.85 \cdot 10^{-3}$
	50 %	$1.46 \cdot 10^{-3}$	$1.24 \cdot 10^{-3}$	$0.95 \cdot 10^{-3}$
+10°	90 %	$1.17 \cdot 10^{-3}$	$0.90 \cdot 10^{-3}$	$0.61 \cdot 10^{-3}$
	70 %	$1.24 \cdot 10^{-3}$	$0.97 \cdot 10^{-3}$	$0.67 \cdot 10^{-3}$
	50 %	$1.29 \cdot 10^{-3}$	$1.02 \cdot 10^{-3}$	$0.72 \cdot 10^{-3}$
+15°	90 %	$1.10 \cdot 10^{-3}$	$0.81 \cdot 10^{-3}$	$0.54 \cdot 10^{-3}$
	70 %	$1.14 \cdot 10^{-3}$	$0.85 \cdot 10^{-3}$	$0.57 \cdot 10^{-3}$
	50 %	$1.17 \cdot 10^{-3}$	$0.89 \cdot 10^{-3}$	$0.59 \cdot 10^{-3}$

2.4 mm, in April (30 days) 18.6 mm and in May during 7 days 5.8 mm.

The increase found by us is rather small in relation to the normal total evaporation in summer and autumn but large in relation to the evaporation in winter over a snow surface or a cover of ice.

In winter, the evaporation conditions over ice-free water surfaces are outstanding. When very cold weather conditions prevail, the monthly evaporation from a water surface that is prevented from ice-covering, is estimated to exceed 5—10 mm.

5. The relation between water temperature and air temperature

We have seen that a lake regulation and a modification of discharge may result in a change of water temperature, mostly not exceeding one to two degrees centigrade.

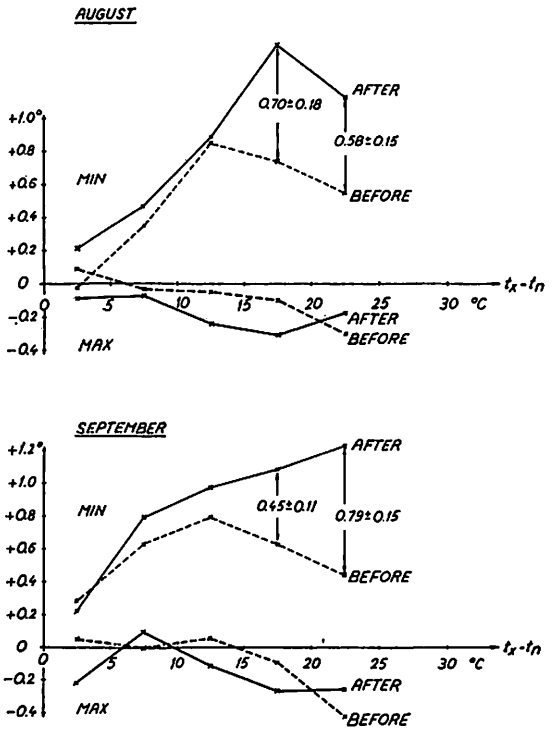

FIG. 4. The change of daily maximum and minimum temperatures at Ljusnedal, caused by enlargement of the lake.
Station close to the submerged area: Ljusnedal II.
Reference station at 2 km distance: Ljusnedal I.
$t_x - t_n$: Difference between daily maximum and minimum temperatures at Ljusnedal I, giving an idea about the actual radiation conditions.
The figures within the diagram are mean differences and their standard errors.
August and September.

TABLE 2. *The value of k in (5)*

$T_w - T_a$	R	$T_w = +20°$	$T_w = +10°$	$T_w = 0°$
+5°	90 %	0.54	0.59	0.62
	70 %	0.52	0.58	0.61
	50 %	0.51	0.58	0.61
+10°	90 %	0.56	0.60	0.62
	70 %	0.56	0.60	0.62
	50 %	0.56	0.60	0.62
+15°	90 %	0.58	0.61	0.63
	70 %	0.58	0.61	0.63
	50 %	0.58	0.61	0.63

The air temperature is mostly unaffected by such a small change of the water temperature.

The influence of lake regulation upon air temperatures is greatest where areas are submerged and new banks are formed. The local climate of a bank is rather particular because of the triple merging atmosphere—water surface—ground with vegetation. So the climate of a bank of a water storage may in some details differ from the climate originally found in the area if the distance between the new and the original bank is great.

For example, a great lake is created close to

the village of Ljusnedal on Ljusnan. There, Ljusnan is a minor stream originally flowing into the lake Lossnen at 13 km distance from village. The lake (original area 8.4 km²) has now been enlarged and a great area (in total 23 km²) is submerged next to the village. The change of daily maximum and minimum temperature in August and September at a site of temperature measurement called Ljusnedal II, once close to the river, now 50 m from the bank of the new lake, is shown in Fig. 4. The temperatures at Ljusnedal II are compared with the readings at another climate station, called Ljusnedal I and situated about 2 km from the new lake and Ljusnedal II. These readings are assumed to be unaffected by the new lake.

For the statistical investigation of the temperature change involved by the submergence, the daily temperature differences between the two sites Ljusnedal I and II are grouped according to the incident difference between the maximum and minimum temperatures at Ljusnedal I, this difference being taken as a measure for the prevailing radiation conditions. Indeed, it is the conditions of radiation which settle the temperature difference between two adjacent sites having different topographic characteristics.

The diagram of the figure shows that the conditions of the daily maximum temperature are not changed by the submergence, likely because of the advection and turbulent mixing being considerable. Frequently, at noon, the winds have such a velocity that the atmospheric temperature differences between sea and land areas are almost eliminated. This is surely not a common feature but rather specific to the mountainous area around Ljusnedal.

When extreme radiation conditions prevail, the minimum temperature at night is raised at Ljusnedal II since the new lake was established. In general, the temperature difference between minimum temperatures before and after submergence is 0.5 to 1.0° C when the most extreme radiation conditions prevail i.e. when the most extreme differences between the maximum temperature at noon and minimum temperature at night occur. The rise is significant from a statistical point of view, the standard error being 0.11 to 0.18°.

6. The formation of fog

In a previous paper (1966), the author has described a formula showing the factors operating to concentrate the liquid water in the atmosphere,

$$\frac{\delta \bar{r}_w}{\delta t} - K\frac{\delta^2 \bar{r}_w}{\delta z^2} = -\left(\bar{u}\frac{\delta \bar{r}_w}{\delta x} + \bar{v}\frac{\delta \bar{r}_w}{\delta y}\right) + \left[\left(\frac{dr_w}{dz}\right)_{ad} - \frac{\delta \bar{r}_w}{\delta z}\right]\left[\bar{w} - \frac{1}{\varrho}\frac{\delta(\varrho K)}{\delta z}\right] + K\left[A\left(\frac{\delta \bar{T}_v}{\delta z}\right)^2 + A\overline{\left(\frac{\delta T'_v}{\delta z}\right)^2} + B\frac{\delta \bar{T}_v}{\delta z} + C\right] - \chi\frac{Q}{L} + P \qquad (6)$$

r_w = the content of liquid water per unit mass of dry air. Negative values refer to the amount of liquid water required to saturate the air in the psychrometer process.
ϱ = the density of dry air.
L = the latent heat at evaporation.
T_v = the wet-bulb temperature.
K = the coefficient of eddy exchange.
u, v, w = the vecolcity components in horizontal (x, y) and vertical (z) directions.

The bars indicate that the symbols refer to mean values covering a spell long enough to make sure that the sum of the eddy variations, e.g. T'_v, is very small, i.e. $\overline{T'_v} = 0$.

There is a spectrum of dynamical processes bringing about the concentration of liquid water in the atmosphere. They are fundamental to the occurrence of condensation and precipitation. The processes are represented by the terms in (6) as follows.

1. The term of advection—e.g. of moving clouds or fog drift—easily gets magnitudes exceeding 10^{-6} sec^{-1}. It is mostly the largest term in the right-hand part of the equation and this agrees to the fact that we quickly notice the motion of the clouds but longer attention is required to observe the change of their shapes.

2. The term of convection specifies the well-known effect of vertical motion. When the vertical displacement is 1 m sec^{-1}, the term is about 10^{-6} sec^{-1}. In convective clouds of

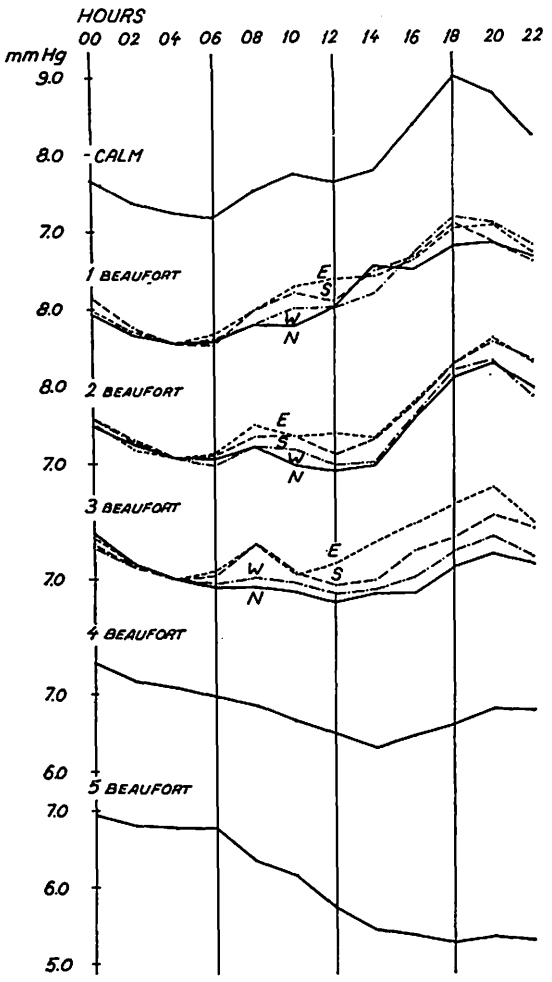

FIG. 5. The diurnal variation of vapour pressure. Nilsböle (Indalsälven). July—September 1953—1961.

The curves refer to samples considering only days when the relative humidity at 14.00 is less than 70 %.

The wind speeds and directions are those observed at a close station (Bölestrand) at 13.00.

Cumulus type the vertical velocity is still greater, and then the rate of the vertical development is visible to the naked eye simultaneously with the horizontal motion of the cloud.

The bracket term includes the derivative $\left(\frac{d\,r_w}{d\,z}\right)_{ad}$ which is the increase of liquid water content in a closed volume of air at a vertical displacement. The total bracket term becomes negative if there is a rapid vertical increase of liquid water content in the surrounding air,

$$\frac{\delta\,\bar{r}_w}{\delta\,z} > \left(\frac{dr_w}{dz}\right)_{ad}.$$

This may for instance happen below a Stratus cloud after sunrise when the air next to the ground is heated by diffuse radiation. Then, the cloud or the fog is dissolved by upward displacements.

The derivative $\frac{1}{\varrho}\frac{\delta\,(\varrho K)}{\delta\,z}$ is the vertical variation of the coefficient of eddy exchange. Below an inversion, it is negative and has the same effect as an upward vertical motion. It brings about an adiabatic cooling and a strengthening of the inversion—and so it operates to increase itself. Thus, it works in a kind of "chain reactions" strengthening the inversion.

At the base of an inversion, there are—in addition to the process specified by the derivative of eddy exchange—two others which both bring about a cloud or a fog. These are turbulent mixing in a temperature transition zone and net loss of heat by radiation.

3. The effect of turbulent mixing is shown by the term

$$K\left[A\left(\frac{\delta\,\bar{T}_v}{\delta z}\right)^2 + A\overline{\left(\frac{\delta\,T'_v}{\delta z}\right)^2} + B\frac{\delta\,\bar{T}_v}{\delta z} + C\right]. \quad (7)$$

The coeffcients A, B and C depend mainly on temperature and only slightly on pressure. They are described by RODHE (1966). The term (7) is always greater than zero and explains the formation of steam found also elsewhere, for instance over boiling water, over a wet warm or hot surface, in the smoke of a chimney, in the exhaust steam from a motor or a jet plane etc.

The turbulent mixing is the primary stage of fog formation when a temperature transition zone is formed by advection or radiative cooling in the boundary layer next to any kind of surface of the earth. When the first traces of fog are formed, the long-wave radiation operates effectively in further developing the fog.

4. The term of radiation $-\chi\frac{Q}{L}$ does not reach the magnitude of 10^{-6} sec^{-1} in clear air but when there are aerosols, these

operate as black bodies raising the net loss of heat at night and in winter. The factor χ depends on temperature and pressure, and ranges from 0.07 (—30° C) to 0.42 (0° C) and 0.85 (+30° C) at 1000 mbs. See for further details RODHE (1966).

5. The last term P represents the fall-out of precipitation. Say, P is -10^{-6} sec^{-1}. This is equivalent to a precipitation of 0.5 mm per hour when the fog or cloud layer is 100 metres deep, or 5 mm per hour when the depth of the cloud is 1000 metres.

Summing up, all the terms mentioned represent processes of fog and cloud formation and dissolution, as identified by $\frac{\delta \bar{r}_w}{\delta t}$. Their integer result depends upon the boundary conditions. In dry conditions r_w remains negative in spite of the existence of even strong vertical motions or considerable temperature transition zones.

At least one of the terms must be in operation within clouds and fogs at stationary conditions since it is necessary that $-\frac{\delta^2 \bar{r}_w}{\delta z^2} > 0$ somewhere and precipitation may fall out ($P<0$).

7. The diurnal variation of absolute humidity

The diurnal variation of vapour pressure in July, August and September, is shown in Fig. 5. The site of investigation is Nilsböle at the lower part of the river Indalsälven. The river flows here in a valley. The temperature and the humidity were recorded along the slopes at heights 0, 10, 34 and 70 metres aboye the level of the river. The investigation started in 1953. The power station Bergeforsen was built in the area and was ready in 1955. Then, the lowermost site of record was submerged and the station, originally at the 10-metre level, got close to the water surface.

The diagrams of Fig. 5 represent the station, at the 34-metre level. The records are grouped according to wind conditions. There is a curve, or a set of curves, for each Beaufort wind force. In the case of Beaufort 1, 2 and 3 the records are moreover classified according to the wind directions.

Since the absolute values of the records are not quite correct, the curves in each set are drawn from a common starting point at 04 o'clock. Thus the curves only pretend to show the diurnal variation, not the magnitude of the vapour pressure itself.

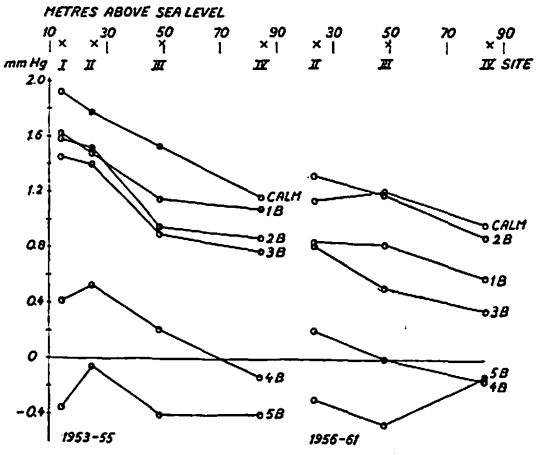

FIG. 6. The diurnal increase (12—18 hours) of vapour pressure at different heights along the slope of the valley. Nilsböle 1953—1955, 1956—1961. See legend to Fig. 5.

The diurnal variation of vapour content in the atmospheric surface boundary layer depends in parts upon the evaporation from the surface and the heat balance prevailing there, in parts upon the atmospheric turbulence transferring the humidity from the boundary layer upwards to higher levels of the atmosphere.

The diagrams show that in total the vapour pressure increases from sunrise to sunset at light wind velocities during the day. However, the increase is not uninterrupted.

In the early morning, the evaporation is considerable but the turbulence is small. Then, the vapour pressure in the surface boundary layer increases. At about 8—10 a.m., the turbulence has increased so much that there is now a net loss of vapour content in the boundary layer. In light winds, the decrease ends at noon. Then, evaporation adds more vapour to the boundary layer than is removed by turbulence. At night, there is a loss of vapour content in the boundary layer because of dew formation.

When the wind is strong, the effect of turbulence predominates and the net loss of vapour in the boundary layer starts early

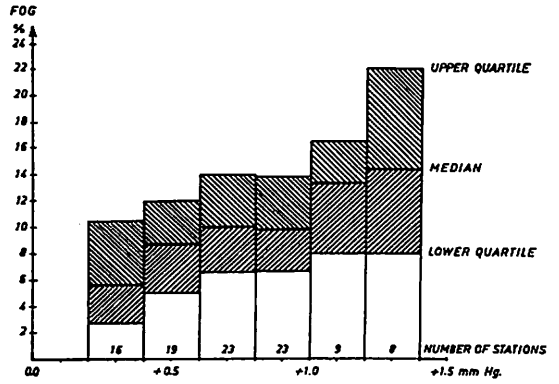

FIG. 7. The relation between the diurnal increase (07—19 hours) of vapour pressure and fog frequency in July, August and September. The increase of vapour pressure is the mean value of days when the windforce and the relative humidity at 13.00 are one Beaufort and less than 70 %, respectively.

in the morning and lasts until after noon. In very strong winds, there is a decrease of vapour content during the whole day.

The curves differ with the wind directions. In E-ly and S-ly wind directions, the air is more stable and the eddy exchange is less then in W-ly and N-ly winds. Thus, the diurnal increase of vapour pressure is greater in winds from south and east than from north and west.

Fig. 6 shows that the diurnal increase of vapour pressure is greater in the lower than in the upper sites of record along the slopes of the valley. The diagram is subdivided into two parts, the right-hand part referring to the records when the water level of the river had been raised to the 10-metre level.

In view of the effect of turbulence on vapour content in the boundary layer, the upward decrease of the diurnal variation is easy to understand.

The river area was enlarged by the rise of the surface level. We might have expected that the increase of the area of evaporation should involve an increase of the diurnal vapour variation. However, the diurnal amplitude has decreased. The period of investigation was indeed short: three years before and six years after the change of river conditions. The decrease is surely due to random variations of weather conditions

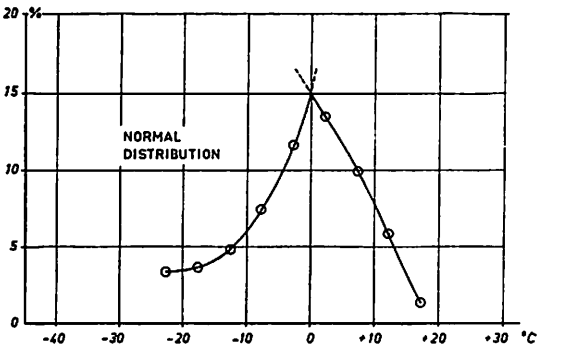

FIG. 8 a. The normal variation of fog probability with air temperature.

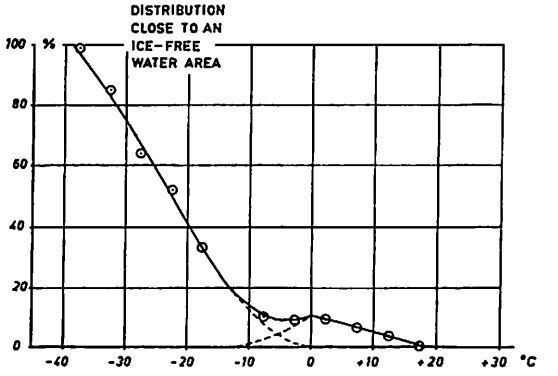

FIG. 8 b. The distribution of fog probability with air temperature close to a river which is always free of ice in winter because of stream velocity.

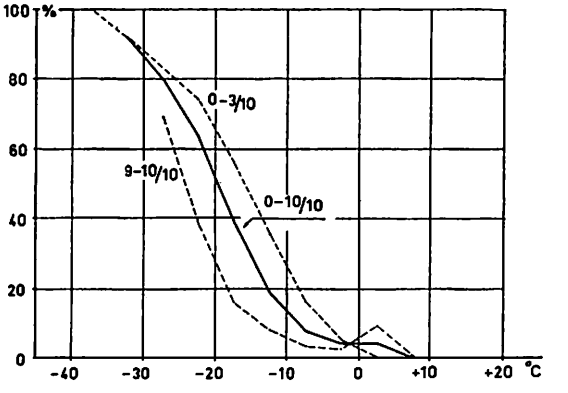

FIG. 8 c. The distribution of fog probability with air temperature close to an ice-free water in different sky conditions. November to February, 1956—62, Lycksele (Norrland).

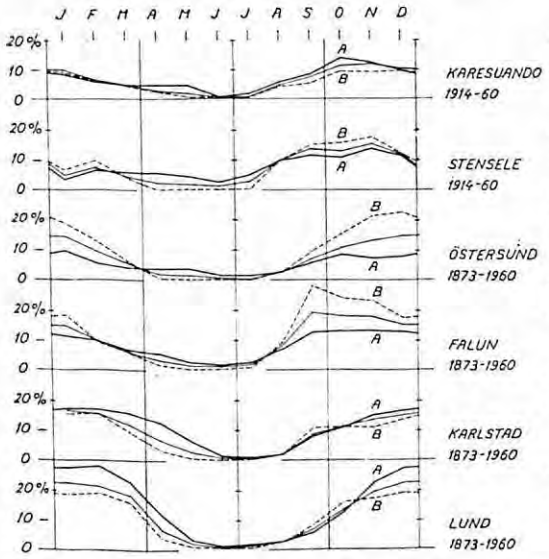

FIG. 9 a. The annual variation of fog frequency, and additionally, fog probability in the following conditions.
(A) Within 24 hours after a fall of precipitation.
(B) On days without precipitation (at least 48 hours after a fall of precipitation).
Inland stations.

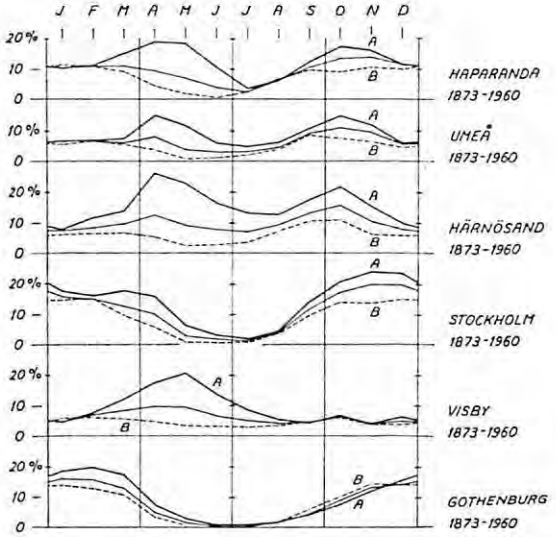

FIG. 9 b. Ditto. Coast stations.

during these rather short periods. Neverthelses we note that the rise of the water level had no considerable effect on the vapour content.

8. The fog frequency

We have shown that the amplitude of diurnal increase of vapour pressure at low wind velocities may be a characteristic feature of the topographic site. The histogram of Fig. 7 shows that fog frequency relates to this amplitude and so, too, is settled by the topographic conditions. The vertical scale refers to the fog frequency in July, August and September, the horizontal scale to the average increase of vapour pressure 07—19 hours on days when the wind force at 01 p.m. was one Beaufort and the humidity less than 70 %. 98 stations are included in the statistics.

The diagram of Fig. 8 a shows the normal distribution of fog frequency in a temperature diagram. There is an increase of fog probability with temperature decreasing towards freezing point. This variation is in agreement with the variations of the coefficients *A*, *B* and *C* in (7). Below freezing point, the fog probability abruptly decreases because of the snow surface cover, the latter having a smaller vapour pressure than the water droplets in fog.

Next to an ice-free water surface (freezing being prevented by a rapid stream flow), the temperature difference between the air and the water surface increases greatly in cold weather conditions. In consequence the fog probability increases when the air temperature decreases below —10° C. At —30°, over an ice-free water surface, fog occurs almost everyday. It is worth mentioning that the probability curve shown in Fig. 8 b has been found to fit wherever the freezing of a river stream is prevented in Sweden.

Fog formation is enforced by radiative cooling. Thus, the probability curve shown in Fig. 8 b refers to a normal distribution of cloud frequency. Fig. 8 c shows the fog probability in winter partly under clear sky (0—3/10) and partly under overcast sky (9—10/10) conditions.

9. The annual variation of fog frequency

The annual variation of fog frequency is shown in Figs. 9 a and b. In agreement with the frequency distribution shown in Fig. 8 a, the annual maximum appears when the tem-

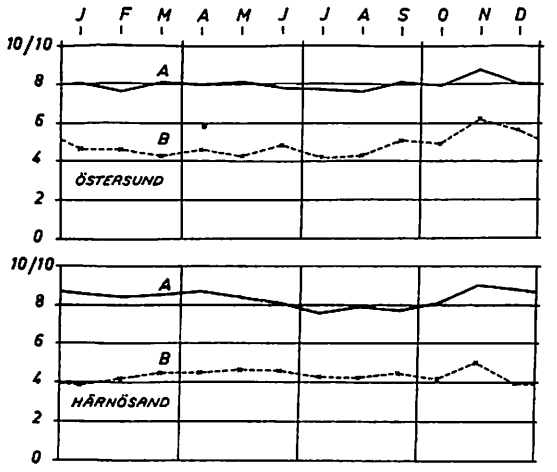

FIG. 10. Annual variation of daily sky conditions at 19.00.
(A) Within 24 hours after a fall of precipitation.
(B) On days without precipitation.
Östersund and Härnösand, 1931—60.

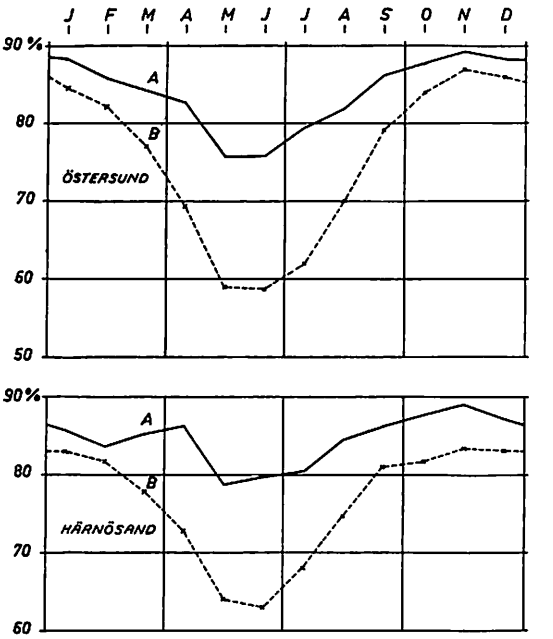

FIG. 11. Annual variation of relative humidity at 19.00.
(A) Within 24 hours after a fall of precipitation.
(B) On days without precipitation.
Östersund and Härnösand, 1931—1960.

perature is about 0° C, i.e. in autumn and spring in the northern part of Sweden, in winter in the southern part. In spring, the low humidity conditions keep the fog frequency low.

In order to show the effect of annual humidity variation on fog frequency, we group the observations of fog in two classes: One class containing the observations on a day with precipitation, the other at least two days after a day of precipitation. As seen in Figs. 10 and 11, the sky conditions as well as the humidity conditions are quite different within these two classes.

The annual variation of fog probability, too, is indeed different between these two classes. We note the following two interesting features in Figs. 9 a and b:

1. Within the class specified by the conditions of high humidity, the maximum of fog probability in spring is outstanding, especially by the sea. Surely, it is the frequent temperature difference between the air and the sea surface that brings about this maximum provided that the humidity is high.

2. The evaporation from the sea is usually not high enough to raise the humidity so much that fog is formed for this reason. Östersund and Stensele being places close to large lakes, but yet fog has hardly never been found there on days without precipitation in April, May, June and July during 50, respectively, 90 years of observations.

3. The fog probability is in autumn often greater on days without precipitation than on days with precipitation, especially at inland stations far from the sea. Thus, the humidity is in autumn mostly great enough for fog to form at night. Nights of low cloud amounts and of effective cooling by long-wave radiation are therefore those most favourable to fog formation.

10. The effect of lake regulation on fog frequency

We have already shown that a change of river flow and rise in lake surface level within moderate limits hardly affects the humidity conditions of the air in summer time. Hence, we do not expect any considerable change of fog frequency in this way.

However, if the discharge from a regulated

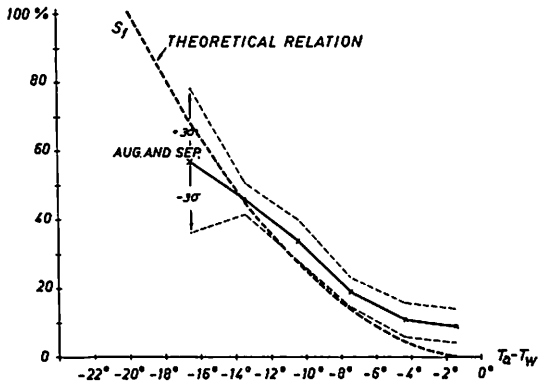

FIG. 12. The relation between the fog probability and the difference between the water surface temperature and the air minimum temperature at night. August and September. The mean values cover twelve stations.
σ = the standard error. The curve S_1 is based upon the coefficient A in (7) and is adapted to the empiric values.

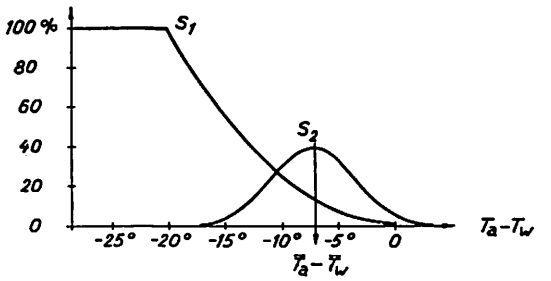

FIG. 13 a. The fog probability (curve S_1, evaluated in Fig. 12) and the frequency distribution of the differences between water surface temperature and nocturnal air minimum temperature (curve S_2).

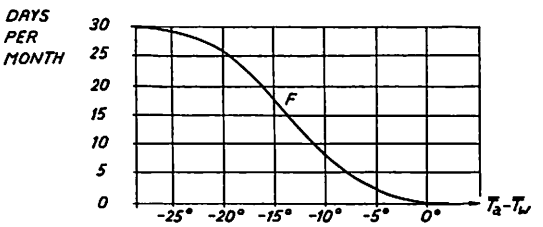

FIG. 13 b. The relation of the monthly fog frequency (F) to the monthly mean difference between water surface temperature and nocturnal air minimum temperature $\bar{T}_a-\bar{T}_w$:

$$F=\int_{-\infty}^{+\infty} S_1 S_2 \, d\,(T_a-T_w)$$

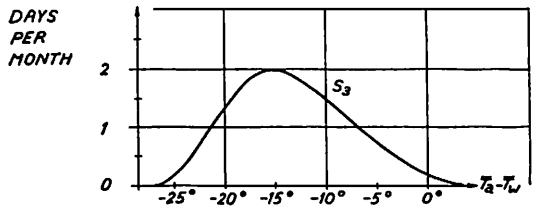

FIG. 13 c. The increase of monthly fog frequency caused by change of the mean water surface temperature:

$$S_3=-dF/d(\bar{T}_a-\bar{T}_w)$$

lake prevents freezing of the river, the fog conditions are radically changed from the type of Fig. 8 a to that of Fig. 8 b. Surely, this is the greatest effect of lake regulation on local climate.

Secondly, a change of the mean surface water temperature in autumn may have an influence upon fog frequency. The fog probability next to the river or a lake depends on the difference between the nocturnal minimum temperature and surface water temperatue as shown in Fig. 12 by means of an empiric curve based on observations at 12 stations, supplemented by a theoretical one derived by means of the coefficient A in formula (7). Fog is formed very often when at night the temperature difference between the water surface and the air exceeds 15°. In consequence, the monthly fog frequency in parts depends on the frequency distribution of nocturnal temperature differences between water surface and air during the month.

Say, the curve S_1 in Fig. 13 a shows the fog probability distribution along the temperature scale. The curve S_2 represents the temperature frequency distribution. The monthly fog frequency F is the integral of the product of S_1 and S_2 along the abscisse. This integral depends upon the average difference between the air and water temperatures. $\bar{T}_a-\bar{T}_w$. Its variation is shown in Fig. 13 b.

Now, say the mean difference $\bar{T}_a-\bar{T}_w$ is increased one degree centigrade by a modification of river flow. That results, according to the curve F, in an increase of fog frequency. The curve in Fig. 13 c shows how great the

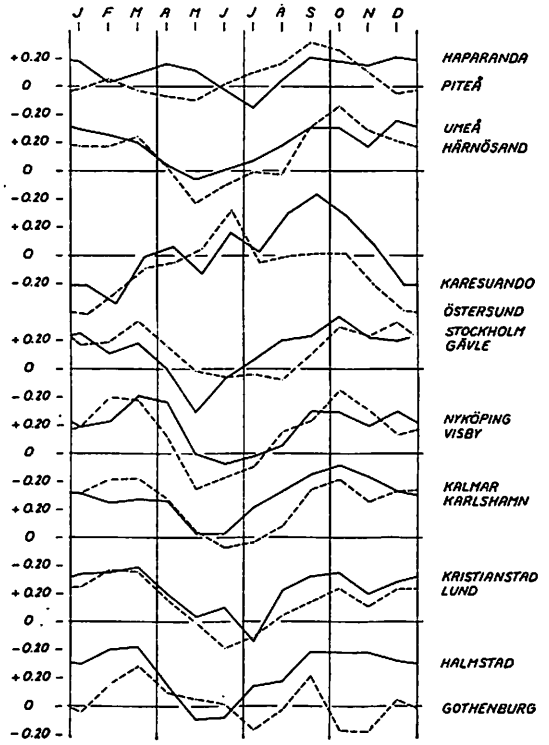

FIG. 14. The annual variation of the correlation between the fog frequency and the monthly mean temperature.

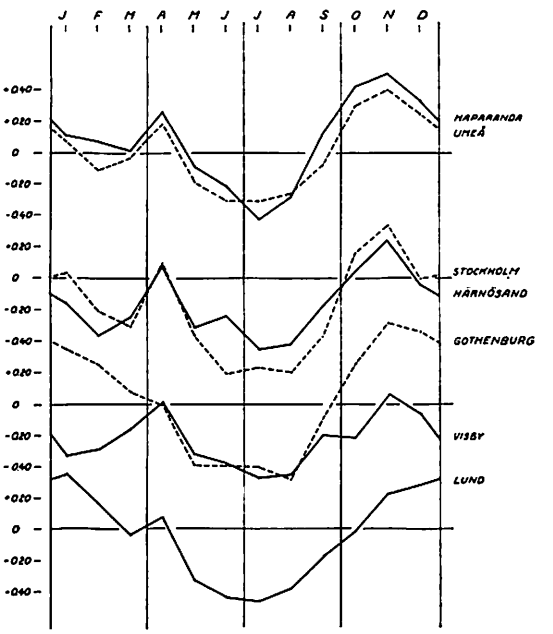

FIG. 15. The annual variation of the correlation between the precipitation frequency and the monthly mean temperature.

increase in fog frequency is per unit increase of the water temperature $\bar{T}_w$. In northern Sweden, the average difference $(\bar{T}_a - \bar{T}_w)$ between the nocturnal air minimum temperature and the water temperature is between —5 and —10° in September and October. Within this range, the fog frequency increases with one day per month when the mean water temperature is raised 1° C.

11. The correlation between fog frequency and monthly mean temperature

The Fig. 14 shows the annual variation of the correlation between fog frequency and monthly mean temperature. The variables are the relative frequencies we get by comparing each month with the preceding and the following ones. Absolute frequencies are not reliable because the interest taken by the observers in fog observations varies very much.

Mostly there is a positive correlation in autumn and winter. In some places, e.g. Östersund and Karesuando, there is a negative correlation in winter. The latter places are close to ice-free water areas so that steam fog is formed during cold winters.

Fig. 15 shows in the same way the correlation between the monthly mean temperature and the precipitation frequency. Since the observers take better care of their precipitation gauges than current weather observations, these curves agree better with each other than the curves referring to fog frequency. The positive correlation coefficients in autumn as well as the negative in summer are outstanding.

12. The secular variation of temperature

The Fig. 16 illustrates the variation of overlapping ten-years mean values of the monthly mean temperatures since the start of observations at Stockholm (1756), Uppsala (1773), Gothenburg (1804), Härnösand (1859), Östersund (1861) and Haparanda

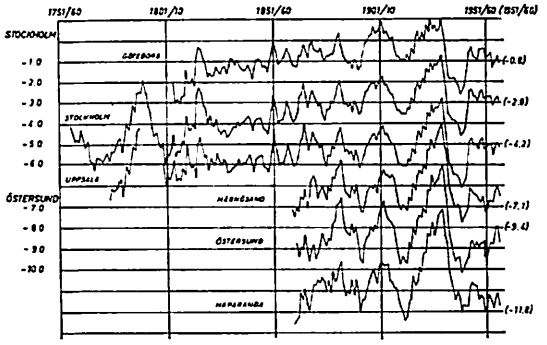

January.

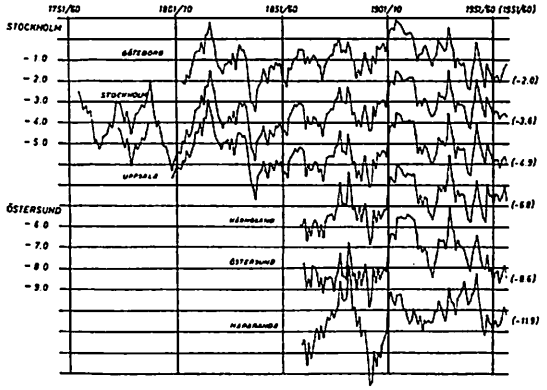

February.

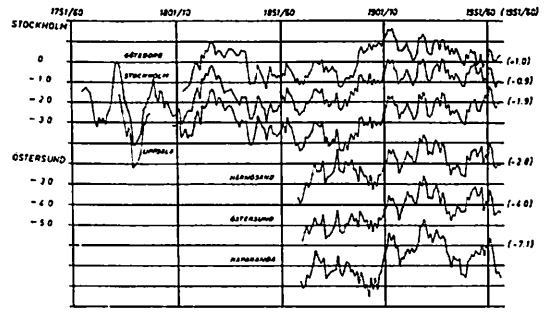

March.

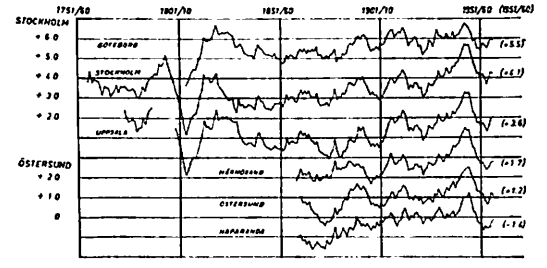

April.

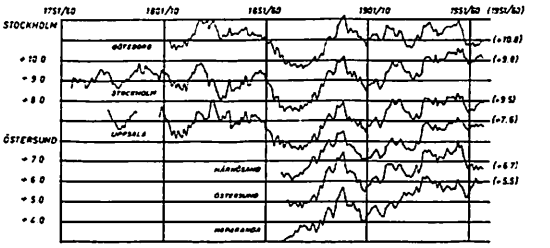

May.

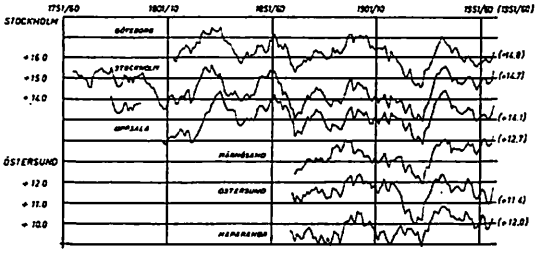

June.

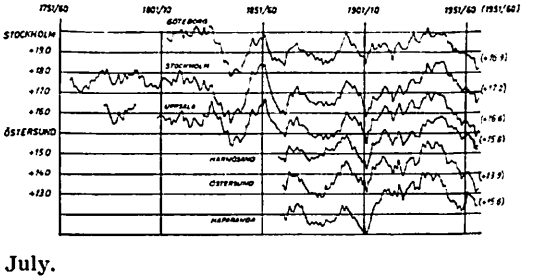

July.

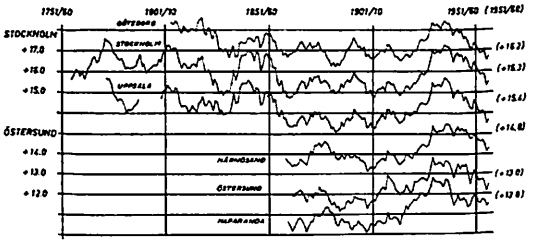

August.

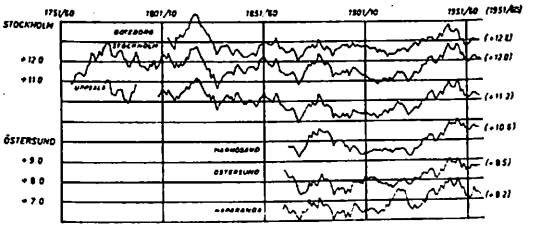

September.

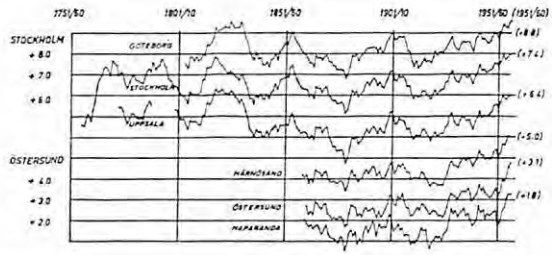

October.

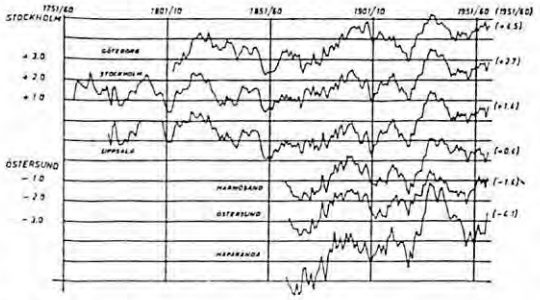

November.

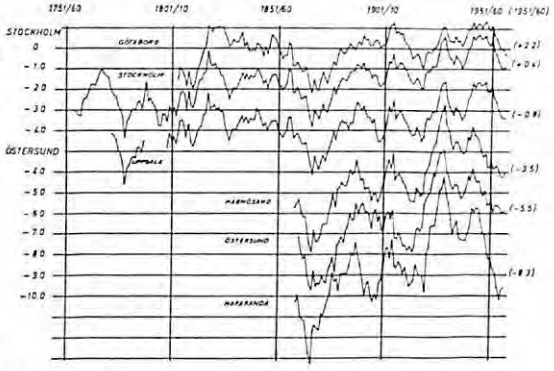

December.

FIG. 16. The secular variation of monthly mean temperatures, overlapping ten-years mean values at Gothenburg since 1804, Uppsala (1773), Stockholm (1756), Härnösand (1859), Östersund (1861) and Haparanda (1860). The vertical scales on the left-hand side refer to Stockholm and Östersund. The other curves are vertically displaced, their temperature ordinates are easily found by means of the figures on the right hand reading the mean temperature of the decade 1951/60.

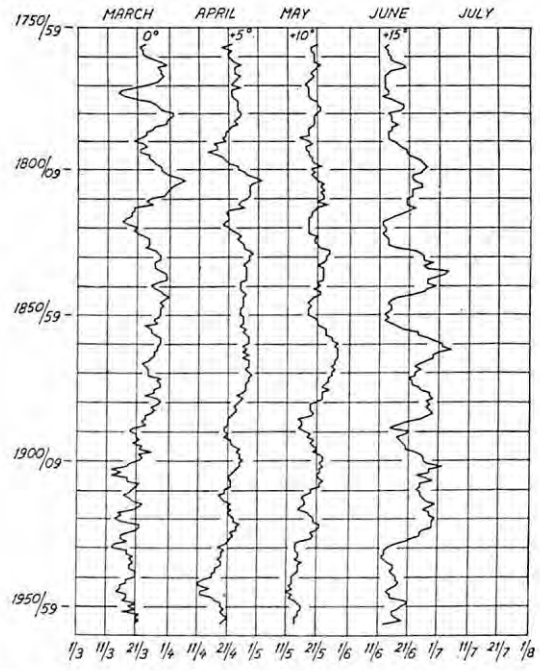

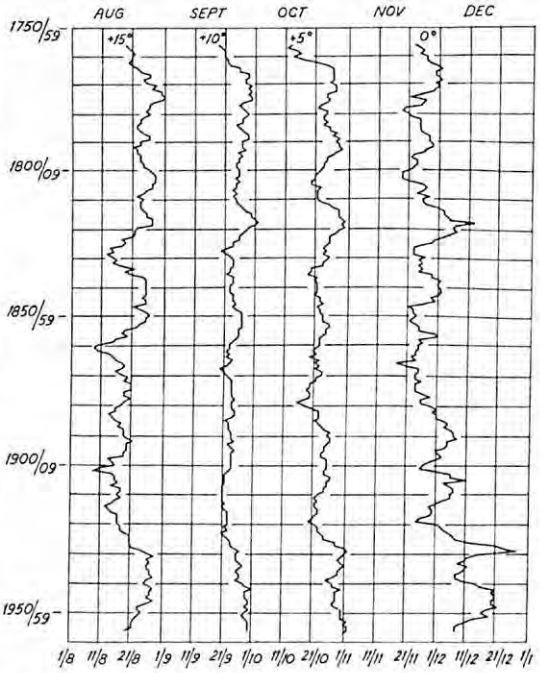

FIG. 17. The variation of the beginning of the annual seasons, represented by the date when the ten-years mean temperature passed 0°, +5°, +10° and +15° C. Stockholm 1756—1966.

(1860). The series cover practically the whole of Sweden and the diagrams show that the secular temperature variation has the same pattern in the whole country. A lot of interesting details are outstanding but we note here only two.

1. The July and August temperatures show a maximum in the nineteenthirties. The cooler summer conditions of our days, are comparable with those in the beginning of the century.

2. There is at present in October a maximum mean temperature. In most of the station series, this October maximum is the highest ever recorded.

The climate temperature variation involves a displacement of the annual seasons. Fig. 17 presents the mean date when according to the overlapping ten-year mean values the temperature passed some values as for instance 0°, 5°, etc. The curves reveal the displacement of the beginning and end of the seasons. There are short-range fluctuations covering less than thirty years. But there are some long-range trends, too. In August the temperature went below +15° earlier at the end than in the beginning of the nineteenth century. The arrival of spring comes nowadays five to ten days earlier than before 1890. The summer and the autumn end later. In total the summer time has been prolonged.

Summing up, we find that the natural temperature variations are large in comparison with those which may result out of lake regulations. Because of the temperature rise in autumn and the correlation between mean temperature and fog frequency, we assume that there has also been a rise of fog frequency during the last decades. It is not possible to see this directly in the series of fog observation because the absolute frequencies are unreliable and series referring to different observers are uncomparable.

We have seen that the lake regulations may result in a small increase of fog frequency in autumn, but likely there has also been trend in the natural variation of climate going in the same direction.

REFERENCES

Bowen, I. C., 1926, *Phys. Rev.*, *27*, p. 779.

Geiger, R., 1959, *Das Klima der bodennahen Luftschicht.* Friedr. Vieweg & Sohn, Braunschweig.

Nyberg, A., 1965, A study of the evaporation and condensation at a snow surface. *Ark. f. Geofysik*, *4*, 30.

Rodhe, B., 1962, The effect of turbulence on fog formation. *Tellus*, *14*, pp. 49—86.

Rodhe, B., 1966, The concentration of liquid water in the atmosphere. *Tellus*, *18*, pp. 86—104.

Rodhe, B., 1967, Report on the effect of lake regulation and electric power station on climate. Report given by the Swedish Meteorological and Hydrological Institute in May 1967.

Wallén, C. C., 1966, Global solar radiation and potential evapotranspiration in Sweden. *Tellus*, *18*, pp. 786—800.

Ångström, A., 1916, Ueber die Gegenstrahlung der Atmosphäre. *Meteorol. Z.* *33*, pp. 529—38.

The temperature of physically well-defined bodies under the influence of various meteorological elements, particularly radiation

By KARIN SCHRAM and J. C. THAMS *Ticinese Observatory of the Swiss Central Meteorological Station. Locarno-Monti*

ABSTRACT

A knowledge of the temperature which a body may assume under the influence of solar radiation in air layers near the ground is of major significance in problems of heliotherapy. The attempt has here been made to explore these conditions with the aid of recordings extending over more than a year on solid copper spheres placed 10 cm and 160 cm above the ground. The results show that in the climatic conditions prevailing just south of the Alps very high temperatures may be attained which are of importance from a physiological viewpoint.

1. Introduction

There can be no doubt that research into atmospheric radiation phenomena received powerful stimuli, particularly in its initial phases, from the medical profession. The discovery of NIELS R. FINSEN (1961) that lupus can be healed by irradiation, and the use of the natural ultra-violet radiation of the high mountains by O. BERNHARD and A. ROLLIER to cure tuberculosis of the bone provided the cue for a thorough investigation of the highradiation climate, particularly in the mountains. The pioneering work on this subject, "Studie über Licht und Luft des Hochgebirges" (A Study of the Light and Air of the High Mountains) by C. DORNO appeared in 1911. Soon afterwards heliotherapy went through a phase of previously unimagined expansion and thousands of persons were healed of serious illness in the mountains. Today heliotherapy plays a minor role only; other and more effective medicines have been discovered for combating tuberculosis, and most of the mountain sanatoria have been converted into sporthotels.

The controlled use of solar radiation by physicians in sanatoria has today been replaced by the uninhibited sun-bathing craze of millions of holiday-makers, a movement which is being followed by the medical world with ever-growing concern. The seasonal migration to the sunny south was never as extensive as in our own day. Here, however, the non-specific effect of optical radiation, the thermal action complex (LOTZ, 1962), plays an important part in addition to the photo-actinic effect. And this influence is still imperfectly understood from a medical viewpoint.

One of the fundamental questions which here await an answer is what temperature the upright or outstretched human body assumes under the influence of the various meteorological factors, and above all of solar radiation. The question is difficult to answer for the human body with its highly developed and very complicated control mechanism. The temperature ranges involved, however, are to a large extent the subject of special climatological research.

2. Test set-up

If a clarification of the basic problems was to be expected, the following requirements had to be fulfilled:

1) The measurements had to be made in a climatic region which attracts thousands of holiday-makers each year because of its high sunshine quota and mild climate.

2) The instruments used had to be of a character qualified to furnish results of an

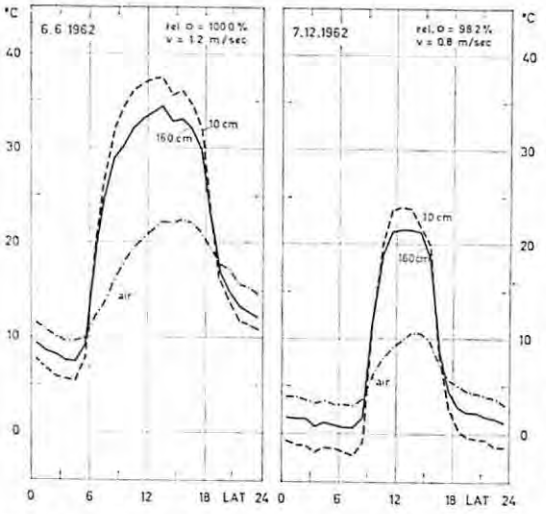

FIG. 1. Diurnal variations of the temperatures [°C] of black copper spheres at heights of 10 cm and 160 cm above the ground and of the air on practically cloudless days in summer and winter, viz. on 6.6.1962 and on 7.12.1962, at Locarno-Monti (rel. ⊙ %: relative duration of sunshine, v: wind velocity).

absolutely satisfactory nature from the physical and climatological viewpoint.

The region concerned in the present instance is the southern foot of the Alps, or to be more exact the lower-lying parts of the Ticino, which fulfil the first requirement in an ideal way. Not only does the area enjoy a good deal of sunshine; the air temperatures are also high compared with those north of the barrier of the Alps. Sunlight therapy is also favoured by the wind velocities, which are in general low.

The test set-up was the following: Two black solid copper spheres of a diameter of 75 mm were placed above a meadow, the grass of which was kept short, at heights of 10 cm (lying posture) and 160 cm (upright posture). In the interior of each sphere was fitted a thermocouple, the tension of which was continuously recorded by a compensograph (made by Leeds & Northrup).

This set-up was frequently calibrated. The mean error for individual readings was $\pm 0.4°$ C. In the immediate proximity of these two black bodies was a Bellani spherical pyranometer made in the workshop of the Physico-Meteorological Observatory in Davos. This instrument measures the energy of the short-wave radiation from sun and sky (day total) falling on a spherical surface. The air temperature was also recorded very close to the test set-up by thermo-electric means in a Stevenson screen. The wind velocity was measured with a Fuess cup anemometer at a height of 1.6 meters above the ground.

Evaluation was based on the mean hourly figures, in view of the problem to be investigated. Higher values may therefore be attained for very short times. The period of measurement extended from August 1961 to December 1962.

The Ticinese Observatory is located about 200 metres above the Lake of Locarno. The situation is typical of a southward facing slope. It is quite possible that still higher temperatures are sometimes reached on the shores of the Lake of Locarno (200 metres above sea level).

3. Results

Continuous recording of the temperature of the black bodies for almost a year and a half supplied a wealth of material from which a few characteristic figures that throw most light on the problem under consideration will be quoted here. We shall therefore restrict ourselves in general to sunny days on which it is likely that people would take sunbaths. Major interest attaches to the maximum temperatures that can be reached, to the frequency with which they occur and to the rate of temperature rise.

Two examples will first of all be given, one from the summer and one from the winter, to show in what way the temperature of a black copper sphere 10 cm or 160 cm above the ground varies on a practically cloudless day (Fig. 1). In the night the temperatures fall because the energy loss of the spheres due to outgoing longwave radiation exceeds the heat input by conduction and convection and by the relatively small long-wave incoming radiation on clear nights. The nearer the sphere is to the ground, the lower is the wind velocity and thus the heat transfer by conduction and convection, which represents a heat gain at night, when the air is warmer than the sphere, but a heat loss in

TABLE I. *Maximum hourly means of the temperature of black copper spheres at heights of 10 cm and 160 cm above the ground measured in the various months, together with air temperatures and wind velocities of the corresponding hours and the relative duration of sunshine for the whole day, measured at Locarno-Monti.*

Date	Hour (a.s.t.)	T max. (10 cm)	T max. (160 cm)	T air	v (m/sec)	rel. ⊙ % (day)
26. 1.1962	13—14	31.1	28.4	16.4	0.9	98.3
6. 2.1962	12—13	32.8	29.0	18.3	1.2	98.6
12. 3.1962	13—14	32.7	29.4	15.9	1.2	90.1
24. 4.1962	13—14	42.4	39.1	24.7	1.1	95.6
10. 5.1962	12—13	40.9	37.0	22.2	1.2	70.9
25. 6.1962	12—13	49.4	44.7	30.2	1.1	70.4
17. 7.1962	12—13	45.9	42.5	29.3	1.1	67.0
14. 8.1962	11—12	45.9	42.5	28.8	0.9	88.0
13. 9.1962	14—15	44.5	40.9	30.2	1.3	98.4
4.10.1962	12—13	40.1	36.3	23.0	0.8	97.0
2.11.1961	13—14	31.2	27.7	15.3	0.9	99.7
13.12.1961	13—14	34.1	31.1	19.1	0.6	90.0

the day. When shortwave irradiation sets in at sunrise the temperature of the spheres at first rises very quickly, at a rate of up to 10° C per hour; then it slows down, reaching its maximum in most cases one to three hours after the sun's culmination. This extremely marked and rapid rise in temperature, which takes place in summer and winter alike as soon as the body is exposed to the short-wave radiation from sun and sky, is of course a tremendous load for the organism, a fact of which most sun-bathers are of course oblivious. The temperature drop in the afternoon is just as steep as the rise in the morning and only flattens out at sunset.

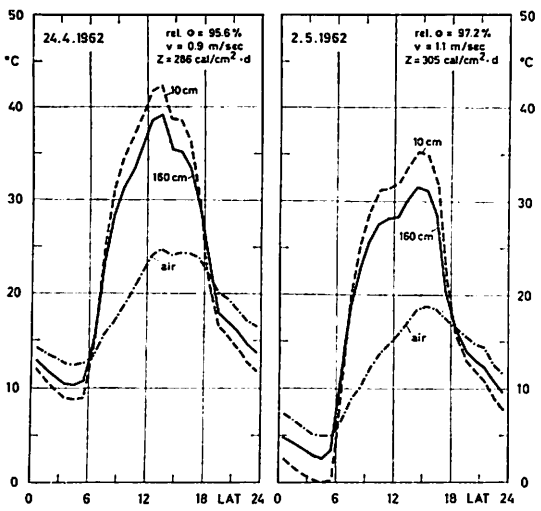

FIG. 2. Diurnal variations of the temperatures [°C] of black copper spheres at heights of 10 cm and 160 cm above the ground and of the air on 24.4.1962 and on 2.5.1962 (rel. ⊙%: relative duration of sunshine, v: wind velocity, z: short-wave radiation incident on a spherical surface).

The diurnal variations of the temperatures shown in Figure 1 were recorded on cloudless days with little wind, but they are not by any means extreme cases. Considerably higher temperatures can in fact be reached (Table 1). The highest measured hourly mean of 49.4° C was registered for a sphere at a height of 10 cm in June, but even in winter the temperature may rise to more than 30° C. The sphere at a height of 160 cm above the ground is exposed to higher wind velocities and therefore becomes less warm. It is a striking point, as revealed by Table 1, that the maximum temperatures, particularly in summer, did not occur on completely cloudless days. This is partly due to the fact that the short-wave radiation of sun and sky is considerably greater when there are clouds near the sun. On the other hand, extremely high temperatures can only be reached when the initial temperatures are high, or in other words the weather conditions prevailing on the preceding days are also of considerable importance. This is demonstrated in Figure 2. Although the wind conditions on the two

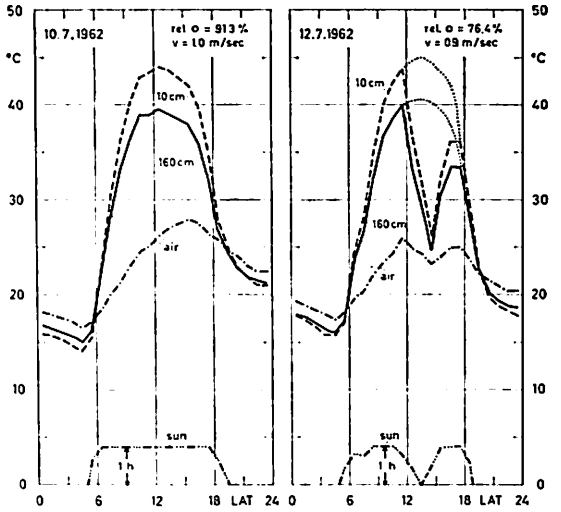

FIG. 3. Diurnal variations of the temperatures [°C] of black copper spheres at heights of 10 cm and 160 cm above the ground, of the air and of the duration of sunshine [h] on 10.7.1962 and on 12.7.1962 at Locarno-Monti (rel. ⊙%: relative duration of sunshine, v: wind velocity).

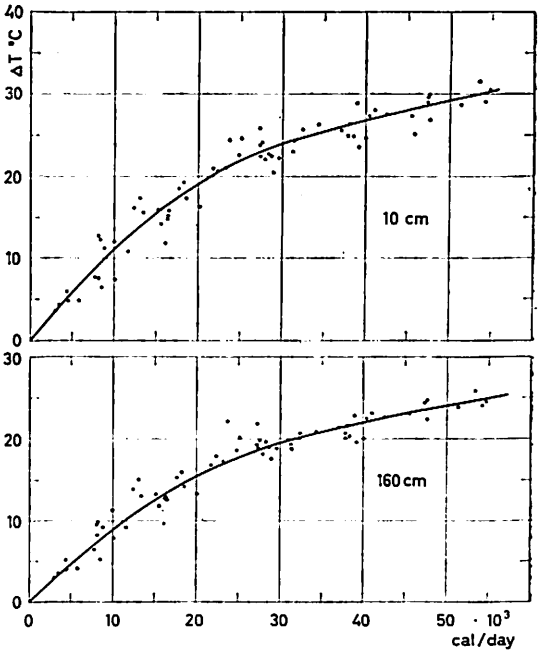

FIG. 4. Relationship between the maximum temperature rise [°C] per day of black copper spheres at heights of 10 cm and 160 cm above the ground and the daily total of short-wave radiation incident on the surface of the spheres [cal], measured at Locarno-Monti.

days represented were practically the same and the radiation on 2.5.1962 was even rather higher than on 24.4.1962, the maximum temperature measured on 2.5. was 7° C lower because the initial morning temperature differed by about the same amount. Before the 24th April the weather was cloudy and temperatures dropped very little in the night, while the 2nd May had been preceded by a period of Nordföhn with clear nights and comparatively low day temperatures. The initial morning temperature is thus chiefly responsible for the absolute value of the maximum temperature on a day of radiation, since a given energy supply by radiation can only produce a given temperature rise. Consequently the heating of the spheres on days with a relative duration of sunshine between 60 and 100 % is fairly constant and amounts to about 30° C for the sphere at a height of 10 cm in summer, and 25° C in winter, while the corresponding figures for the sphere 160 cm above the ground are 25° C in summer and 20° C in winter. The human body is at a temperature of about 36.5° C at the beginning of exposure and must therefore become much warmer than the copper spheres. It is clear that its control mechanism cannot deal with this high energy supply and that the result must be a build-up of heat in the body and possibly lasting damage if this overloading is frequently repeated.

The majority of the incoming short-wave radiation is due to direct sunlight. If the sun's rays are screened off by clouds, the spheres cool down comparatively quickly. This can be demonstrated very clearly by the example of the 12th July 1962 (Fig. 3). The rise of the temperatures on the morning of this day, and the drop in that part of the afternoon when the sun was practically unobscured by clouds, were the same as on the cloudless 10th July 1962. But from 11.00 o'clock onwards the sun was obscured more and more by clouds and from 13.00 till 14.00 was not visible at all. The temperature of the sphere 160 cm above the ground sank 15° C in this period, that of the sphere at 10 cm even dropping by 18° C. The sky then cleared

TABLE 2. *Number of cases in which the hourly means of the temperatures of the black copper spheres at heights of 10 cm and 160 cm above the ground were 36.5° C, 40.0° C, 45.0° C or more at Locarno-Monti in the year 1962.*

Month		A.s.t.																		
		10 cm above ground										160 cm above ground								
		8—9	9—10	10—11	11—12	12—13	13—14	14—15	15—16	16—17	17—18	8—9	9—10	10—11	11—12	12—13	13—14	14—15	15—16	16—17	17—18
T ⩾ 36.5° C	April			4	5	5	3	4	3						3	3	3				
	May			4	5	6	8	6	3						1	1	1	1			
	June	5	10	14	15	19	19	16	11	8	3	1	7	9	9	8	10	10	7	3	
	July	3	17	23	24	25	24	22	18	9	1		4	13	22	18	18	16	8	2	
	August	3	21	24	25	25	24	24	25	20	1		4	20	21	22	21	22	19	8	
	September		3	11	12	14	14	13	8	3				3	6	7	6	4	3	2	
	October				4	6	6	3	1												
T ⩾ 40.0° C	April				3	4	2														
	May				1	1	1	1	7	3											
	June	1	5	10	9	8	11	12	9	2			1	3	2	4	4	4	3	1	
	July		5	15	19	19	19	16	19	7				2	3	7	4	3			
	August		3	19	20	21	21	22	3	2				1	7	10	9	6	3		
	September			3	6	7	6	5										1	1		
	October					1															
T ⩾ 45.0° C	June			2	2	2	2	1	1												
	July				1	4	3														
	August				2	2	2	3													

again and the temperatures which the spheres would have had with a completely cloudless sky were again reached.

Figure 4 shows the relationship between the heating of the spheres and the short-wave radiation. The days were divided into classes based on the relative duration of sunshine for each month of the year, and for each day the difference between the highest temperature about noon and the lowest in the morning was calculated. The individual points in Figure 4 are the mean values of this maximum temperature rise and of the daily sum of the short-wave radiation on the spheres, measured with a Bellani spherical pyranometer, for each class and each month. The comparatively marked scatter of the points was to be expected, since the short-wave radiation is not the only component in the heat balance of the spheres. Wind conditions and precipitation both have an influence on the range of the temperature rise. At high wind velocities more heat is extracted from the spheres by conduction and convection than at low wind speeds. Above all, however, the heating and evaporation of precipitation on the spheres represents a considerable loss of energy.

The question now arises of how often high temperatures are attained in the spheres in the sunny and not very windy climate of Locarno. Table 2, in which the frequency of high temperature recordings in 1962 is summarized, confirms the long-known fact that the Ticino is one of the warmest regions of Switzerland and one of the richest in radiation. Even in April the temperature of the two spheres was above 36.5° C at noon on approximately a tenth of all days, and that of the sphere at a height of 10 cm was even above 40.0° C. In June the sphere at this height already attained a temperature of 36.5° C in the hour between 8.00 and 9.00 and did not sink below it till after 18.00. In July and August the temperature remained above this level from 10.00 to 15.00

on four fifths of all days, and on most was above 40.0° C. The sphere at a height of 160 cm was also at a temperature of more than 36.5° C on a large number of days, and the 40.0° C level was exceeded fairly frequently.

The small investigation described here naturally furnishes information only on the behaviour of a physically well-defined body at various heights above the ground under the influence of the meteorological elements. Transference of the results to the human body still remains an extremely difficult problem which can only be solved in close collaboration with physiologists and physicians.

REFERENCES

Dorno, C., 1911, *Studie über Licht und Luft des Hochgebirges*. Vieweg & Sohn.

Lotz, R., 1962, Unspezifische Wirkungen optischer Strahlung. „Thermischer Wirkungskomplex". *Handbuch der Bäder- und Klimaheilkunde*, Stuttgart.

Progress in Photobiology. The Finsen Memorial Congress, Copenhagen, 1960. Elsevier Publishing Company, 1961.

Rayonnement (Tiros IV) et pluviosité au Congo[1]

Par WALTER SCHUEPP

Astronomisch-Meteorologische anstalt der Universität Basel

ABSTRACT

From charts of daily precipitation, of the daily sum of global radiation and from infrared radiation in the region 8—12 μ (HRIR) measured by satellite TIROS IV, the meteorological evolution over Central Africa during the period 1st to 3rd May, 1962, is analyzed. Table 1 shows that a relatively strong correlation exists between radiation intensity in this range and precipitation. Even between the daily sum of global radiation from sun and sky and precipitation a similar relation exists (Table 2). A radiation chart taken from a satellite and distributed sufficiently fast may greatly facilitate the synoptic information.

Le satellite météorologique TIROS IV a collectionné dans la période du 26 avril jusqu'au 9 mai 1962 un grand nombre d'observations au-dessus de l'Afrique.

Tandis qu'en latitudes moyennes l'intérêt se rapporte en premier lieu aux photos des nuages, les données de rayonnement infrarouge 8 à 12 μ sont plus significatives dans les tropiques humides. En effet ce rayonnement indique grossièrement le niveau où se trouve la surface moyenne des nuages dans le secteur visé. Même en régions tropicales il faut en général que les nuages pénètrent l'isotherme de 0° pour provoquer des pluies importantes. Cette isotherme se situe vers les 5000 m d'altitude, tandis que la température au sol varie entre 20 et 35°. Les régions de pluie se trouvent donc principalement aux endroits où le rayonnement 8 à 12 μ indique de basses températures. Alors une corrélation entre la carte synoptique et les zônes de faible ou forte radiation infrarouge est indiquée.

Le nombre de stations pluviométriques munies de pluviographes qui permettraient l'évaluation de l'intensité et la quantité de pluie tombant au moment du passage du satellite est trop faible pour attaquer le problème ainsi. Mais la république du Congo dispose d'un réseau de stations pluviométriques où la quantité journalière est évaluée à 06 GMT le matin, tandis que le passage du satellite a lieu entre 08 et 12 GMT. S'il pleut à la station au moment du passage, il est fort probable qu'une partie de la pluie a été mesurée à 06 GMT du jour et que le reste ne sera lu qu'à l'observation prochaine du lendemain à 06 GMT. Beaucoup plus représentative aurait été la quantité de pluie tombée entre 00 et 12 GMT. Néanmoins le tableau 1 montre déjà une relation étroite entre le rayonnement infrarouge 8 à 12 μ et la quantité de pluie mesurée à 06 GMT (donc précèdent le passage) ainsi que celle mesurée à 06 GMT du lendemain (tombée pendant et après le passage du satellite). S'il n'y a que 14 à 16 % de risque de pluie pour un rayonnement 8 à 12 μ supérieur à 37 unités, il y a 100 % de risque quand ce rayonnement est inférieur à 21 unités. Même en classant en deux groupes uniquement, le risque de pluie augmente de 36 % pour rayonnement infrarouge $>$ 31 unités à 74 % pour rayonnement $<$ 30 unités. Cette relation prouve que les systèmes de nuage de grande étendue et à surface élevée relevés par le detecteur TIROS IV sont de première importance pour le régime de précipitation au Congo.

Un autre moyen de caractériser la densité du système nuageux est la somme journalière du rayonnement global (du ciel et du soleil) mesurée à 30 stations environ. La variation journalière n'est enregistrée qu'à 3 points, il n'est donc pas possible d'en déduire la

[1] Cette étude était faite au « Service Météorologique, Kinshasa, République Démocratique du Congo » avec le concours du U.S. Weather Bureau, Dep. Satellite Meteorology, Washington, D.C. U.S.A. qui a mis les observations du satellite TIROS IV à la disposition.

TABLEAU 1. *Rayonnement infrarouge 8 à 12 μ de TIROS IV et pluviosité au Congo.*

1ère colonne: pluie tombée avant le passage
2ème colonne: pluie tombée pendant et après le passage.

Rayonnement	19 à 21	22 à 24	25 à 27	28 à 30	31 à 33	34 à 36	37 et plus	jusqu'a 30	31 et plus	
Pluviosité										
0	0 (0)	4 (7)	14(10)	19(18)	47(27)	33(27)	6(15)	37(35)	86(69)	cas
gouttes à 0.3 mm	1 (1)	4 (1)	6 (9)	9 (4)	8 (5)	5 (7)	0 (0)	20(15)	13(12)	
0.4 à 1.0 mm	0 (0)	1 (1)	4 (2)	4 (5)	2 (0)	0 (1)	0 (0)	9 (8)	2 (1)	
1.1 à 3.0 mm	0 (0)	4 (6)	5 (2)	11(10)	5 (6)	4 (0)	0 (0)	20(18)	9 (6)	
3.1 à 10.0 mm	0 (0)	4 (9)	7(11)	11 (9)	6 (8)	4 (4)	1 (1)	22(29)	11(13)	
10.1 à 30.0 mm	0 (1)	9 (5)	6 (7)	8(11)	4 (5)	3 (1)	0 (2)	23(24)	7 (8)	
plus que 30 mm	1 (0)	3 (5)	4 (2)	1 (3)	2 (0)	3 (0)	0 (0)	12(10)	5 (0)	
% jours de précipitation	100(100)	75(79)	70(77)	71(70)	37(47)	37(33)	14(16)	74(75)	35(37)	%

TABLEAU 2. *Rayonnement global G et pluviosité au Congo.*

Pluie tombée dans l'intérval de 24 heures pendant et après le passage.

Rayonnement	jusqu'à 100	101 à 200	201 à 300	301 à 400	401 à 500	501 et plus	jusqu'à 400	401 et plus	cal/cm² d
Pluviosité									
0	0	1	5	38	109	49	44	158	cas
gouttes à 0.3 mm	1	0	5	9	20	1	15	21	
0.4 à 1.0 mm	0	0	7	7	4	2	14	6	
1.1 à 3.0 mm	0	0	3	15	16	6	18	22	
3.1 à 10.0 mm	2	5	9	13	15	6	29	21	
10.1 à 30.0 mm	0	5	11	18	16	1	34	17	
30 mm et plus	0	1	7	11	10	1	19	11	
% jours de précipitation	100	92	89	66	43	26	75	38	%

densité au moment même du passage du satellite; mais le tableau 2 nous indique que la pluviosité et le rayonnement global sont liés étroitement. Par rayonnement très fort > 500 cal/cm² d (nébulosité faible pendant les heures de jour) il n'y a que 26 % de risque de pluie; par rayonnement faible < 200 cal/cm² d le risque de pluie augmente jusqu'à 94 %. Même si on ne sépare le collectif qu'en deux groupes (> 400 et < 400 cal/cm² d) les risques de pluie se chiffrent à 38 % par rayonnement fort et 75 % par rayonnement faible. Cette relation prouve que les systèmes de nuages denses relevés par les pyranomètres au sol sont la source principale des précipitations au Congo (SCHÜEPP, 1963).

Il paraît qu'en régions tropicales humides l'évolution du temps joue à deux échelles de caractère fort différent, pour ne pas dire contradictoire.

a) L'échelle perceptible à l'observateur au sol. On sait que les cellules individuelles d'orages et de précipitations ne dépassent pas en général les dimensions de 10 à 50 km de diamètre. La durée de vie d'une telle cellule ne dépasse guère quelques heures et souvent les trajets des cellules s'avèrant assez indépendants l'un de l'autre surtout aux journées de vent faible en altitude.

Par conséquence parmi les pluviographes de stations voisines, souvent l'un n'indique rien au moment où une forte averse se déverse sur l'autre. Un exemple particulier pour l'indépendance apparente du temps entre deux stations voisines est l'observation du rayonnement global journalier à Bukavu et L'wiro, deux stations situées au bord du lac Kivu à moins de 100 km de distance, où aucune correspondance entre les observations aux deux postes n'a pu être détectée. C'est ainsi que les météorologistes sont tentés de parler d'un climat autochtone. Une

statistique de JOHNSON (1962) du réseau pluviométrique Est-Africian confirme l'indépendence des stations éloignées de plus de 200 km, tandis qu'une faible correlation est indiqueé entre stations distantes de 50 km seulement.

b) A l'échelle du satellite la situation se présente tout autrement. Encore il arrive que parfois à un lieu de rayonnement infrarouge élevé une pluie tombe dans les 24 heures avant ou après le passage, mais on constate qu'il doit exister des systèmes nuageux très étendus et assez réguliers se déplaçant d'une façon ordonnée pour que l'image momentanée soit représentative pour une période d'au moins 12 heures avant et après le passage. Donc l'individualisme arbitraire frappant l'observateur au sol est en réalité englobé dans des systèmes assez ordonnés à l'échelle supérieure. L'ensemble des cellules convectives avec leur courte durée de vie et ses motions arbitraires forme un collectif. Déjà les cartes journalières du rayonnement global (SCHÜEPP 1963) ont montrés qu'aux cas d'insolation nulle, le rayonnement de plusieures stations voisines était fortement réduit. Un autre phénomène marqué particulièrement bien à Léopoldville —Kinshasa (SCHÜEPP, 1956) est le fait, que les cellules orageuses épargnent certaines stations à le première occasion—surtout les orages d'après-midi évitent le large du bassin du Stanley-Pool — tandis que les lignes de grains suivantes — surtout les orages de nuit — y passent par préférence. Enfin les lignes de grains matinales souvent ont l'aspect assez compacte et ne sont pas déformées par l'orographie.

Il resulte donc un parallelisme très marqué entre

a) la carte rayonnement 8 à 12 μ lors du passage du satellite TIROS IV
b) la carte de la somme journalière du rayonnement global, et
c) la carte de pluviosité journalière RR sur les 24 heures précédent — ou suivant le passage du satellite.

Ceci est illustré par les 10 figures indiquant l'évolution du 1er au 3 mai 1962 entre 10° latitude N et 15° latitude S, ainsi que les longitudes de 10 à 35° E. Pour bien pouvoir suivre l'évolution il faut voir l'ensemble des 10 tableaux.

Les 3 tableaux TIROS sont des prises « momentanées » composées des passages captés pendant deux ou trois vols entre 10 à 12 GMT le 1er, entre 9 et 11 GMT le 2 et entre 8 et 10 GMT le 3 mai; ce qui correspond à midi local le premier, 11 heures local le 2 et 10 heures local le 3 mai.

Le carte du rayonnement global pour la journée du 1er mai est assez représentative, car le passage du TIROS se situé au mileu de la journée. Pour la carte du 2 mai et encore plus pour celle du 3 mai il faut tenir compte, que le rayonnement global est mesuré surtout après le passage du satellite.

Enfin les cartes de pluies sont celles de 06 GMT de la veille à 06 GMT du jour, donc la carte du 1er mai indique la pluie tombe longtemps avant le passage de TIROS IV, la carte du 2 mai indique la pluie tombée du 1er au 2 période où se situe le passage TIROS du 1er, il faut donc s'attendre à une correspondance entre la carte TIROS du 1er, et la carte rayonnement global du 1er et la carte précipitations lue le 2 à 06 GMT. En effet aucune précipitation n'est observée du 1er au 2 au Katanga, région où le rayonnement en général dépasse les 400 cal/cm² d, bien qu'à cette époque le soleil soit assez bas avec seulement 60° à midi, et le rayonnement 8 à 12 μ indique entre 30 et 34 unités. Par contre la région centrale et occidentale du pays indique (sauf la station de Banane au bord de la mer) une forte pluviosité dépassant 10 mm et sur de vastes régions même 40 mm. De même le rayonnement global est en dessous de 300 cal/cm² d dans toute la partie centrale du Congo avec des noyaux en dessous de 200 cal/cm² d au Mayumbe, dans la région du Lac Léopold et au Kwilu, aux mèmes endroits où le rayonnement 8 à 12 μ est en dessous de 26 unités.

Toute différente est la situation du 2 au 3 mai 1962. La région de faible rayonnement 8 à 12 μ < 26 unités s'est déplacée vers le nord, tandis que la zone avec rayonnement >33 unités s'est avancée au dessus de la capitale. De mème la carte du rayonnement global ne montre plus qu'une zone au N et à l'E où la valeur n'atteint pas les 300 cal/cm² d. Regardant les deux cartes de la pluviosité du 1er au 2 mai et du 2 au 3 mai on a l'impression qu la zone de pluie se soit déplacée vers le NE. Derrière cette zone le ciel

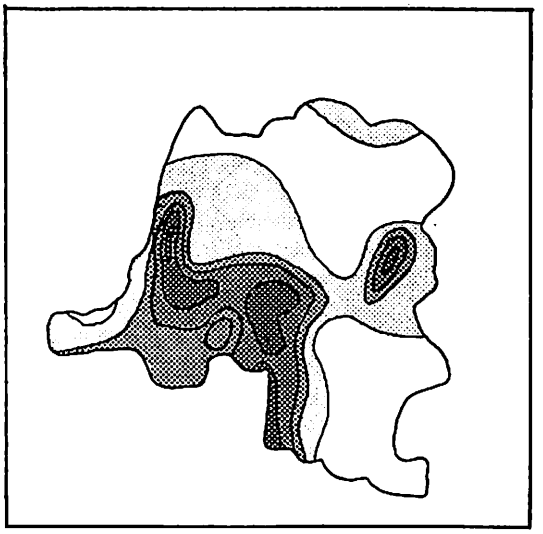

Précipitation 01-05-62
24h RR 0600Z

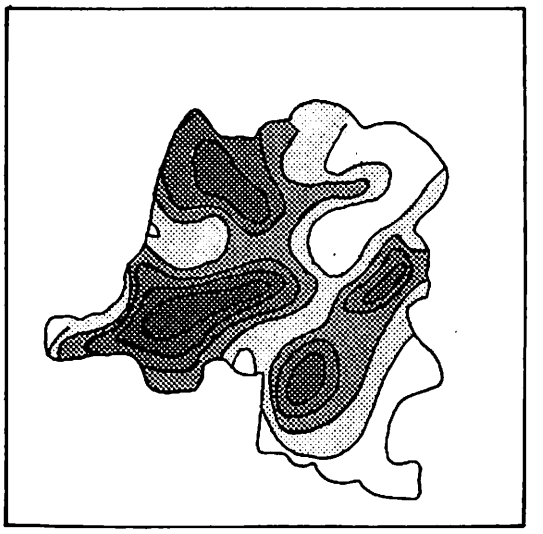

Précipitation 02-05-62
24h RR 0600Z

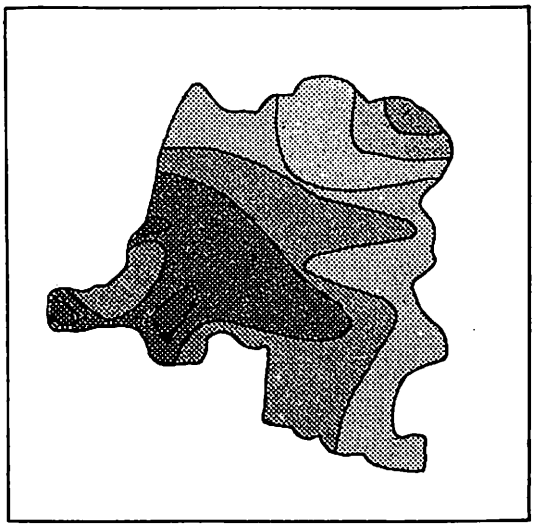

Rayonnement global 01-05-62

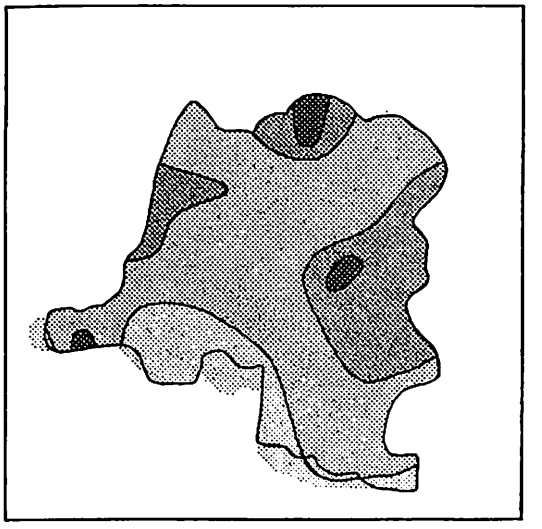

Rayonnement global 02-05-62

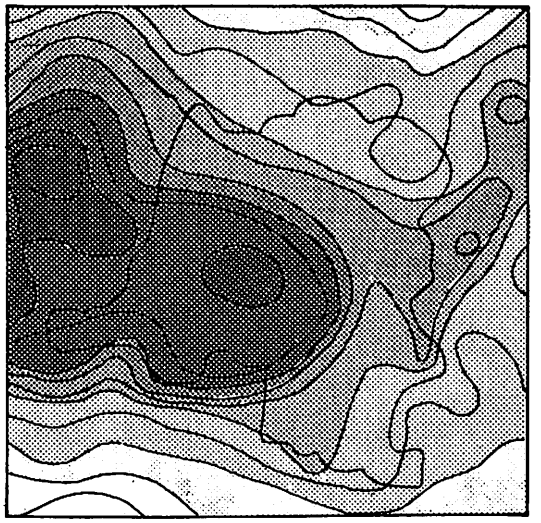

Tiros rayonnement 01-05-62
8à10 10-12Z

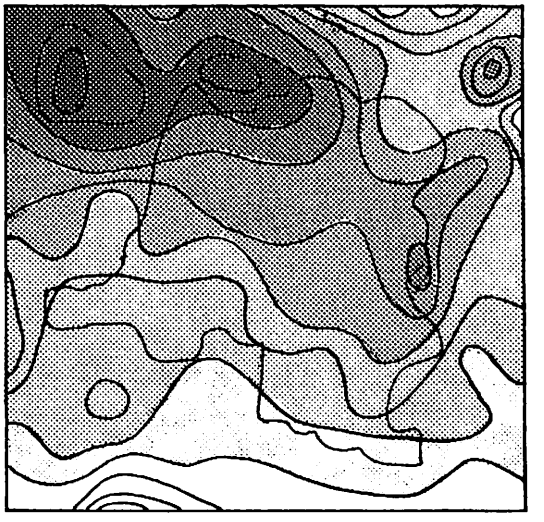

Tiros rayonnement 02-05-62
8à10 09-11Z

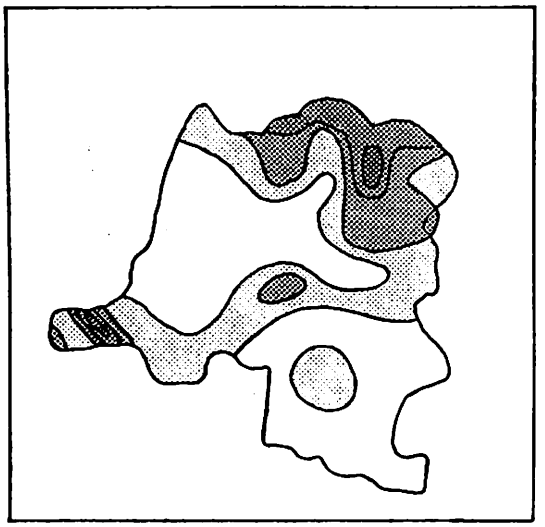

Précipitation 03-05-62
24h RR 0600Z

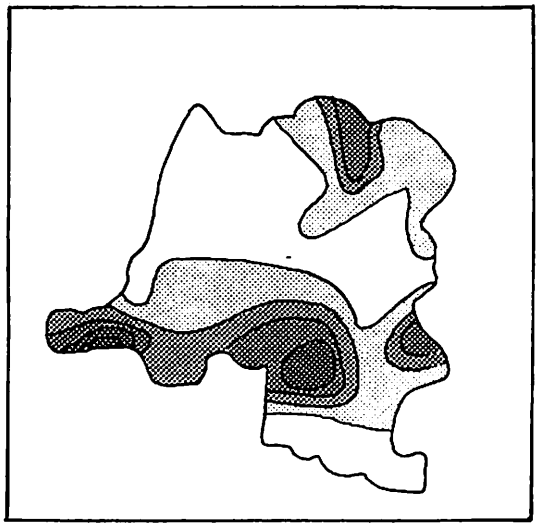

Précipitation 04-05-62
24h RR 0600Z

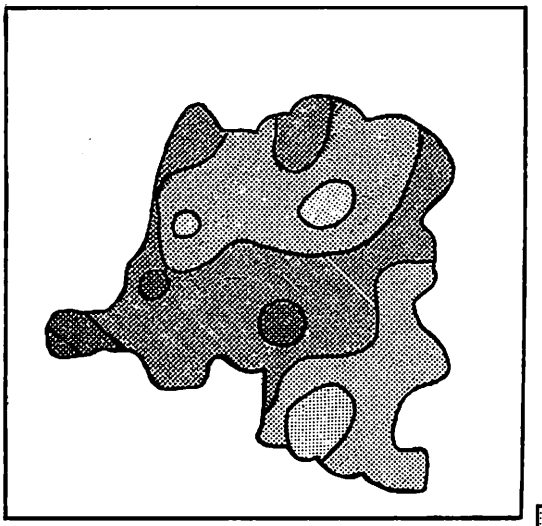

Rayonnement global 03-05-62

Tiros rayonnement 03-05-62
8 à 10 08-10Z

0 mm
Spur - 5
5-10
10-20
20-40
> 40 mm

cal/cm^2 d

> 500
400 - 500
300 - 400
200 - 300
0 - 200

HRIR unités

> 38
36 - 38
32 - 36
30 - 32
28 - 30
26 - 28
22 - 26
< 22

s'est éclairci au SW du pays, laissant le rayonnement global au dessus de 400 cal/cm² d au W de 25° longitude et au S de l'équateur; la mème région où le 2 à 11 heures local TIROS indique un rayonnement 8 à 12 μ au dessus de 30 unités. Par contre le NE de la République pratiquement sans pluie du 1er au 2 mai reçoit beaucoup du 2 au 3 mai avec le système nuageux centré le 2 à 5° N et 20° E et le 3 mai à 8° N et 30 ° E. Ce changement brusque de la pluviosité sur un pays si vaste apparait selon les observations TIROS en premier lieu comme simple déplacement d'un système nuageux. Mais avant que ce système disparaisse au N un nouveau système apparait au SW indiqué sur la carte du 3 mai le long du 5ème parallèle S aussi bien dans la bande 8 à 12 μ au TIROS qu'au rayonnement global et déjà la carte de pluviosité du 3 mai indique de nouvelles précipitations au Bas-Congo et à quelques stations du Kasai. La carte de pluviosité du 4 mai montre cette nouvelle zone pluvieuse assez étendue tandis qu'un petit noyau de l'ancien système persiste encore au NE.

La comparison entre carte TIROS et carte rayonnement global du 3 mai indique que la zone de nébulosité assez élevée au N ne persistait pas toute la journée, car le rayonnement global y était assez fort, de mème cette région restait en grande partie sans précipitations. Est-ce que c'était des couches Ac très transparentes pour le rayonnement solaire mais assez denses pour l'infrarouge 8 à 12 μ?

Il est curieux de constater que tandis que les lignes de grains se déplacent en général avec le vent d'E en altitude vers l'W, à l'échelle supérieure les zones nuageuses et régions de pluies indiquent un déplacement du SW vers NE, phénomène déjà signalé par BULTOT (1952).

Un détail particulier apparait fréquement sur les cartes TIROS analysées, c'est une singularité dans la région du Lac Victoria centré à 2° S et 33° E où le rayonnement était en dessous de 28 unités le 1er. Cette singularité est bien connue des météorologistes qui ont observé une pluviosité et activité orageuse nocturne maxima au centre du lac Victoria (JOHNSON, 1962). L'extension du cumulonimbus se formant fréquemment pendant la nuit sur le lac atteint donc l'échelle du champ de vision du détecteur infrarouge utilisé par le TIROS IV.

Ainsi des balayages reguliers de la surface terrestre par les éléments infrarouges de satellites TIROS, NIMBUS ou ESSA aidera sensiblement à l'étude synoptique dans les régions tropicales où ni le champ de pression ni celui de la température peuvent servir d'indicateur sur la situation générale.

BIBLIOGRAPHIE

BULTOT, F., 1952, Sur le Caractère Organisé de la Pluie au Congo-Belge Pub. I.N.E.A.C. Bruxelles. *Bureau Climatologique Conum. No 6*

JOHNSON, D. H., 1962, Rain in East Africa *Q. J. Roy. Meteor. Soc. 88*, p. 1.

SCHÜEPP, W., 1956, L'influence du fleuve au climat étudié à l'exemple du rayonnement à Léopoldville *Misc. Geofisica Angola*. Luanda.

SCHÜEPP W., 1963, Cartes journalières du rayonnement au Congo. *Archiv für Meteorol. Geoph. u. Biokl. B. 12*, p. 475.

A modified method to determine the annual precipitation in the Scandinavian mountains

By CARL CHRISTIAN WALLÉN, *Swedish Meteorological and Hydrological Institute, Stockholm*

ABSTRACT

Various methods have been applied earlier to determine the annual precipitation in Swedish mountain areas outgoing from measurements of precipitation and run-off as well as from estimates of evaporation. A modified method is described to map precipitation in the Scandinavian mountains based on a study of the relationship between calculated precipitation on the one hand and height above sea level and distance from the sea on the other. A map showing the annual precipitation is constructed with the aid of the relationship found.

1. Introduction

It is generally only with difficulties and with a great deal of approximation that the amounts of precipitation which fall in mountain areas may be determined and mapped. This is particularily true in mountainous regions of scarce population where observation stations may be established only in those valleys where the population is concentrated. The local topography at the same time is so varied that rather a denser network of precipitation stations should be required in such areas than in flat regions. It is consequently inevitable to try to develop a method to calculate precipitation amounts at a number of points where no measurements are made so as to increase the network of precipitation values in the area.

In Sweden A. WALLÉN as early as in 1923 developed a method to calculate annual precipitation in the Swedish mountains from run-off values obtained from a number of catchment areas spread over the mountains taking into account reasonable amounts of evaporation. This method was used also by the author in his presentation of maps of the precipitation in Sweden for the period 1901—30 (1951) however in a slightly modified form.

In connection with plans to publish for the climatological normal period 1931—60 new maps of precipitation for the whole of Scandinavia and Finland it has been considered necessary to adopt a method by which annual precipitation might be calculated not only for the Swedish but also for the Norwegian part of the mountain area. In fact in 90 % of Norway the topographical conditions make it impossible to map precipitation only by means of data obtained from precipitation stations.

The author consequently has developed a modification of the original method to determine precipitation from both precipitation and run-off values which seems to be acceptable to apply also in the Norwegian mountain regions.

2. Available basic data

The modified method has been developed for that part of the Scandinavian mountain area which is situated between latitudes 64° N and 68° 30′ N. In this area all available original data of the following kind have been used:

1. Mean annual precipitation values for all Norwegian stations giving reliable values which could possibly be reduced to the normal period 1931—60.
2. Mean annual precipitation values for all Swedish stations giving reliable values and which could possibly be reduced to the normal period 1931—60.
3. Mean annual run-off values for all acceptable run-off stations in Norway calculated for or reduced to the period 1931—60.

4. Mean annual run-off values for all acceptable run-off stations in Sweden, calculated for or reduced to the period 1931—60.
5. Values of the mean altitude above sea-level of the catchment areas corresponding to the run-off values in both Norway and Sweden.

In order to increase the number of available basic data mean values from certain precipitation stations and run-off stations which have been operating during periods of years outside the normal period 1931—60 have also been applied after having been reduced to that period.

The Norwegian data has been kindly placed at the author's disposal by the Norwegian Meteorological Institute and the Norwegian Water Development Board.

3. Estimation of evapotranspiration

All methods of the actual kinds are based on the assumption that annual precipitation may be estimated from run-off values by adding amounts of annual evaporation which are reasonable for the area in question.

The mean annual amount of evapotranspiration over a period of years from catchment areas in the Swedish mountains has been considerably discussed in the past. A. WALLÉN (1923, 1924) who first applied the actual method to calculate precipitation in the Swedish high mountains estimated the mean annual evapotranspiration to be between 300 to 400 mm based on the relation between run-off and evapotranspiration in Swedish catchment areas in general.

MELIN (1942) found in his experimental investigation of precipitation and run-off conditions in the Malmagen mountain area (Lat. 62° 35′ N. and Lond. 12° 10′ E, height 781 m) during the 1930-ies the mean annual evapotranspiration to be considerably lower i.e. around 150 mm. He concluded that this value would be a reasonable amount for most of the Swedish mountain areas.

BERGSTEN (1950) made a thorough investigation of the increase of the evaporation in Sweden which had taken place from the period of maritime climatic conditions during the first decades of this century to the period of more continental conditions with warmer summers during the 30-ies and the 40-ies. In the forest lands of Norrland Bergsten estimated the increase to have been from around 200 to 240 mm i.e. about 20 %. It is reasonable to assume that a corresponding increase must have taken place in the mountain areas. The values of Melin refer mainly to the 1930-ies and therefore should be higher than those occurring in earlier decades. According to Bergsten the maximum of evaporation occurred in the 1940-ies and considering that summer temperature in Sweden has declined since then a mean value for the period 1931—60 may be estimated to correspond to Melin's value i.e. to be around 150 mm.

Further investigations indicate, however, that this value may be somewhat too low. TAMM (1959) in his extensive investigation of the evapotranspiration in Sweden found by making use of his emperical formula based on temperature conditions that the annual mean evapotransspiration even in the upper forested region of Swedish Norrland close to the mountain region is slightly above 200 mm. Considering that the temperature difference between this zone and the mountain zone not covered by forest is only small in summer while the winds must be considerably stronger in the upper region than in the lower it is not likely that evapotranspiration there is much less than in the lower regions. This assumption is confirmed by recent calculations of potential evapotranspiration in Sweden carried out by the author (C C WALLÉN 1966). The amount of annual potential evapotranspiration calculated by the Penman formula is between 250 and 300 mm and considering that from comparisons with Tamm's values the relation between actual and potential evapotranspiration in this part of Sweden is around 0.7 we arrive at a value of 180 mm for the Swedish mountain regions. In estimating reasonable values for various catchment areas their height above sea level and latitude have to be considered. In doing so we have added to the run-off values those evapotranspiration values given in table 1 for different catchment areas in the Swedish mountains. They all lie between 150 and 200 mm.

Thus the values estimated in this study are around 50 mm higher than those applied in my investigation of 1951 but still consider-

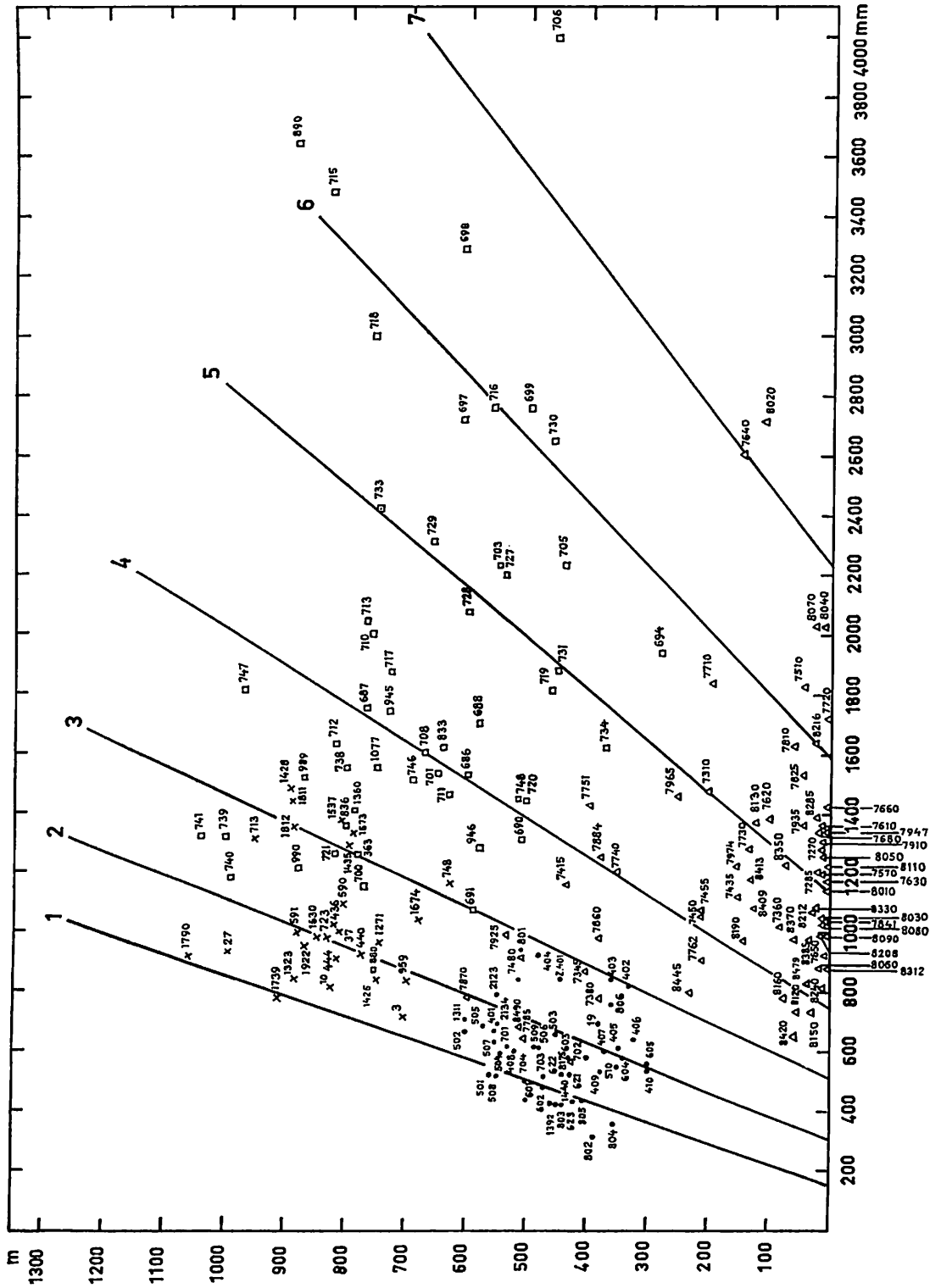

FIG. 1. Scatter diagram for the relationship between annual precipitation (in mm, abscissa) and height above sea level (ordinate) in the Scandinavian mountains, Regression lines are given for different areas. Rainfall stations are indicated by dots (Swedish) and triangles (Norwegian) and gauges by crosses (Swedish, see table 1) and squares (Norwegian, see table 2).

ably lower than those applied by A. Wallén in his calculation of the precipitation in the mountains of 1923.

Another reason to use somewhat higher values for evapotranspiration in the Swedish mountains are the values of potential evapotranspiration recently determined for Norway by WERNER-JOHANNESSEN (1968). For the latitudes under consideration which all are mountainous areas Werner-Johannesen's values for potential evapotranspiration have rendered estimates of 180—260 mm of actual evapotranspiration for those catchment areas situated at an altitude above 500 m (Table 2).

4. Mean annual precipitation for catchment areas

The mean annual precipitation values obtained for Swedish and Norwegian catchment areas by adding the above discussed estimates of evapotranspiration to the mean annual run-off values are also given in tables 1 and 2. These values represent the mean annual precipitation over rather big areas as the catchments vary in size between about 50 km² and 3 000 km². They therefore seem not to be clearly comparable with those precipitation values obtained at precipitation stations. It is clear enough on the other hand that those values, which we obtain by precipitation measurements, also are representing areas. We do not know, however, the size of these areas, although we suspect them generally to be smaller than catchments.

Considering the approximations involved in this method as a whole it has been taken for acceptable to compare the two kinds of precipitation values with relation to altitude provided that this comparison only is made for values from stations and catchment areas located fairly close to each other. The catchment values in most cases represent areas situated at higher elevations than the areas which are represented by the station values.

5. Precipitation in relation to altitude and distance from the sea

All the applied values of annual precipitation both from stations and catchment areas were plotted in an ordinary diagram with height above sea level as ordinate and precipitation as abscissa. The height above sea level of the field centres of gravity were used for the catchment areas, so that in fact the precipitation values of them also represent a point. In this diagram the precipitation values from stations generally are situated at lower altitudes than the values representing the catchments. It is now possible to draw a series of straight lines representing the increase of precipitation with altitude in various regions of the mountain area keeping in mind that values representing points below each other should be compared. It is evident from fig. 1 that the inclination of these lines is increasing from the continental inner parts of Sweden to the Atlantic coast of Norway and it seems as this change of inclination is almost mathematically regular.

The regions of different increase of precipitation with altitude were now possible to map for the whole area of the Scandinavian mountains under consideration. Fig. 2 gives a picture of this map showing that it is possible to draw continuous but of course windling lines corresponding to each one of the straight lines in fig. 1. In this manner and if interpolation between these lines is allowed the amount of annual precipitation is possible to determine at every point over the mountain area provided the altitude is known.

6. Mapping of the annual precipitation

It is now possible to proceed to mapping of the precipitation in different ways. In the final mapping a topographical map with isohypses for equal intervals over the whole mountain area will be used but as this map is not yet available it has been necessary to apply a net of grid points to the area under consideration in the test that has been carried out for this preliminary note namely the one located between 65° N and 66° N. Both the intersection points of full degree latitudes and longitudes as well as intermediate points between those were selected for this grid (fig. 2).

As a first step the altitude of each one of these grid points was determined from Norwegian and Swedish topographical maps. At certain occasions a grid point happened

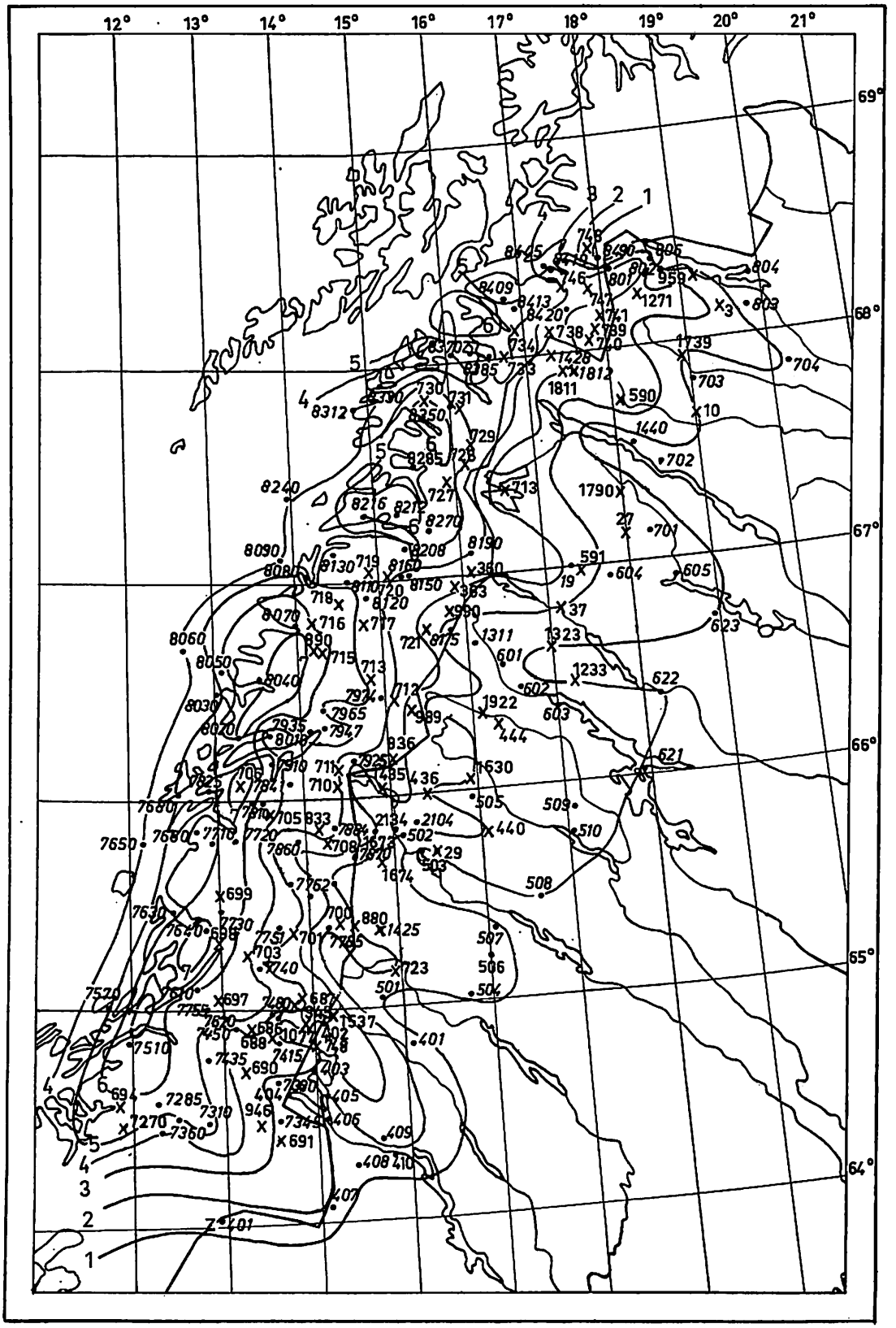

FIG. 2. Isolines for the interrelationship between annual rainfall and height above sea level (see Fig. 1). Station numbers are given for rainfall stations (dots) and gauges (crosses).

TABLE 1. *Hydrological data and estimates of precipitation for catchment areas in the northern part of the Swedish mountains. Discharge 1931—1960 from gauges in the mountains*

Gauge		Center of gravity of catchment area Latitude (North)	Longitude (East)	Mean altitude (m above sea level	Discharge m^3/s	Catchment area km^2	Discharge (mm/year)	Evapo-transpiration (estimated)	Annual precipitation (approximate values)
1-1738	Kummajoki	68° 57′	20° 29′	720	8,5	390	687	165	850
1-1780	Mertajärvi	68° 16′	22° 04′	420	3,8	370	324	190	515
4-1739	Laukujärvi	67° 55′	18° 50′	915	23	1166	621	160	780
9- 1428	Sitasjaure	67° 59′	17° 16′	895	41	982	1317	160	1480
9-1811	Autajaure	67° 55′	17° 20′	890	45	1101	1288	150	1440
9-1812	Teusajaure	67° 55′	17° 25′	890	51	1339	1197	150	1350
9-1790	Kåbtåjaure	67° 19′	17° 58′	1060	17	696	769	150	920
28-1922	Gautojaure	66° 20′	16° 05′	870	36	1448	784	160	950
28-1630	Gauträsk	66° 05′	15° 55′	845	33	1280	813	160	980
28-1673	Tängvattnet	65° 51′	14° 45′	790	7.3	197	1167	160	1330
28-1674	Nedre Jovattnet	65° 43′	14° 49′	680	9.8	358	863	170	1040
38-1425	Fättjaure	65° 19′	14° 45′	750	8.0	385	655	180	840
38-1537	Ankarvattnet	64° 59′	14° 12′	810	16.7	430	1197	170	1370
1-959	N. Abiskojokk	68° 20′	19° 15′	700	71	3290	681	150	830
1-3	Jukkasjärvi	68° 10′	19° 25′	705	99.4	6000	522	190	710
1-1271	Pahtajaure	68° 26′	18° 25′	745	2.7	103	825	140	965
4-10	Fjällåsen	67° 40′	19° 0′	825	44.4	2260	620	190	810
9-713	Virihaure	67° 20′	16° 35′	950	51.2	1380	1170	140	1310
9-590	Satisjaure	67° 45′	18° 5′	805	69.0	2320	936	150	1090
9-591	Niavve	67° 0′	17° 25′	880	45.6	1700	844	160	1000
9-1427	Skalka	67° 10′	17° 55′		110.1	4830	718	200	920
9-27	Tjåmotis 1	67° 10′	18° 0′	990	58.1	2290	800	150	950
13-37	Stenudden	66° 50′	17° 5′	810	64.1	2440	826	170	1000
20-1323	Rebnesjaure	66° 38′	16° 59′	885	21.2	1000	668	170	840
28-1435	Överuman +								
28-435	Umasjö	66° 3′	14° 54′	795	22.3	634	1109	180	1290
28-436	Solberg	66° 0′	15° 28′	820	28.5	1070	838	180	1020
28-440	Slätvik	65° 48′	16° 4′	770	9.4	407	728	190	920
28-444	Hällbacken	66° 20′	16° 20′	815	40.8	1790	718	190	910
38-723	Saxnäs +								
38-1631	Kultsjön	65° 10′	14° 55′	825	43.3	1720	793	190	980
38-748	Gäddede 1 +								
38-1383	Gäddede 5	64° 50′	14° 0′	630	78.6	2580	960	200	1160

As observations at some of the gauges are available for only a small part of the period 1931—60, a reduction method has been applied to obtain the mean values for these stations.

TABLE 2. *Hydrological data and estimates of precipitation for catchment areas in the Norwegian mountains between 64° 30′ and 68° 30′ N 1931—60*

Gauge		Center of gravity of catchment area Latitude (North)	Longitude (East)	Mean altitude (m above sea level)	Catchment area (km²)	Discharge (mm/year)	Evapo-transpiration (estimated)	Annual precipitation (mm) (calculated appr.values)
686	Limingen	64° 51′	2° 52′	600	653	1324	200	1530
1077	Landbru	64° 56′	3° 13′	750	56	1348	200	1550
687	Namsvatn	65° 05′	3° 07′	770	702	1554	200	1750
945	Bjørnstad	65° 05′	3° 00′	730	1051	1544	200	1740
688	Fiskumfoss o	64° 55′	2° 40′	580	3302	1460 M	240	1700
690	Tunnsjøplass	64° 43′	2° 36′	510	475	1072	240	1310
691	Otersjø ovf.	64° 26′	2° 51′	590	573	829	240	1070
946	Trangen	64° 29′	2° 42′	580	852	1042	240	1280
694	Salsvatn	64° 41′	1° 10′	280	425	1636 M	300	1940
697	Åbjørvatn	65° 06′	2° 13′	610	384	2452	270	2720
698	Strompdal	65° 27′	2° 15′	620	196	3020	270	3290
699	Hundålvatn	65° 45′	2° 15′	500	150	2479 M	280	2760
700	Hattfjelldal	65° 25′	3° 35′	770	1831	967	180	1150
701	Laksfoss	65° 25′	3° 05′	650	3647	1331	200	1530
880	Unkervatn	65° 25′	3° 55′	750	780	663	210	870
703	Kapskarmo	65° 17′	2° 34′	540	475	1973 M	230	2200
705	Fustvatn	65° 55′	2° 49′	440	520	2006 M	225	2230
706	Storvatn	66° 07′	2° 32′	460	43.5	3770 M	260	4000
708	Tustervatn	65°r45′	3° 30′	670	1500	1400	200	1600
833	Sjofoss	65° 50′	3° 25′	640	1880	1436	180	1620
710	Lille Målvatn	66° 04′	3° 37′	760	273	1798 M	200	2000
711	Store Akersvatn	66° 09′	3° 41′	630	129	1258	200	1460
989	Krokstrand	66° 24′	4° 37′	870	736	1325	190	1520
712	Nevernes	66° 30′	4° 25′	820	1849	1441	190	1630
713	Reinfosshei	66° 35′	4° 05′	770	3113	1859	180	2040
836	Jordbru	66° 12′	4° 17′	800	337	1169	190	1360
890	Storglåmvatn ndf.	66° 43′	3° 30′	890	230	3392	250	3640

TABLE 2. *(Cont.)*

Gauge		Center of gravity of catchment area Latitude (North)	Longitude (East)	Mean altitude (m above sea level)	Catchment area (km²)	Discharge (mm·year)	Evapo-transpiration (estimated)	Annual precipitation (mm) (calculated approx.values)
715	Fykanvatn	66° 44′	3° 29′	830	288	3230	250	3480
716	Ågnes	66° 51′	3° 28′	560	200	2504	260	2760
717	Selfoss	66° 51′	4° 04′	730	790	1632 M	240	1870
718	Arstadfoss	66° 56′	3° 44′	760	195	2722 M	280	3000
719	Oldereidvatn	67° 05′	4° 10′	460	50	1535	280	1810
720	Skarsvatn	67° 01′	4° 19′	500	141	1156 M	280	1440
721	Russånes	66° 45′	4° 50′	820	1151	1067	180	1260
990	Junkerdalselv	66° 48′	5° 04′	880	422	1032	180	1210
360	Fjell	67° 04′	5° 18′	790	695	1223	180	1400
363	Daja	66° 59′	5° 12′	780	411	1082	180	1260
727	Lakshola	67° 27′	5° 12′	550	220	1972 M	260	2230
728	Sørfjordvatn	67° 33′	5° 22′	600	111	1828 M	240	2070
729	Kobbvatn	67° 39′	5° 28′	660	390	2089 M	220	2310
730	Storvatn	67° 52′	4° 57′	460	72	2274 M	380	2650
731	Rotvatn	67° 49′	5° 17′	450	233	1602	280	1880
733	Ovre Sørfjordvatn	68° 01′	6° 01′	750	64	2165	250	2420
734	Forsavatn	68° 15′	6° 08′	370	150	1373	250	1620
738	Kjårdaelv	68° 09′	6° 36′	800	68	1352	200	1550
739	Gamnes	68° 08′	7° 08′	1000	804	1155	160	1320
740	Sørelv bru	68° 03′	7° 06′	990	373	1011 M	170	1180
741	Nordelvkors	68° 11′	7° 12′	1040	404	1172	150	1320
746	Høibakfoss	68° 20′	6° 46′	690	74	1256	250	1510
747	Sildvikvatn	68° 21′	7° 09′	970	18.5	1605	200	1810
748	Nygård	68° 30′	7° 11′	510	30	1210	240	1450

Figures marked M are mean values based on observations during the period concerned. All other figures have been obtained by reducing mean values valid for the period 1901—30 to the more recent normal period. This reduction was made by means of a map showing the geographical distribution of the quotient between the normals concerned.

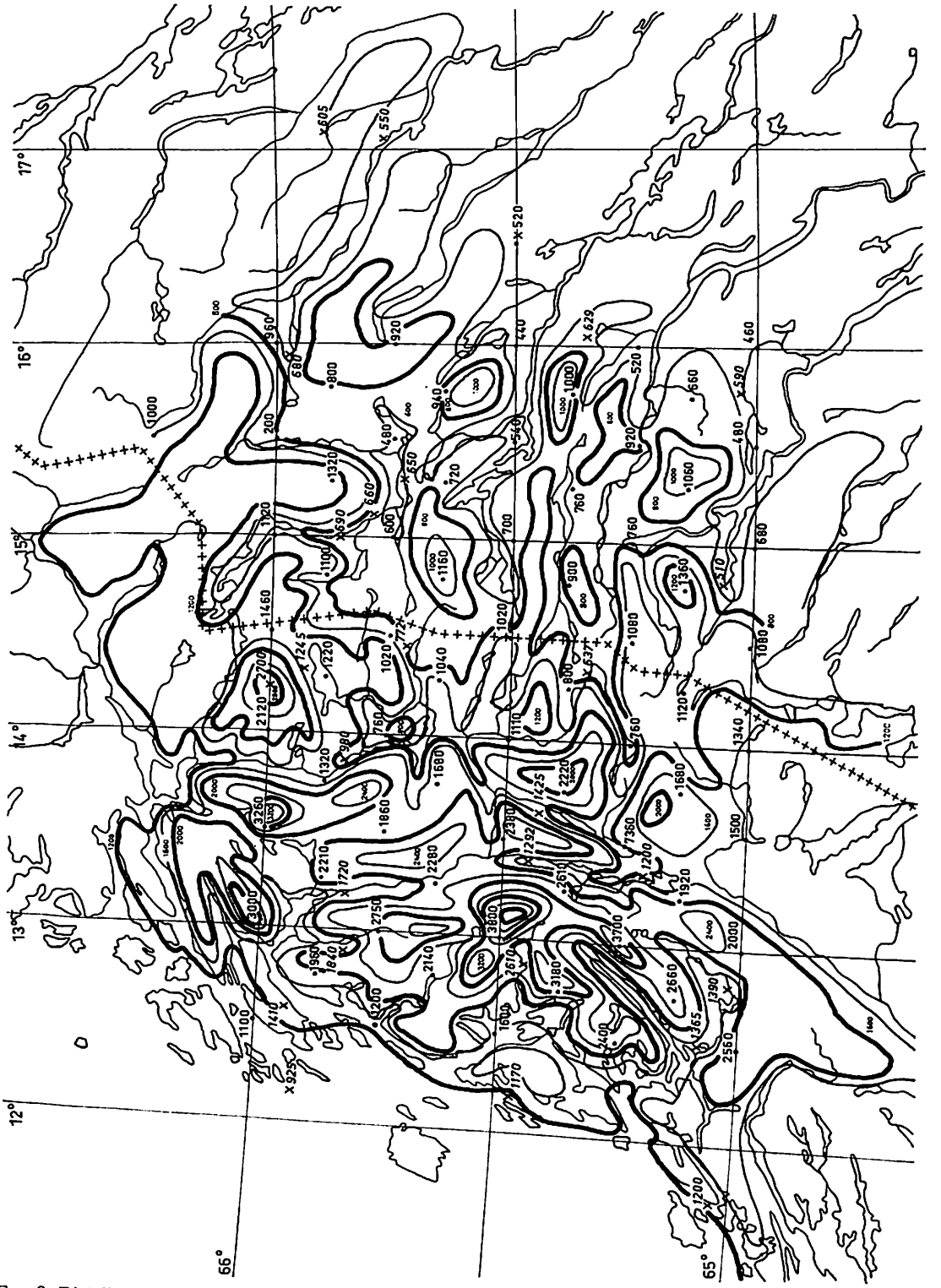

FIG. 3. Distribution of annual precipitation with due regard taken to the relationship between this quantity and height above sea level. Observed values are given by numbers in conjunction with crosses, computed values by numbers in conjunction with dots.

to be located on the top of a mountain or even in the sea. In such cases the altitude of a more topographically representative point somewhat aside the original grid point was determined.

As the second step the annual precipitation at the altitudes of the grid points was determined from the diagram in fig. 1 and the values entered on a transparent paper which was fixed on the top of a map of the latitude zone giving a general outline of the topographical features. The precipitation values from existing stations in the area were also entered on the transparent paper in order to increase the number of points. The isohyets were finally drawn taking into consideration not only the precipitation values but also the topographical features.

The picture of the distribution of the annual precipitation as given in fig. 3 indicates that the modified method will when applied to the whole area of the Scandinavian mountains render a much more detailed and as we think also more correct picture of the distribution of precipitation than we have earlier had.

REFERENCES

BERGSTEN, F., 1950. Contribution to study of evaporation. *SMHI, Communications, Series D, No. 3.*

MELIN, R., 1943. Nederbörd och vattenhushållning inom Malmagens fjällområde. *SMHI, Communications, Series Upps. No. 44.*

TAMM, O. F. S., 1959. Studier över klimatets humiditet i Sverige. *Bull. Royal School of Forestry, No. 39,* Stockholm.

WALLÉN, A., 1923. L'eau tombée dans la haute montagne de la Suède. *Geogr. Ann, Vol. 5 No. 1.*

WALLÉN, A., 1924. Nederbördskartor över Sverige. *SMHA, Communications, Bd 2, No. 3.*

WALLÉN, C. C., 1951. Nederbörden i Sverige. Medelvärden 1901—1930. *SMHI, Communications, Series A, No. 4.*

WALLÉN, C. C., 1966. Global radiation and potential evapotranspiration in Sweden. *Tellus.* Vol. 18, No 4.

WERNER JOHANNESSEN, T., 1968. Climate of Scandinavia and Finland. World Survey of Climatology. (In print)

Turbidity at Uppsala from 1909 to 1922 from Sjöström's solar radiation measurements[1]

By F. E. VOLZ *Astronomisches Institut der Universität Tübingen, Aussenstelle Weissenau bei Ravensburg*[2]

ABSTRACT

In the course of investigations on attenuation by dust from violent volcanic eruptions, the blue filter measurements of direct solar radiation at Uppsala by SJÖSTRÖM from 1908 to 1922 have been evaluated. For about 2,5 years, attenuation by the dust from the Katmai eruption (1912) was well above normal turbidity, while dust from weaker eruptions and from an Indonesian volcano was hardly detectable. Furthermore, the annual and daily courses of normal turbidity at Uppsala are compared with those at Stockholm in later years. There are also indications of an increase of turbidity by industrial activity in the course of the years.

1. Introduction

Old series of pyrheliometric measurements of direct solar date are dating back as far as about 1884, covering the great eruptions of volcanos Krakatoa (1883) and Mount Pelée (1902). However, it is difficult to derive from these measurements of total radiation turbidity data unaffected by the variable water vapor content of the atmosphere. It was not before 1930 that filters were introduced in regular pyrheliometric measurements for direct separation of haze and water vapor attenuation. However, a large body of spectrobolometric measurements of solar radiation at high altitude stations has been published by the Astrophysical Observatory of the Smithonian Institution from 1906 up to 1945 (Annals *4*, 1922; *5*, 1932). From these series, turbidity has recently been evaluated (VOLZ, 1968). One of the earliest series of pyrheliometric measurements in different spectral ranges has been obtained by SJÖSTRÖM (1930) at the Solar Observatory at Uppsala, from 1909 to 1922.

An evaluation seems not yet to have been made. These measurements, made in a clean northern country, are interesting because some large volcanic eruptions took place during that period, and because normal atmospheric turbidity can be studied at the start of indstrialization. Daily, seasonal, and annual course of turbidity will also be discussed, partly by comparison with later measurements at Stockholm.

2. Evaluation of the measurements

SJÖSTRÖM has measured the solar radiation without filter as well as with blue and yellow filters of spectral transmissions different from today's standard filters. We derived the turbidity coefficient only from the blue filter intensities because of the negligible influence of ozone absorption and since the other filter had much stronger secondary transmission in the infrared. For construction of a turbidity diagram, pure air intensities of the blue filter range for different air masses M were calculated by multiplying SCHÜEPP's (1949) tabulated intensities I_λ^0 for small spectral ranges by the transmission T_λ of the blue filter (which also included a water cell). The integrated pure air intensities

$$I_b^0(M) = \int_b I_\lambda \, d\lambda$$

follow the relation

$$\mathrm{d} \log I_b^0 / dM = 0.108$$

for $M < 4$, i.e. the filter rangeof half width 80 mμ can be considered monochromatic, and the effective wavelength

[1] Veröffentl. Nr. 103 des Astronomischen Institutes der Universität Tübingen.

[2] Now with Air Force Cambridge Research Laboratories, Hanscom Field, Bedford, Massachussetts, USA.

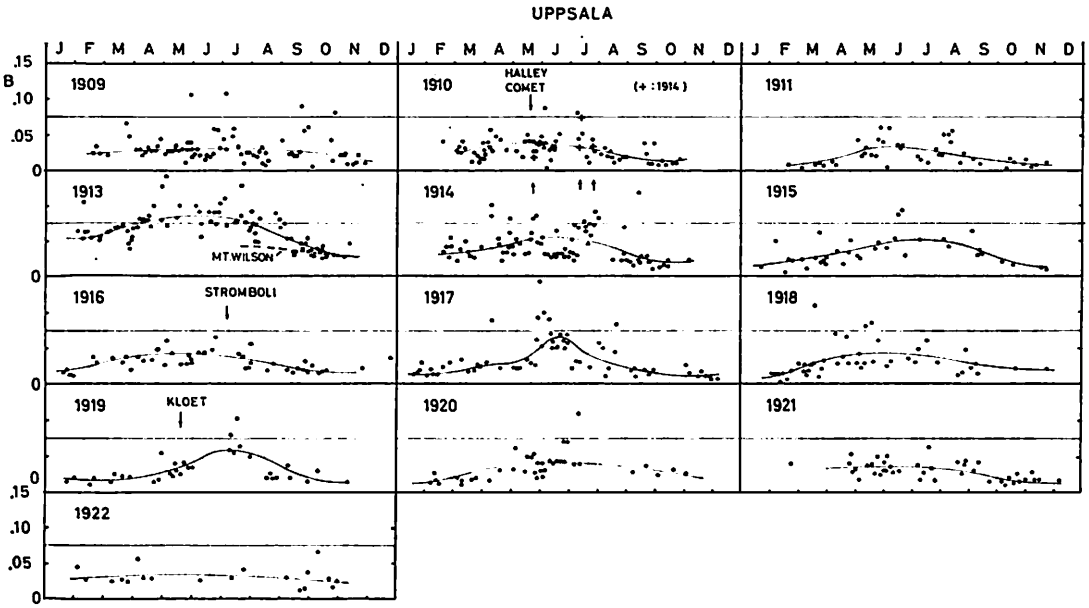

FIG. 1. Turbidity (daily minimum values) at Uppsala, 1909 to 1922 (data of 1912 in Fig. 1a).

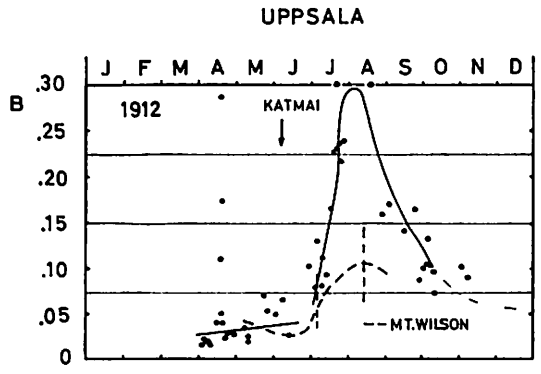

FIG. 1a. Turbidity in the year of the Katmai eruption.

(equivalence to pure air attenuation) is 440 mμ. The near infrared transmission amounted, even at $M=4$, to only 1.6 per cent of I_b^0.

The turbidity diagram was then constructed for the turbidity coefficient B, i.e. the decadic haze attenuation coefficient at λ 500 mμ, by subtracting log $I=1{,}21 \cdot B \cdot M$ from log $I_b^0(M)$ assuming a $\lambda^{-1.5}$ dependency of haze attenutation $\left(\left(\frac{440}{500}\right)^{-1.5}=1{,}21\right)$. The extraterrestrial intensity I_b^0, of the blue filter range, which for unknown reasons, is about 30 per cent smaller than the computed I_b^0, has been checked by us by extrapolating a sufficiently large number of measurements on Summer days to $M=0$. Up to 1910, a value of 0.074 (SJÖSTRÖM's tabulation) has been used, and later on has been changed to 0.070. This variation is roughly in agreement with the course of the calibration factor for total radiation as obtained by SJÖSTRÖM by comparison with other instruments.

3. Results

The annual course of B from 1909 to 1922 is presented in Fig. 1. The values of 1912, which are very high because of volcanic dust, are shown separately in Fig. 1a. For conformity with our other turbidity investigations, only the daily minimum value B_{min} (if it seemed reliable) has been plotted if more than one observation had been made.

3.1. Turbidity in normal years. In Figs 1 and 1 a, the seasonal trend of the turbidity coefficient has been indicated by freehand lines. The years 1909 to 1911, 1915 and 1916, and 1920 to 1922 obviously represent only normal haziness with a typical seasonal course which will be discussed in Sect. 4 in more detail.

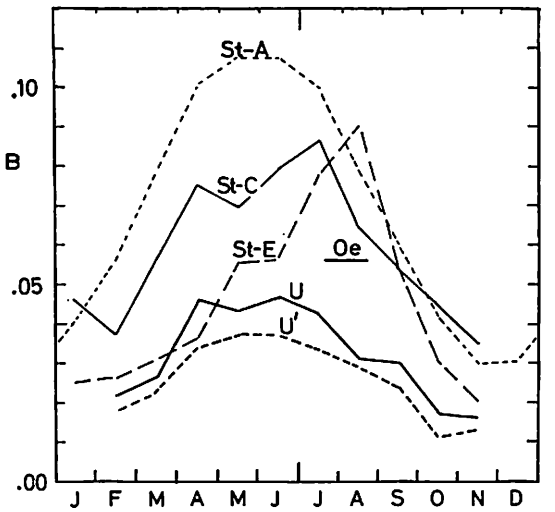

FIG. 2. Seasonal course of turbidity at Uppsala and Stockholm. Uppsala: (U), all data in undisturbed years between 1910 and 1921; (U'), only daily minima in undisturbed years; Stockholm: City (St-A), all data 1921 to 1929 (ÅNGSTRÖM, 1930); Experimentalfältet (St-E), 1938 to 1940, and City (St-C), 1941 to 1950 (SCHÜEPP, 1959): Östersund: (Oe), Summer 1958.

3.2. Disturbed years. On June 6, 1912, the volcano *Katmai* in Alaska had its most violent eruption. Large amounts of dust, partly raised up to 30 km, spread mainly over the arctic circle. In the Uppsala measurements, the first turbidity increase occurred by the end of June, though faint, high dust clouds were already observed in the Alps at the day of the main eruption. The attenuation peak, with $B \approx 0.30$, was from mid July to mid August. At Mount Wilson in California (VOLZ, 1968), the turbidity increase started a few days later than at Uppsala, and seems to have reached the much smaller maximum, with peak values of $B \approx 0.15$, before the end of August, shortly before the 1912 measurements were determined. Thus a strong meridional gradient of dustiness existed as also indicated by a large day to day variability of B at Mount Wilson. In the following Summer, the volcanic dust component ($\Delta B \approx 0.04$) was about constant at Uppsala and had by Spring 1914 about the same value (0.02) as Mount Wilson half a year ago. However, some values were still high in Summer 1914 at Uppsala. Bright, colored purple lights were not observed in Germany before Fall 1912, because the initial turbidity was too strong. They ceased by February 1914, but sky polarization was still abnormal in this year. (Brief accounts and references on visual twilight observations, measurements on sky polarization and neutral points regarding abnormal atmospheric turbidity have been given by GRUNER (1958) and JENSEN (1958); publication of a compilation of such data by the author is in preparation).

The tropopheric dust cloud by the strongest eruption of *Lassen Peak* (near San Francisco) in May 1915 had no effect on Uppsala turbidity. It is doubtful whether the eruption of *Stromboli*, Southern Italy, on July 4, 1916 may have caused some high turbidity values at Uppsala in 1917. However, high dust clouds and colored twilights have been observed in the Alps, and in Southern USA, up to November 1916. Turbidity at Mt. Wilson was slightly ($\Delta B \approx 0.015$) increased during this period.

A few months after the eruption of the volcano *Kloet* on Java on May 19, 1919, both Mt. Wilson and Uppsala show a small increase of turbidity. Twilights in Germany were slightly enhanced up to the end of 1920.

4. Normal seasonal course

The mean seasonal course of turbidity at Uppsala, derived from the undisturbed years 1910, 11, 15, 18, 20, and 1921 is shown in Fig. 2 by heavy lines. Curve U is computed from all data of these years, while curve U' with about 20 per cent lower values, comprises only daily minimum values as presented in Fig. 1. For comparison, Fig. 2 also includes monthly means of turbidity from pyrheliometric filter measurements at Stockholm, 60 km south of Uppsala. Curve ST-A has been obtained by ÅNGSTRÖM (1930) from only 46 measurements, mainly in Spring, between 1921 and 1929 in Stockholm City. SCHÜEPP (1950) evaluated measurements at Stockholm Experimentalfältet (St-E, 3 km north of the city, 1938—40) and from the City (St-*C*, 1941—50).

Regarding the seasonal course, turbidity at Uppsala as well as at St-*A* had their

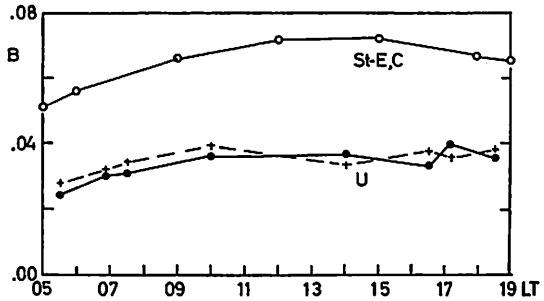

FIG. 3. Daily course of turbidity, May to August. U at Uppsala, undisturbed years between 1909 and 1920 (×1920 and 1911, 116 measurements on 41 days; ● 1909, 1915, 1918, 1920 (72 measurements in 25 days). St-E,C at Stockholm (1938—1950, SCHÜEPP, 1950).

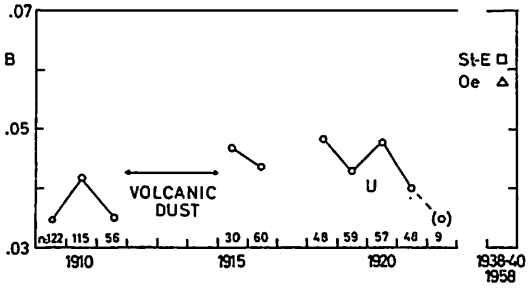

FIG. 4. Annual turbidity (all data between April and August) at Uppsala (o, number of measurements indicated), and at Stockholm (□ St-E, 1938—1940). Measurements at Östersund (and Stockholm) from 10 July to 20 August 1958 (△, Oe).

maximum in Spring, but SCHÜEPP's data give a strong maximum in July resp. August.

Although a more or less continuous turbidity increase may have occurred during the years discussed here, thus making comparison of absolute values difficult, we note that turbidity at St-*E* and *U* were of similar magnitude only during late winter, up to April, while Stockholm City values (St-*C* and St-*A*) were much higher. In the second half of the year all Stockholm values were of the same order, and much higher than *U* data.

In these comparisons, however, one has to keep in mind that the St-*E* series, and especially St-*A*, may have been of insufficient duration for elimination of fortuities of turbidity.

5. Daily course of turbidity

In Fig. 3, the daily course of *B* at Uppsala has been compared with that at Stockholm (SCHÜEPP, 1950), each for the period May to August. Since measurements at Uppsala were seldomly made throughout the day, the daily course had to be computed mainly from days with measurements up to or after noon, so the result may be somewhat questionable. Similar difficulties seem to have existed with the Stockholm data. However, both series give a slight increase of turbidity in the morning hours and practically constant values later on, in contrast to high morning dustiness common for continental stations, especially in industrialized areas. At the Swedish coast, a nightly air flow from the low mountains to the sea together with the prevailing winds from the West could probably explain the morning dust minimum. This seems to be supported by a similar daily course of precipitable water vapor as deduced by Schüepp.

6. Secular increase of turbidity due to industrialization?

Mean turbidity values for Summer periods, April to September, at Uppsala for undisturbed years between 1909 and 1922 are shown in Fig. 4. Excluding 1921 (and 1922 because of the small number of data), the Summer turbidity shows an increasing trend. The countryside measurements at Stockholm (St-*E*, 1938—40) seem to fit well to the trend. This seems to be supported by numerous measurements by the author during 29 days, from 10 July to 20 August 1958, mainly near Östersund (730 m altitude, 420 km in NNW of Uppsala), and in the outskirts of Stockholm. They resulted in a mean *B* of 0,058 with about 20 per cent of the data <0.03, whereas the mean turbidity at Uppsala for the same season (Fig. 2) was only 0.038[1].

[1] Added during proof reading: A similar turbitity trend and its implications have recently been discussed by R. A. McCormick and J. H. Ludwig, Science 156, No. 3780, 1358 (1967). They report an increase of mean annual turbidity by B=0.06 at Washington, D. C. since 1903—05 (then B=0.104), and by 0.022 at Davos since 1914—16 (then B=0.026).

7. Concluding remarks

Although the Uppsala turbidity was rather small, it was difficult to detect the influence of volcanic dust for more than 2 years after a major dust ejection. Regarding the investigation on seasonal course in Uppsala and Stockholm, no typical annual variation could be obtained from the different series of observations. Highly interesting is the likelihood of a considerable turbidity increase during the last decades. Not included in these studies of daily, seasonal and annual course of turbidity are the pyrheliometric measurements at Stockholm-Experimentalfältet from 1930 to 1936, since the rough data (ÅNGSTRÖM, 1937) have not yet been evaluated.

Acknowledgement

I thank Dr. Schüepp, University of Basel, for making available to me his manuscript on the Stockholm data.

REFERENCES

GRUNER, P., 1958, Dämmerungserscheinungen. *Handb. Geophys. 8, Phys. der Atmosphäre I* (Herausg. F. Linke u. F. Möller), Bornträger, Berlin.

JENSEN, CHR., 1958, Die Polarisation des Himmellichts. Ibid.

SCHÜEPP, W., 1949, Die Bestimmung der atmosphärischen Trübung aus Aktinometermessungen. *Arch. Met, Geoph., Bioklim., B 1*, pp. 257—346.

— 1950, Actinometermessungen in Stockholm 1938—1950 (manuscript).

SJÖSTRÖM, M., 1930, Pyrheliometric measurements of the solar radiation in Uppsala during the years 1909—1922. *Nova Acta Reg. Soc. Scient. Upsal. Ser. IV, Vol. 6, Nr. 6.*

VOLZ, F. E., 1968, Normal and volcanic turbidity from Smithonian mountain solar spectrobolometry 1905 to 1950. In preparation.

ÅNGSTRÖM, A., 1930, On the atmospheric transmission of sun radiation II. *Geograf. Ann., 12*, pp. 130—159.

Nr 30. Bibliographie Hydrologique de l'Année 1938. Suède . . . . . Kr. 1: —
31. G. Slettenmark: Current meter discharge measurements for the testing of hydraulic turbines . . . . . » 1: —
32. A. Nyberg: The lag-coefficient of aerological instruments and the function of hair hygrometers at low temperatures . . . . . » 1: 50
33. C. J. Östman: Den svåra isvintern 1939—1940 (with an English summary) . . . . . » 2: —
34. O. Tryselius: A short comparison between the Finnish and the Swedish snow samplers . . . . . » 0: 50
35. G. Liljequist: Winter temperatures and ice conditions of lake Vetter with special regard to the winter 1939/40 . . . . . » 1: 50
36. F. Bergsten: Undersökningar rörande sekulära ändringar i avrinningen i vissa svenska vattendrag (with an English summary) . . . . . » 1: —
37. A. Ångström: Nederbördsklimatets ändring i nuvarande tid (with an English summary) . . . . . » 1: 50
38. C. J. Östman: Isvintern 1940/41 (with an English summary) . . . . » 1: —
39. G. L. Eriksson: Untersuchung der Periodizitäten der Wasserstände und der abfliessenden Wassermengen von Norslund am Dalelf . . . . . » 1: —
40. A. Nyberg und E. Palmén: Synoptisch-Aerologische Bearbeitung der internationalen Registrierballonaufstiege in Europa in der Zeit 17.—19. Oktober 1935 . . . . . » 3: —
41. A. Nyberg: Jämförelser mellan olika instrument för mätning av temperatur och fuktighet i högre luftlager (with an English summary) . . » 1: —
42. A. Ångström: Principiella synpunkter på undersökningar över klimatets förändring med tillämpning på det svenska klimatet (with an English summary). . . . . » 1: —
43. G. H. Liljequist: Isvintern 1941—42 (with an English summary) . . . » 1: —
44. R. Melin: Nederbörd och vattenhushållning inom Malmagens fjällområde. (Precipitation and water-economy within the mountain area of Lake Malmagen, with an English summary.) . . . . . » 3: —
45. O. Tryselius: Rekonstruktion av de naturliga vattenstånden i reglerade sjöar. (Reconstruction of natural water levels in regulated lakes, with an English summary.) . . . . . Utgången (out of print)
46. G. H. Liljequist: The severity of the winters at Stockholm 1757—1942 Kr. 1: —
47. N. G. Johnson and H. Olsson: On the standardization of photoelectric elements by means of solar radiation. The total energy of incident radiation computed from records with photo-electric elements . . . . . » 1: 50
48. A. Nyberg: Synoptic-aerological investigation of weather conditions in Europe 17—24 April 1939 . . . . . » 6: 50
49. F. Bergsten: Metoder för bestämning av vindens inflytande på havets vattenstånd och deras tillämpning vid landhöjningsberäkningar (with an English summary) . . . . . » 1: 50
50. C. C. Wallén: Studier över Skånes nederbördsklimat (with an English summary.) . . . . . » 2: —

Meddelanden. Serie B.

Nr 1. Lindholm, F., Modén, H., Persson, W. och Ångström, A., Åsk- och överspänningsforskning. Åskvädrens geografiska fördelning i Sverige. Synoptisk-aerologisk studie över åskväder under sommaren 1944. Om sambandet mellan solaktivitet och åskfrekvens. (Summary and review.) Kr. 2: —

2. Nyberg, A., A comparison between the Väisälä radiosonde and the Friez radiosonde . . . . . » 0: 50

3. Lindholm, F., Propagation to great distance of air-waves from the explosion of Oslo on December 19th 1943 as an indication of conditions in the upper atmosphere . . . . . » 1: —

4. Lönnqvist, O., Förenkling av höjduträkningen vid radiosondering. (A new method for simplifying aerological height computation, with an English summary.) . . . . . » 1: —

5. Liljequist, G. H., Isvintern 1946—47 (with an English summary) . . . » 1: —

6. Nyberg, A., On liquid water content in fogs and clouds . . . . . » 1: 50

7. Liljequist, G. H., On fluctuations of the summer mean temperature in Sweden . . . . . » 1: 50

8. Similä, A., En ny synoptisk-aerologisk metod att förutsäga åska
Utgången (out of print)

9. Nyberg, A., On the comparison of radiosonde data in Payerne May 1950
Utgången (out of print)

10. Rodhe, B., On the relation between air temperature and ice formation in the Baltic . . . . . Kr. 1: —

11. Lindholm, F., Sunshine and cloudiness in Sweden 1901—1930
Utgången (out of print)

12. Rohde, B., A study of the correlation between the ice extent, the course of air temperature and the sea surface temperature in the Åland Archipelago . . . . . Kr. 1: 50

13. Courvoisier, P., Contributions to standard pyrheliometry. With an introduction by A. Ångström and W. Mörikofer . . . . . » 3: —

14. Lönnqvist, O., Diurnal temperature variation at the surface of the earth » 2: 50

15. Lönnqvist, O., A window radiation chart for estimating surface temperature from satellite observations . . . . . » 3: —

16. Högström, U., An experimental study on atmospheric diffusion . . . . » 4: 50

17. Berggren, R., The vertical distribution of ozone over Arosa on 16 April 1962 and the synoptic situation . . . . . » 3: 50

18. Nyberg, A., A study of the evaporation and the condensation at a snow surface . . . . . » 3: 50

19. Modén, H. & Nyberg, A., Stockholmsområdets klimat. 1. Nederbörden » 5: 00

20. Nyberg, A., A computation of the evaporation in Southern Sweden during 1957 . . . . . » 5: 50

21. Eriksson, B., A climatological study of persistency and probability of precipitation in Sweden . . . . . » 5: 50

22. Rodhe, B. & Ångström, A., Pyrheliometric measurements with special regard to the circumsolar sky radiation . . . . . » 6: 50

23. Rodhe, B., The concentration of liquid water in the atmosphere . . . » 6: 50

24. Wallén, C. C., Global solar radiation and potential evapotranspiration in Sweden . . . . . » 6: 50

25. Berggren, R. & Labitzke, K., Detail study of the horisontal and vertical distribution of ozone. . . . . » 6: 50

26. Berggren, R. & Nyberg, A., Eddy vertical transport of latent and sensible heat . . . . . » 6: 50

27. Wallén, C. C., Aridity definitions and their applicability . . . . . » 6: 50

28. Scientific papers dedicated to dr Anders Ångström . . . . . » 23: —

KUNGL. BOKTR. STHLM 1968